

On the Signatures of Magnetic Reconnection at Current Sheets using Cluster and MMS Multi-satellite Constellation Observations

Stefan Eriksson

Laboratory for Atmospheric and Space Physics, Boulder, Colorado



Image: Petr Horálek, hybrid solar eclipse on 20 April 2023, <https://www.petrhoralek.com/?p=23566>

On the Signatures of Magnetic Reconnection at Current Sheets using Cluster and MMS Multi-satellite Constellation Observations

Stefan Eriksson

Laboratory for Atmospheric and Space Physics, Boulder, Colorado

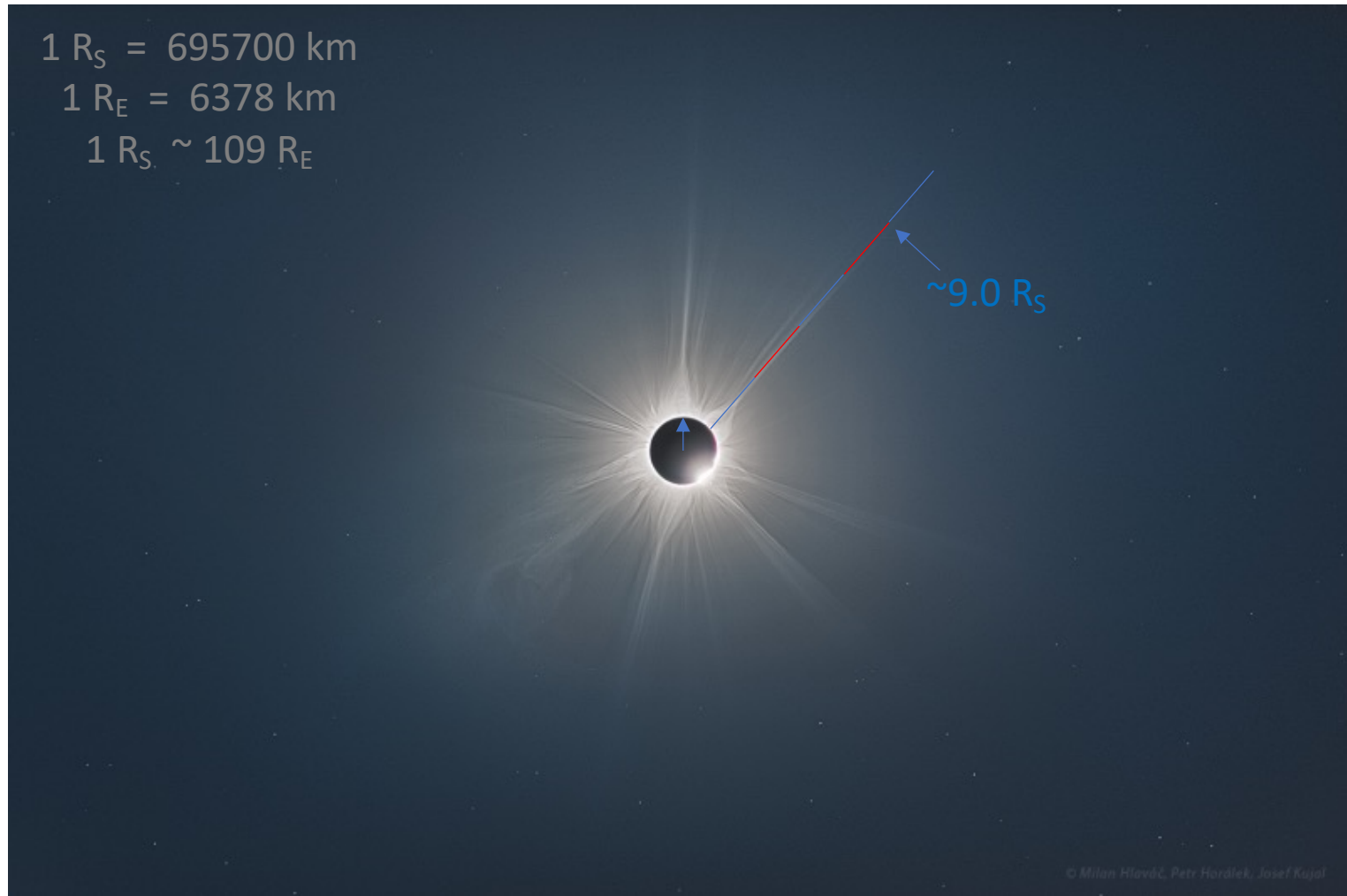


Image: Petr Horálek, hybrid solar eclipse on 20 April 2023, <https://www.petrhoralek.com/?p=23566>

On the Signatures of Magnetic Reconnection at Current Sheets using Cluster and MMS Multi-satellite Constellation Observations

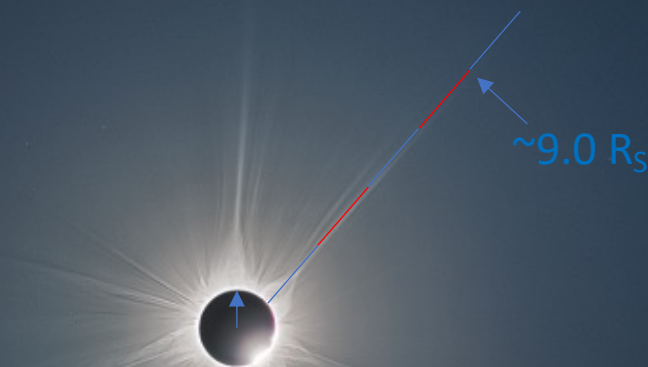
Stefan Eriksson

Laboratory for Atmospheric and Space Physics, Boulder, Colorado

$1 R_S = 695700 \text{ km}$

$1 R_E = 6378 \text{ km}$

$1 R_S \sim 109 R_E$



The Parker Solar Probe will approach to within $9.86 R_S$ from the center of the Sun on 2024-12-24/11:20 UT (1st of 3 planned perihelia) to “taste the Solar Corona” at this closest proximity. Two more scheduled on 2025-03-22 and 2025-06-19.

PSP will travel at $V=690,000 \text{ km/h} \sim 1 R_S/\text{hour}$ or 0.064% the speed of light.

It will then become the fastest man-made object ever ...

© Milan Hlaváč, Petr Horálek, Josef Kujal

On the Signatures of Magnetic Reconnection at Current Sheets using Cluster and MMS Multi-satellite Constellation Observations

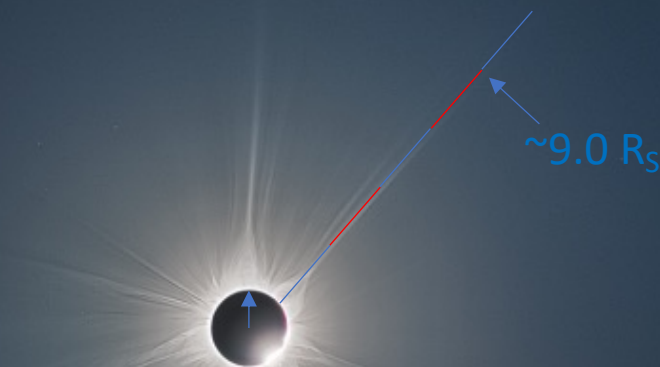
Stefan Eriksson

Laboratory for Atmospheric and Space Physics, Boulder, Colorado

$1 R_S = 695700 \text{ km}$

$1 R_E = 6378 \text{ km}$

$1 R_S \sim 109 R_E$



The Parker Solar Probe will approach to within $9.86 R_S$ from the center of the Sun on 2024-12-24/11:20 UT (1st of 3 planned perihelia) to “taste the Solar Corona” at this closest proximity. Two more scheduled on 2025-03-22 and 2025-06-19.

PSP will travel at $V=690,000 \text{ km/h} \sim 1 R_S/\text{hour}$ or 0.064% the speed of light.

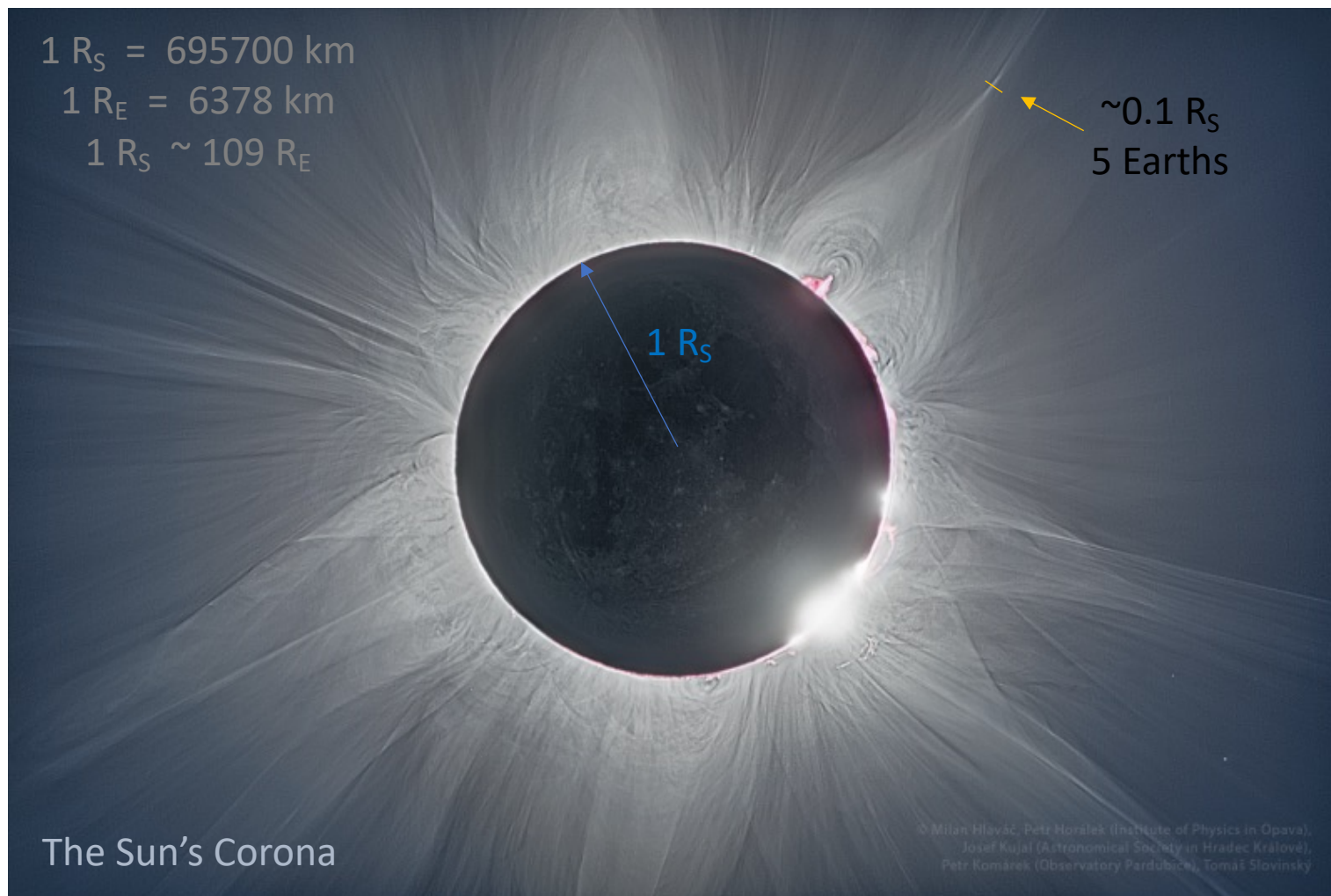
A typical bullet is fired at $\sim 3000 \text{ km/h} \dots V \sim 230 \times$ bullet

© Milan Hlaváč, Petr Horálek, Josef Kujal

On the Signatures of Magnetic Reconnection at Current Sheets using Cluster and MMS Multi-satellite Constellation Observations

Stefan Eriksson

Laboratory for Atmospheric and Space Physics, Boulder, Colorado



On the Signatures of Magnetic Reconnection at Current Sheets using Cluster and MMS Multi-satellite Constellation Observations

Stefan Eriksson

Laboratory for Atmospheric and Space Physics, Boulder, Colorado

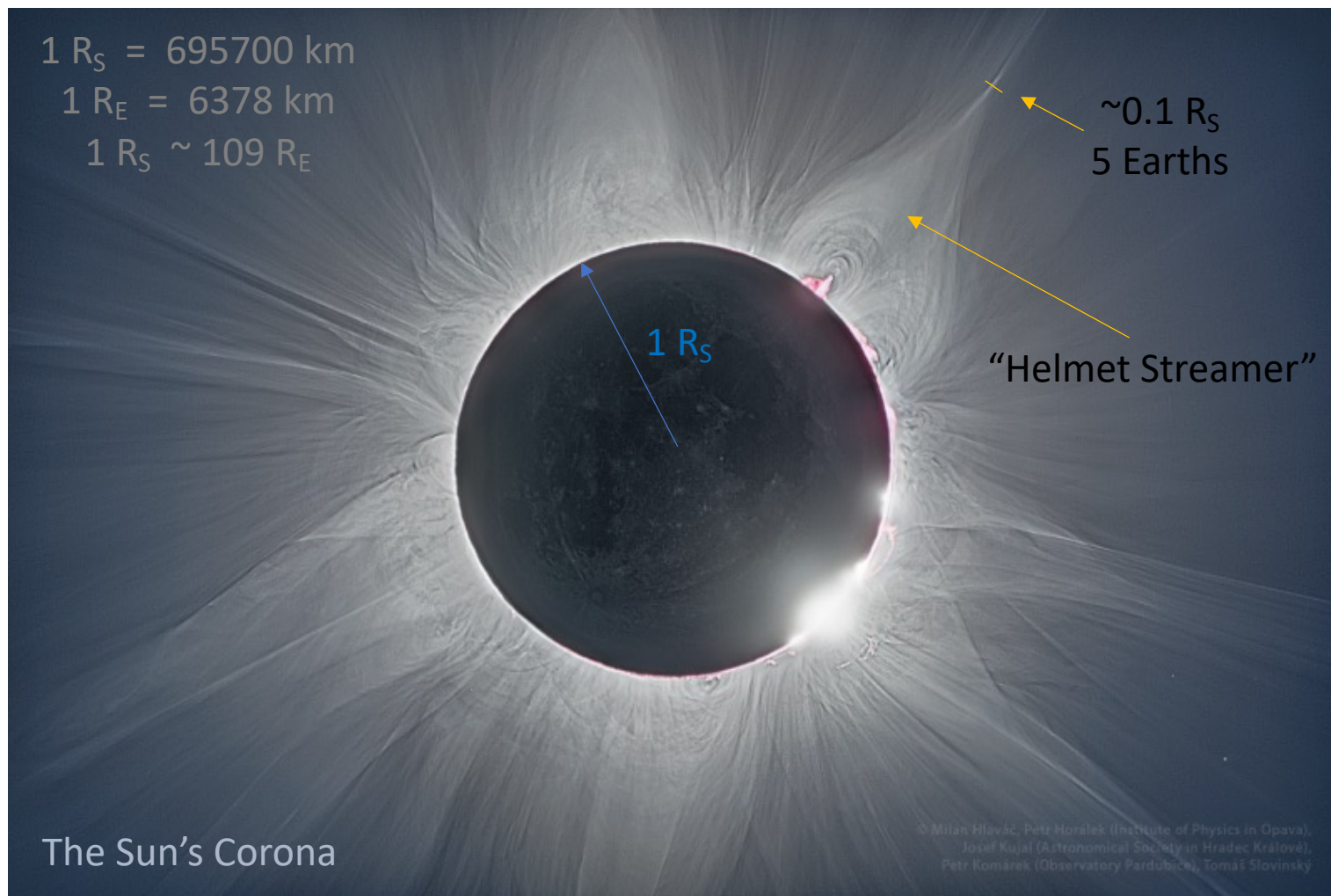


Image: Petr Horálek *et al*, hybrid solar eclipse on 20 April 2023, <https://www.petrhoralek.com/?p=23566>

On the Signatures of Magnetic Reconnection at Current Sheets using Cluster and MMS Multi-satellite Constellation Observations

Stefan Eriksson

Laboratory for Atmospheric and Space Physics, Boulder, Colorado

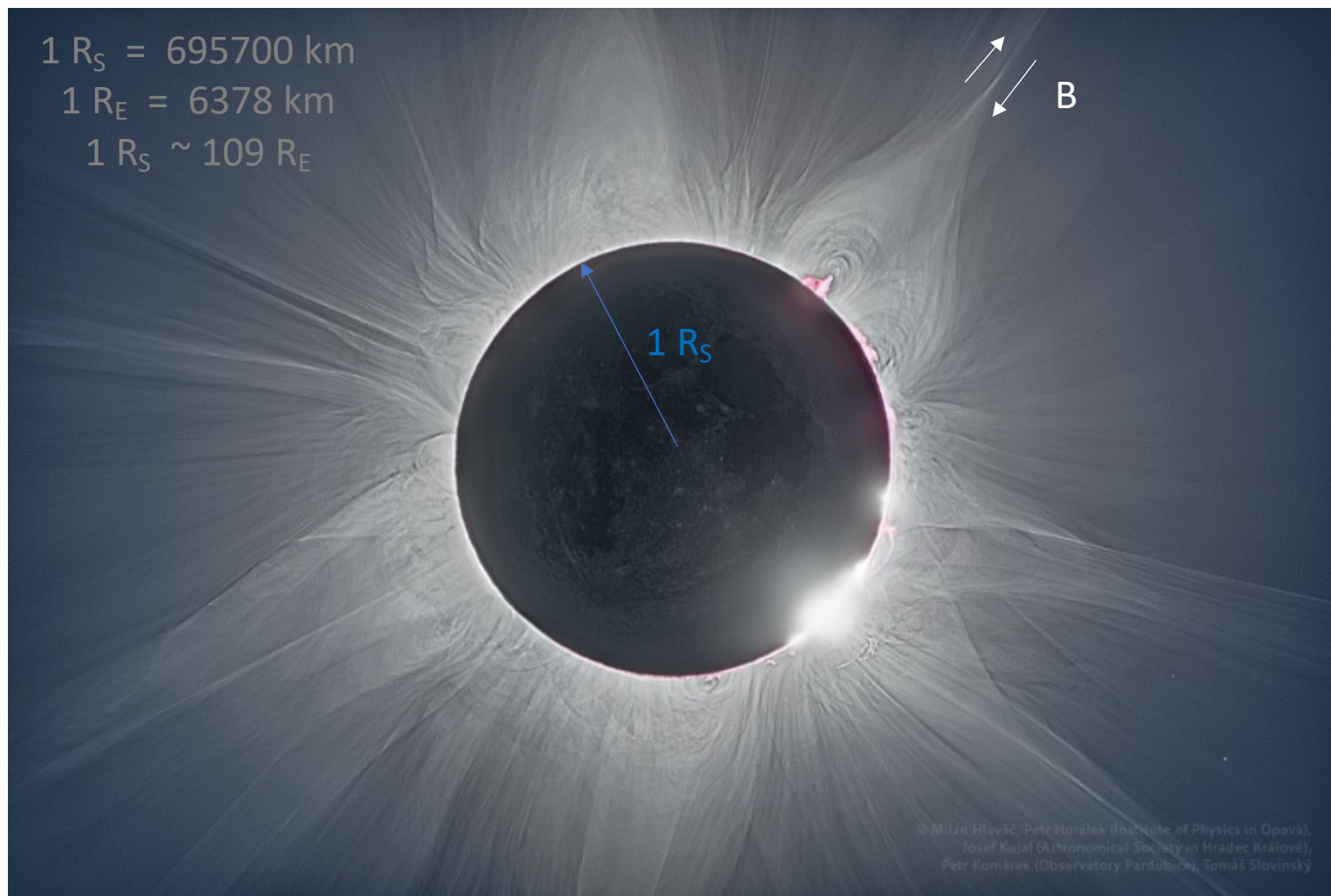


Image: Petr Horálek *et al*, hybrid solar eclipse on 20 April 2023, <https://www.petrhoralek.com/?p=23566>

Overview

- **Current sheets: *Magnetic field rotations* [$J = \nabla \times B / \mu_0$] from the very wide *Heliospheric Current Sheet* to “narrow” *M’pause***
- Multi-spacecraft missions: *A brief introduction to tetrahedron formations and the Curlometer technique*
- Near-Earth space regimes & boundaries
- The magnetic reconnection process at current sheets:
 - (a) *Schematic overviews, 2D vs 3D & ion (di) scale*
 - (b) *“To be or not to be” frozen-in? The G.O.L. vs Hall ☺*
 - (c) *Reconnection rate v_{in}/v_{out}*
- Observations of Reconnection Jets:
 - (a) *Cluster in the solar wind vs “timing normal” concept*
 - (b) *MMS at the magnetopause: J from “curlB” vs $J = Ne(V_i - V_e)$*
- Summary

Heliospheric Current Sheet



SMITH: REVIEW

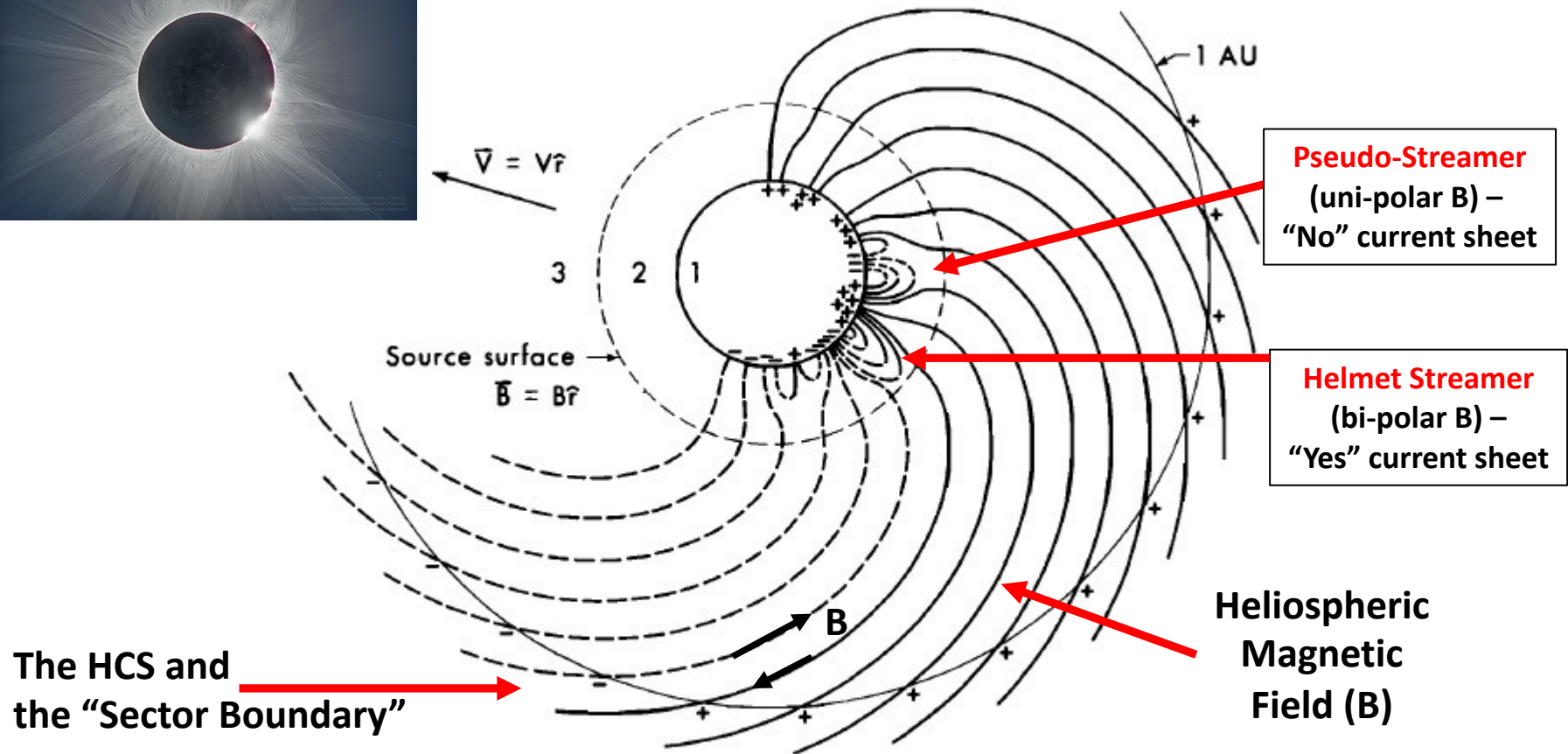


Figure 7. Schematic of the solar wind magnetic field source surface. The photospheric magnetic field, routinely observed by ground-based magnetographs, is extrapolated upward using a magnetic potential to the “source surface” at which the field is required to become radial. The differing magnetic polarities along the photosphere associated with both low- and high-latitude fields are indicated. Only the largest-scale fields reach the source surface. Both positive and negative fields are shown. From *Schatten* [1972].

Heliospheric Current Sheet

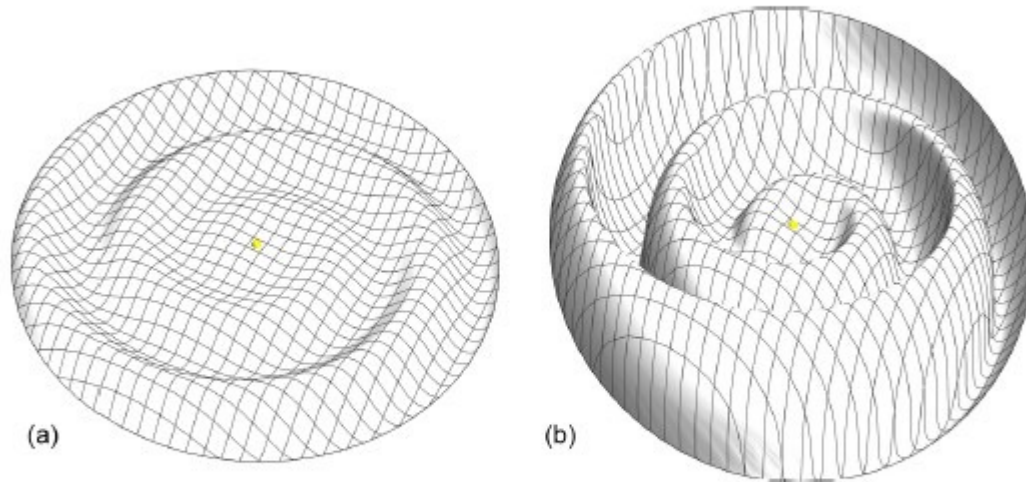


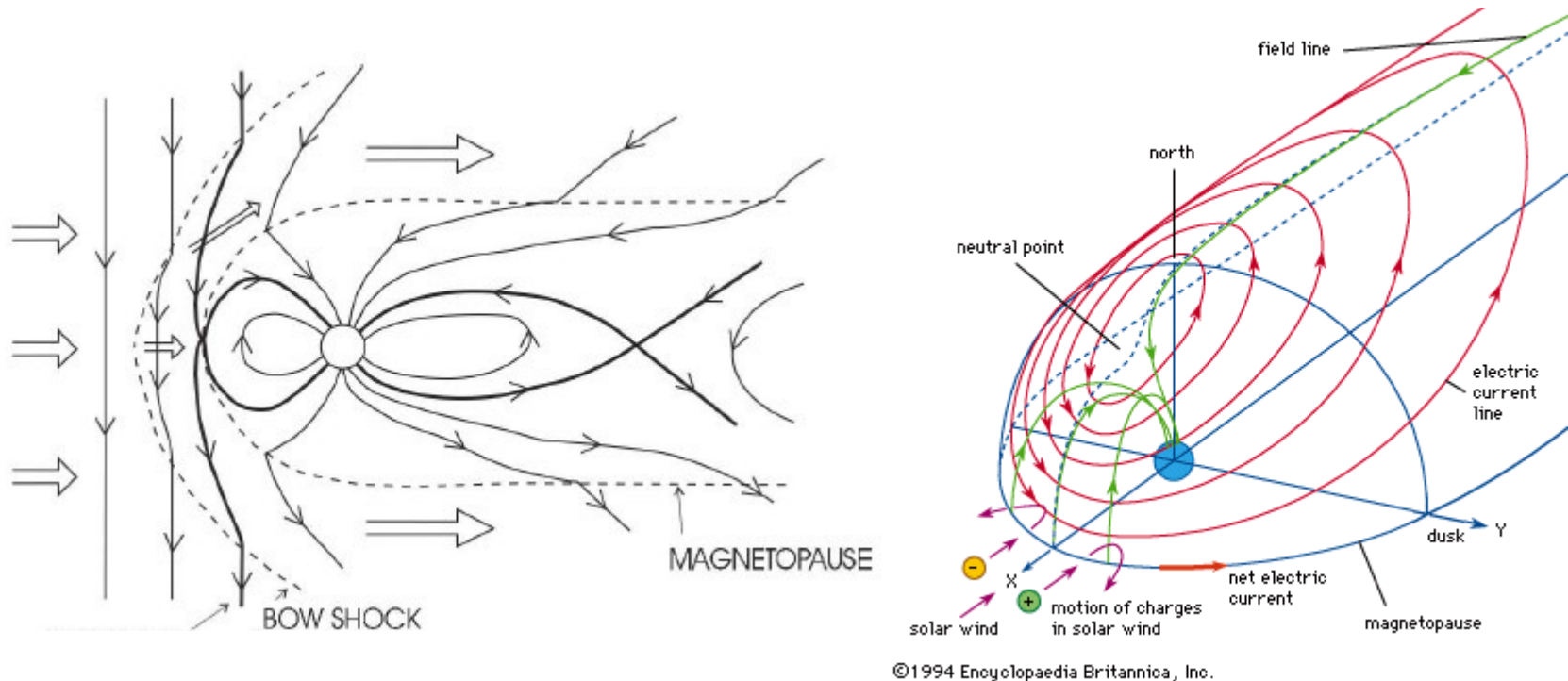
Figure 5. Shape of the “ballerina skirt” model of the heliocentric current sheet defined by $\cos\theta^* = \cos\theta$. Topology at $t = 0$ and for $\theta_{t0} = 5^\circ$ (a) and $\theta_{t0} = 30^\circ$ (b).

Lhotka, C. & Y. Narita, Kinematic models of the interplanetary magnetic field, *Annales Geophysicae*, 37, 299–314, 2019

Ref	HCS min (km)	HCS max (km)	<HCS> (km)
19 HCSs (1)	3500	12000	9100 (median)
212 HCSs (2)	-	-	64000 (average) ~10 R _E

1. Winterhalter et al., The heliospheric plasma sheet, *J. Geophys. Res.*, 99, A4, 6667-6680, 1994
2. Lepping et al, Large-scale properties and solar connection of the heliospheric current and plasma sheets: WIND observations, *Geophys. Res. Lett.*, 1996.

Earth's Magnetopause Current



Principles of Heliophysics, V2.0

<https://www.britannica.com/science/geomagnetic-field/The-magnetopause-current>

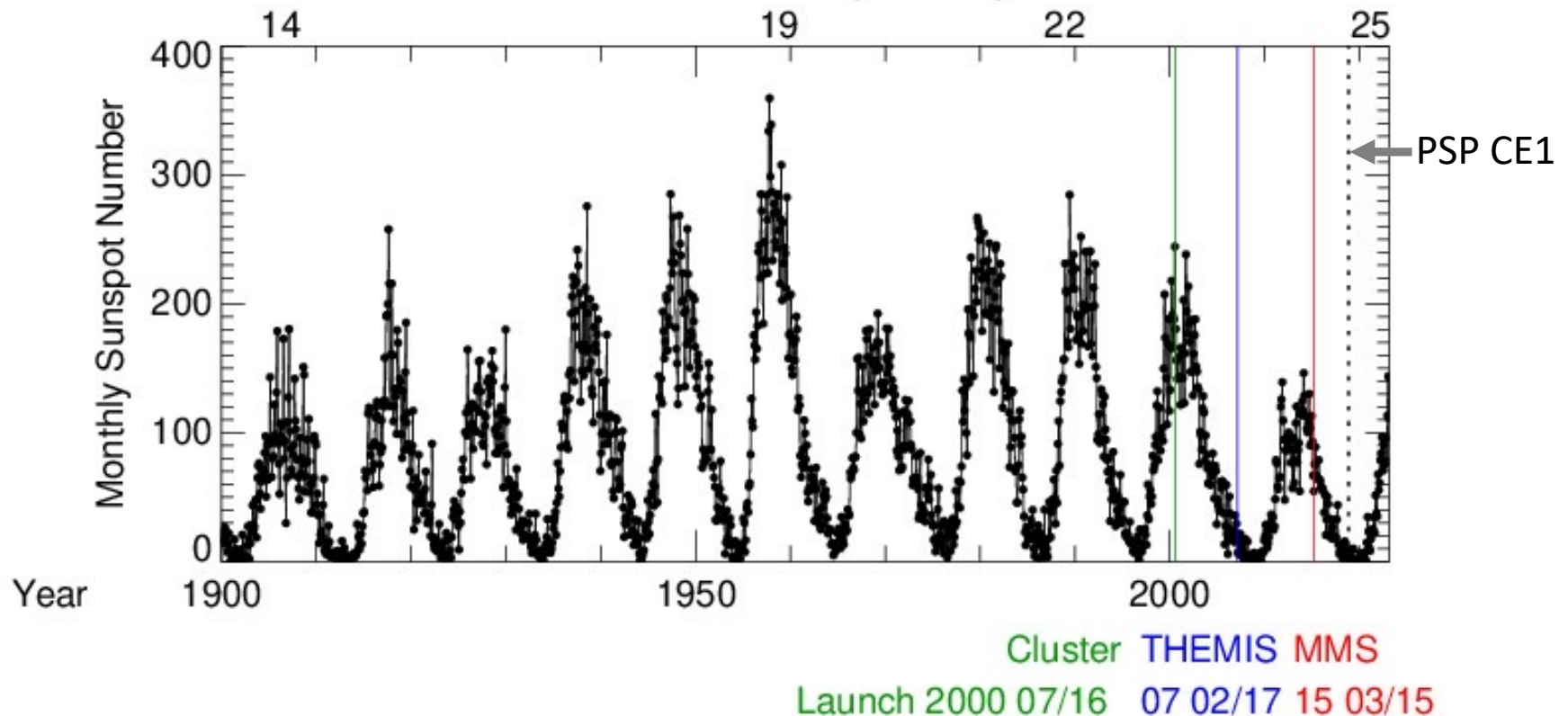
The Earth's magnetopause current layer is typically ~200-600 km thick.

[Le & Russell, The thickness and structure of high beta magnetopause current layer, *Geophys. Res. Lett.*, 1994]

Overview

- **Current sheets: Magnetic field rotations** [$J = \nabla \times B / \mu_0$] from the very wide Heliospheric Current Sheet to “narrow” M’pause
- **Multi-spacecraft missions: A brief introduction to tetrahedron formations and the Curlometer technique**
- Near-Earth space regimes & boundaries
- The magnetic reconnection process at current sheets:
 - (a) Schematic overviews, 2D vs 3D & ion (d_i) scale
 - (b) “To be or not to be” frozen-in? The G.O.L. vs Hall 😊
 - (c) Reconnection rate v_{in}/v_{out}
- Observations of Reconnection Jets:
 - (a) Cluster in the solar wind vs “timing normal” concept
 - (b) MMS at the magnetopause: J from “curlB” vs $J = Ne(V_i - V_e)$
- Summary

11-Year Sunspot Cycle



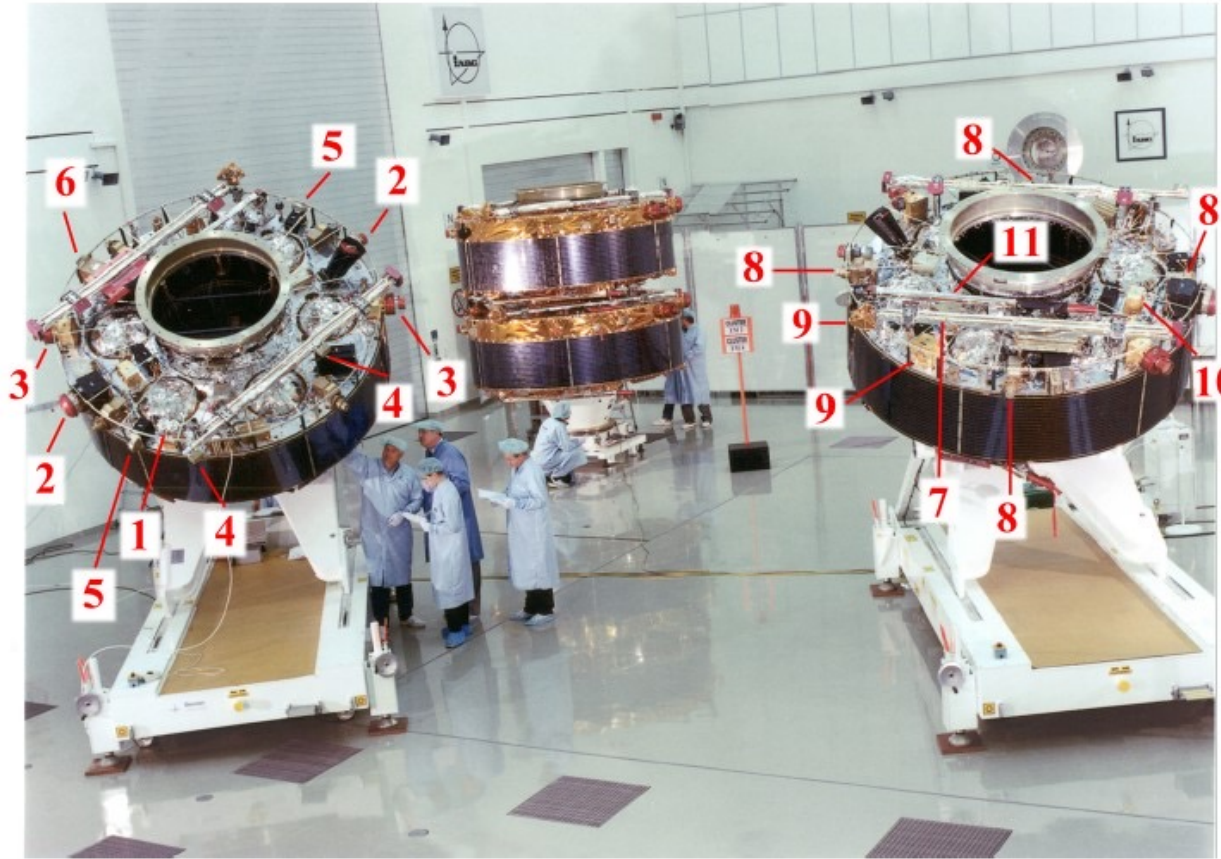
Cluster: 4 s/c - first (ion-scale) tetrahedron formation mission (ESA/NASA)

THEMIS: 5 s/c – no tetrahedron requirement (NASA)

MMS: 4 s/c – first electron-scale tetrahedron mission (NASA)

HelioSwarm: 9 s/c multi-scale turbulence mission (NASA: Launch~2028)

The four-spacecraft Cluster mission



Cluster II is an ESA space mission with NASA participation, to study the Earth's magnetosphere from a $4 \times 19.6 R_E$ elliptical orbit.

This mission is composed of four identical spacecraft flying for the very first time in a **tetrahedron formation.**

The Cluster II spacecraft launched in pairs in July and August 2000 from Baikonur, Kazakhstan.

First scientific measurements made on February 1, 2001. As of March 2023, its mission has been extended until September 2024.

Fig. 3. Position of the 11 instruments on the spacecraft. ASPOC (1), CIS (2), EDI (3), FGM (4), PEACE (5), RAPID (6), DWP (7), EFW (8), STAFF (9), WBD (10), WHISPER (11)

Escoubet et al, The Cluster mission, *Annales Geophysicae* (2001);

Escoubet et al, Recent highlights from Cluster, the first 3-D magnetospheric mission, *Ann. Geophys.* (2015)

What is a Tetrahedron?

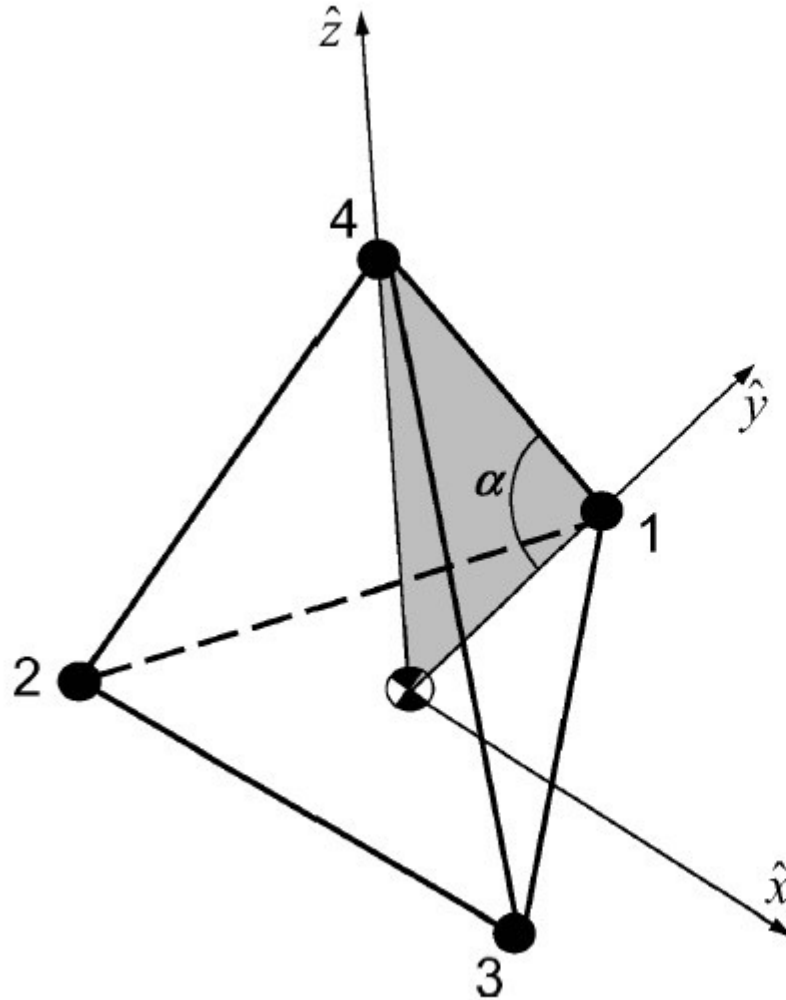


Fig. 5 Regular tetrahedron illustrating V frame and internal angle α .

What is a Tetrahedron?

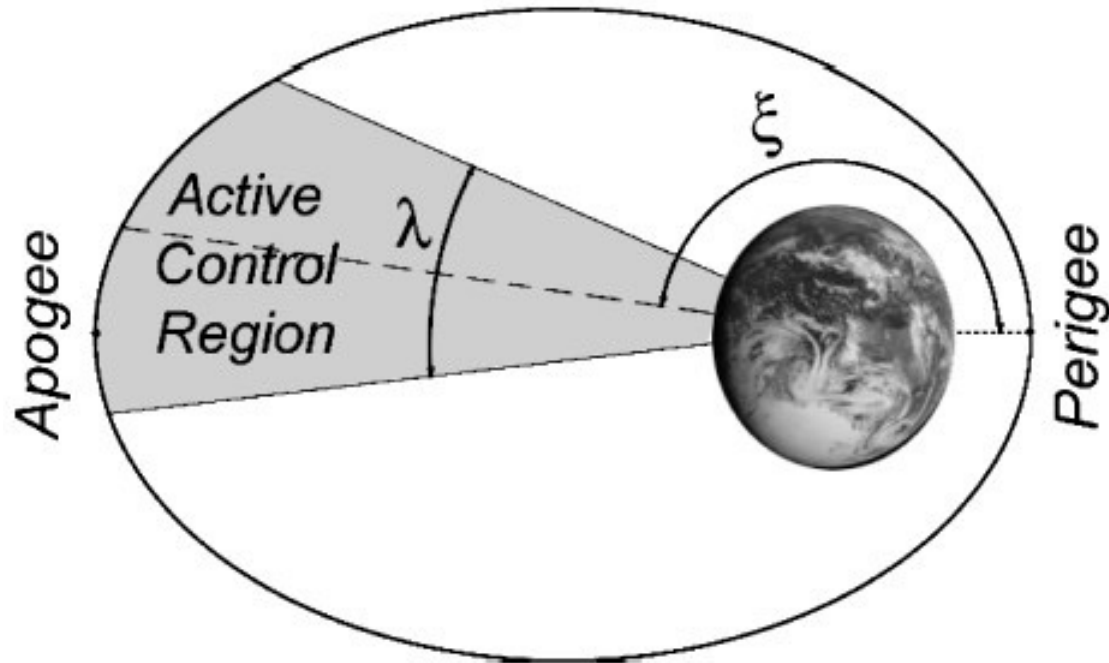


Fig. 2 Location and width of active control region for an elliptical orbit.

Why fly a Tetrahedron mission?

There is a need to know the current density (\mathbf{J}) in space due to its importance in many space plasma applications, such as magnetic reconnection.

The MMS FPI instrument measurements of electron velocity (\mathbf{V}_e at 30 ms cadence) is very high-quality, such that a local (s/c) measurement can be obtained as $\mathbf{J} = n \cdot e \cdot (\mathbf{V}_i - \mathbf{V}_e)$ at the ion cadence (interpolation of \mathbf{V}_e to \mathbf{V}_i 150-ms cadence).

However, before MMS, those high-quality measurements were not available, and the need to estimate \mathbf{J} from a tetrahedron formation, **curlometer technique** is/was crucial.

Tetrahedron allows the **gradients** of any vector/matrix to be evaluated. E.g., divergence of \mathbf{B} ($\nabla \cdot \mathbf{B} = 0$) or electron pressure tensor ($\nabla \cdot \mathbf{P}_e$).

The Curlometer Technique

At low frequencies (much less than the plasma frequency) the electrical current density and the magnetic flux vector in a plasma are related by Ampere's law,

$$\mu_0 \mathbf{J} = \text{Curl } \mathbf{B} \quad (1)$$

For a cartesian coordinate system, for instance, taking the z component of the equation yields

$$\frac{\partial B_x}{\partial y} - \frac{\partial B_y}{\partial x} = \mu_0 J_z \quad (2)$$

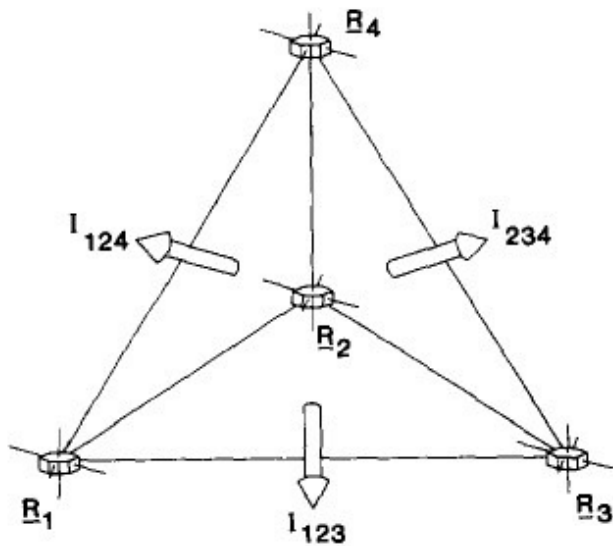


Fig. 1: The CLUSTER spacecraft tetrahedron.

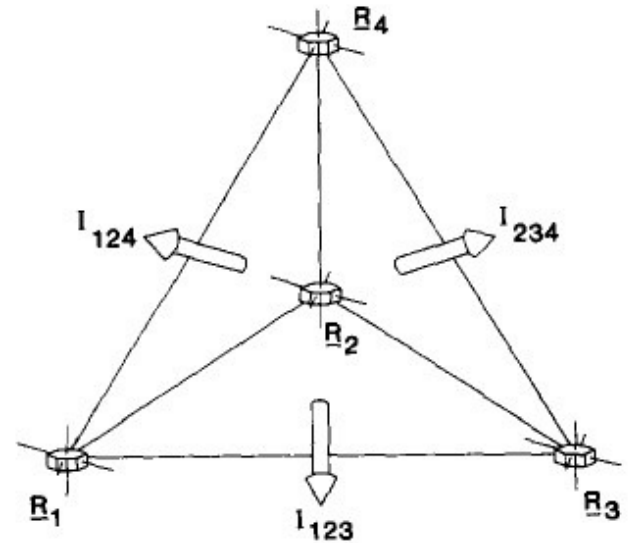
A typical configuration of the CLUSTER spacecraft is depicted in Figure 1. In general the tetrahedron formed will not be regular. Each spacecraft measures a time series of \mathbf{B} at each vertex of the tetrahedron. The vector separation of spacecraft i and j is $\Delta \mathbf{R}_{ij}$ and the vector field difference between the spacecraft is $\Delta \mathbf{B}_{ij}$. One can produce difference estimates for each component of \mathbf{J} so long as a least three of the separation vectors are linearly independent as follows.

It is useful to have a procedure for current calculation that is coordinate-independent. The integral definition of the **curl** \mathbf{B} , arising from Stokes' theorem, gives

The Curlometer Technique

$$\mu_0 \mathbf{J} \cdot (\Delta \mathbf{R}_i \times \Delta \mathbf{R}_j) = \Delta \mathbf{B}_i \cdot \Delta \mathbf{R}_j - \Delta \mathbf{B}_j \cdot \Delta \mathbf{R}_i$$

where \mathbf{J} represents the **average current density** in the s/c volume and $\Delta \mathbf{B}_i$ is the difference in \mathbf{B} between s/c 1 (ref s/c) and s/c $i=2,3,4$.



$\Delta \mathbf{R}_i$ is the vector separation of s/c 1 (ref s/c) and s/c $i=2,3,4$.

By cyclically taking i and j through values 2,3,4 one derives a set of three equations for three independent components of curl \mathbf{B} .

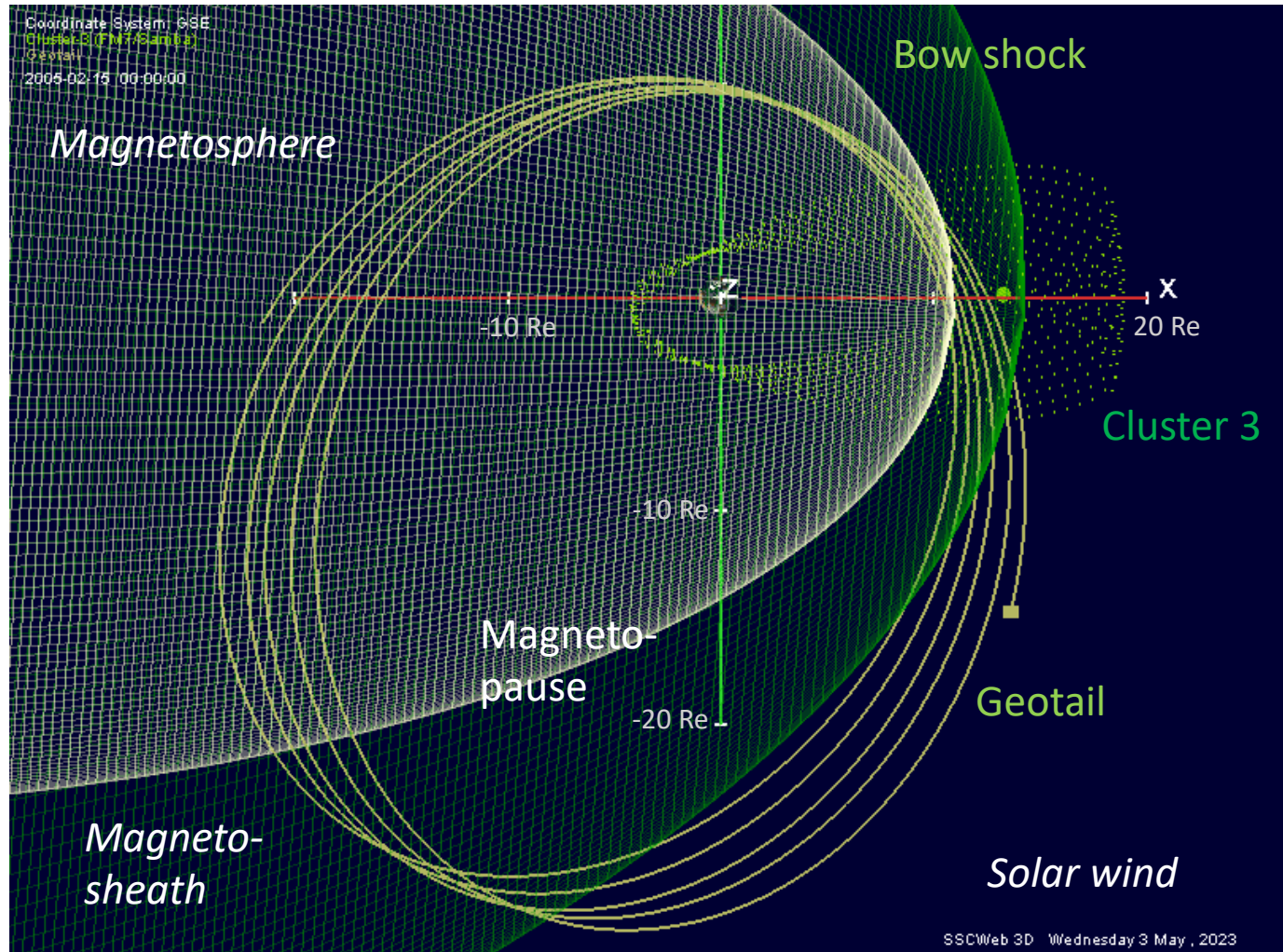
M. W. Dunlop et al., ANALYSIS OF MULTIPOINT MAGNETOMETER DATA, Adv. Space Res. Vol. 8, No. 9—10, 1988.

Dunlop, M. W., et al. (2021). Curlometer technique and applications. Journal of Geophysical Research: Space Physics, 126, e2021JA029538. <https://doi.org/10.1029/2021JA029538>

Overview

- *Current sheets: Magnetic field rotations [$J = \nabla \times B / \mu_0$] from the very wide Heliospheric Current Sheet to “narrow” M’pause*
- *Multi-spacecraft missions: A brief introduction to tetrahedron formations and the Curlometer technique*
- **Near-Earth space regimes & boundaries**
- The magnetic reconnection process at current sheets:
 - (a) *Schematic overviews, 2D vs 3D & ion (d_i) scale*
 - (b) *“To be or not to be” frozen-in? The G.O.L. vs Hall 😊*
 - (c) *Reconnection rate v_{in}/v_{out}*
- Observations of Reconnection Jets:
 - (a) *Cluster in the solar wind vs “timing normal” concept*
 - (b) *MMS at the magnetopause: J from “curlB” vs $J = Ne(V_i - V_e)$*
- Summary

The four-spacecraft Cluster mission: Orbit configurations



2005-02-15 to 2005-03-15: $4.0 \times 19.6 R_E$

Near-Earth Space Plasma Boundaries

Magnetosphere (A):

Hot and tenuous plasma in the Earth's geomagnetic field

Magnetopause (1):

Current density (J) boundary layer that resists ($J \times B$ force) the oncoming (shocked) solar wind plasma

Magnetosheath (B):

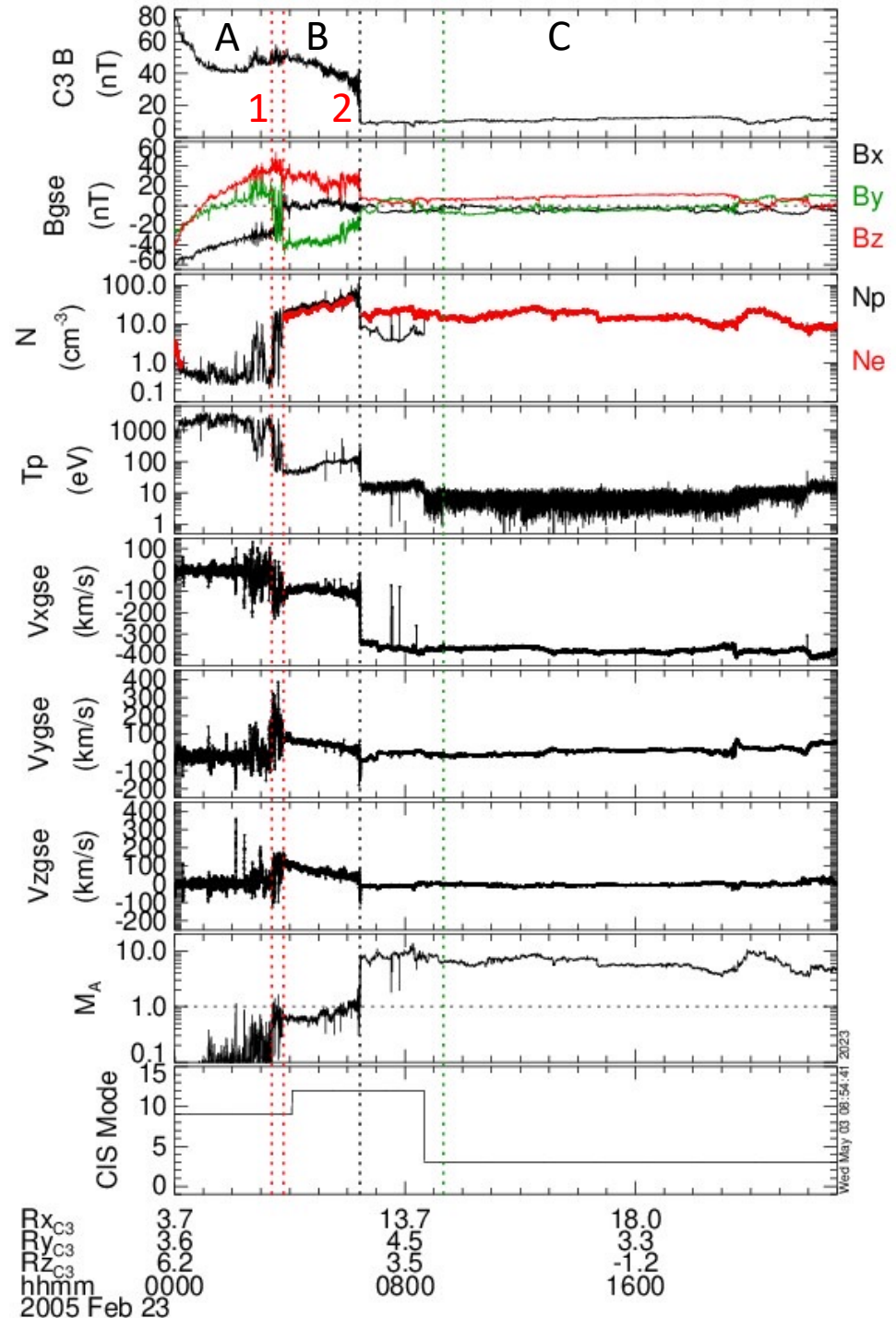
The region of turbulent and shocked ('slow') solar wind plasma

Bow shock (2):

Transition layer from super-Alfvénic ($M_A > 1$) to sub-Alfvénic ($M_A < 1$) plasma motion

Solar wind (C):

Solar origin B and $M_A > 1$ plasma streaming away from the Sun



Near-Earth Space Plasma Boundaries

Magnetosphere (A):

*Hot and tenuous plasma in
the Earth's geomagnetic field*

Magnetopause (1):

*Current density (J) boundary layer that
resists ($J \times B$ force) the oncoming (shocked)
solar wind plasma*

Magnetosheath (B):

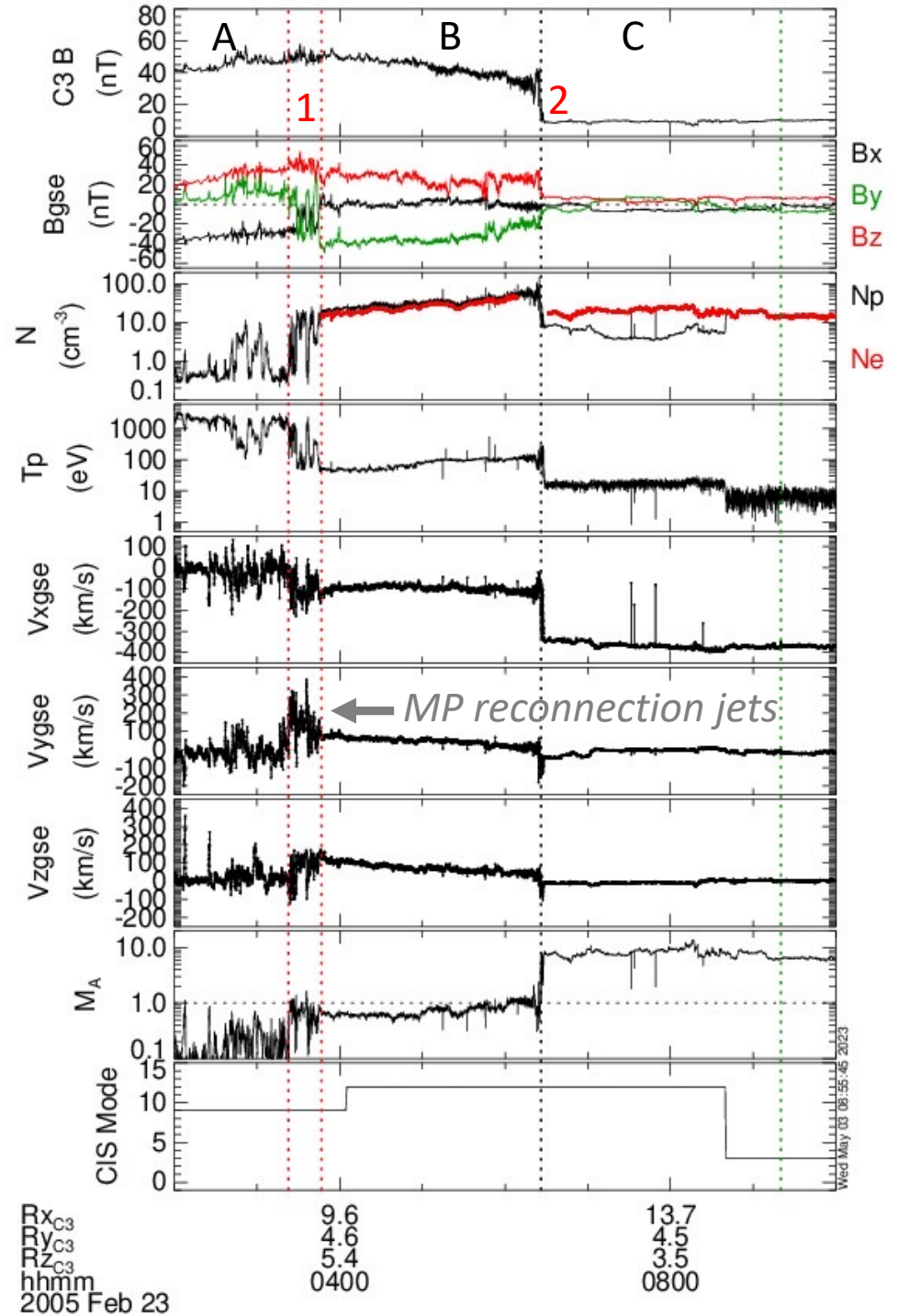
*The region of turbulent and shocked
(‘slow’) solar wind plasma*

Bow shock (2):

*Transition layer from super-Alfvénic ($M_A > 1$)
to sub-Alfvénic ($M_A < 1$) plasma motion*

Solar wind (C):

*Solar origin B and $M_A > 1$ plasma
streaming away from the Sun*

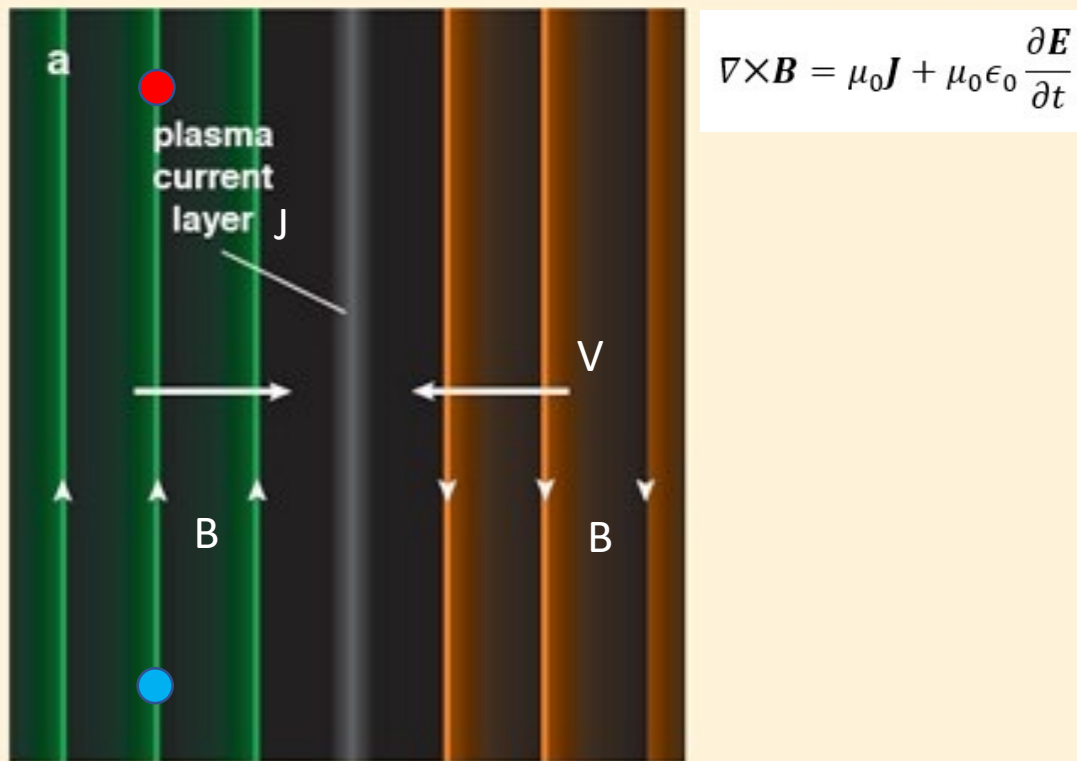


Overview

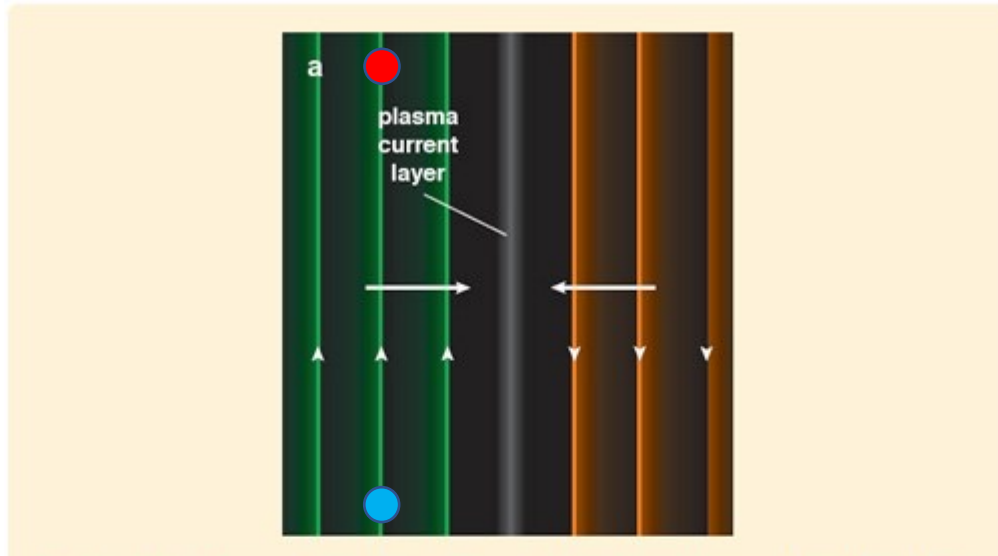
- **Current sheets: Magnetic field rotations** [$J = \nabla \times B / \mu_0$] from the very wide Heliospheric Current Sheet to “narrow” M’pause
- **Multi-spacecraft missions: A brief introduction to tetrahedron formations and the Curlometer technique**
- **Near-Earth space regimes & boundaries**
- **The magnetic reconnection process at current sheets:**
 - (a) **Schematic overviews, 2D vs 3D & ion (di) scale**
 - (b) “To be or not to be” frozen-in? The G.O.L. vs Hall 😊
 - (c) Reconnection rate v_{in}/v_{out}
- **Observations of Reconnection Jets:**
 - (a) Cluster in the solar wind vs “timing normal” concept
 - (b) MMS at the magnetopause: J from “curlB” vs $J = Ne(V_i - V_e)$
- **Summary**

Magnetic Reconnection at Current Sheets

- **Ideal MHD:** frozen-in field lines – “At its simplest, the *frozen-in-field-line theorem* states that if two fluid elements lie on a common field line at one time, then they lie on a common field line at all times past and future.” [*Principles of Heliophysics, p55*]

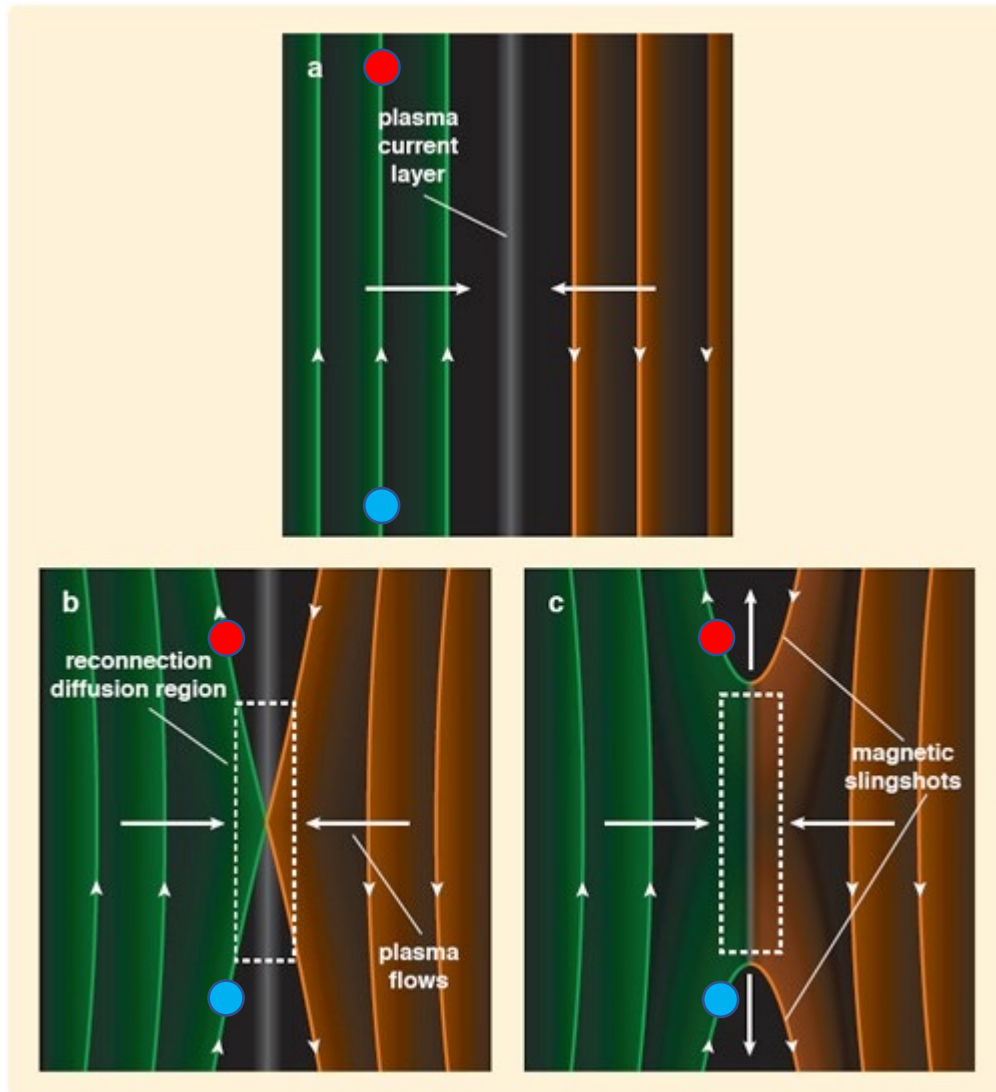


Magnetic Reconnection at Current Sheets



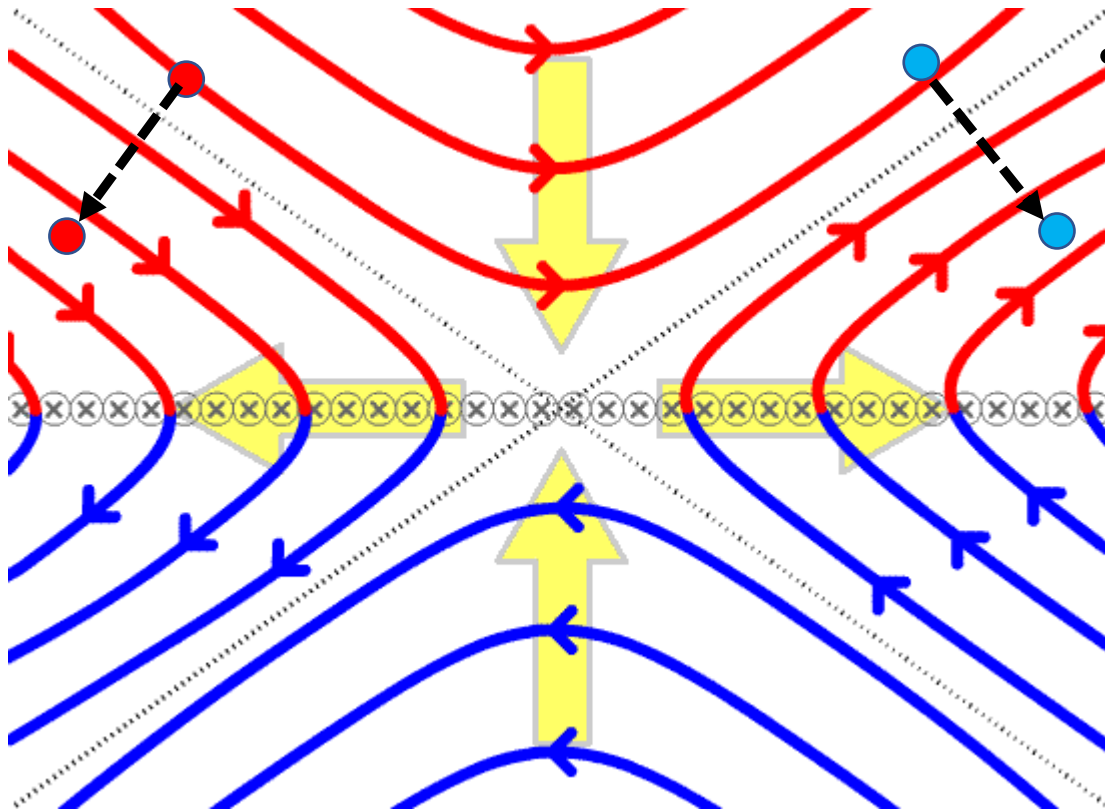
- “Failure of the “field-line” concept ... is captured by the term *reconnection* ... this term can be used to refer to the **changing connectivity** in a vacuum potential field ...or... the **decoupling of particle motions from the background magnetic field** ... we can say that **reconnection occurs whenever the approximation of frozen-in flux fails.**”

Magnetic Reconnection at Current Sheets



- “Failure of the “field-line” concept ... is captured by the term *reconnection* ... this term can be used to refer to the **changing connectivity** in a vacuum potential field ...or... the **decoupling of particle motions from the background magnetic field** ... we can say that **reconnection occurs whenever the approximation of frozen-in flux fails.**”

Magnetic Reconnection at Current Sheets



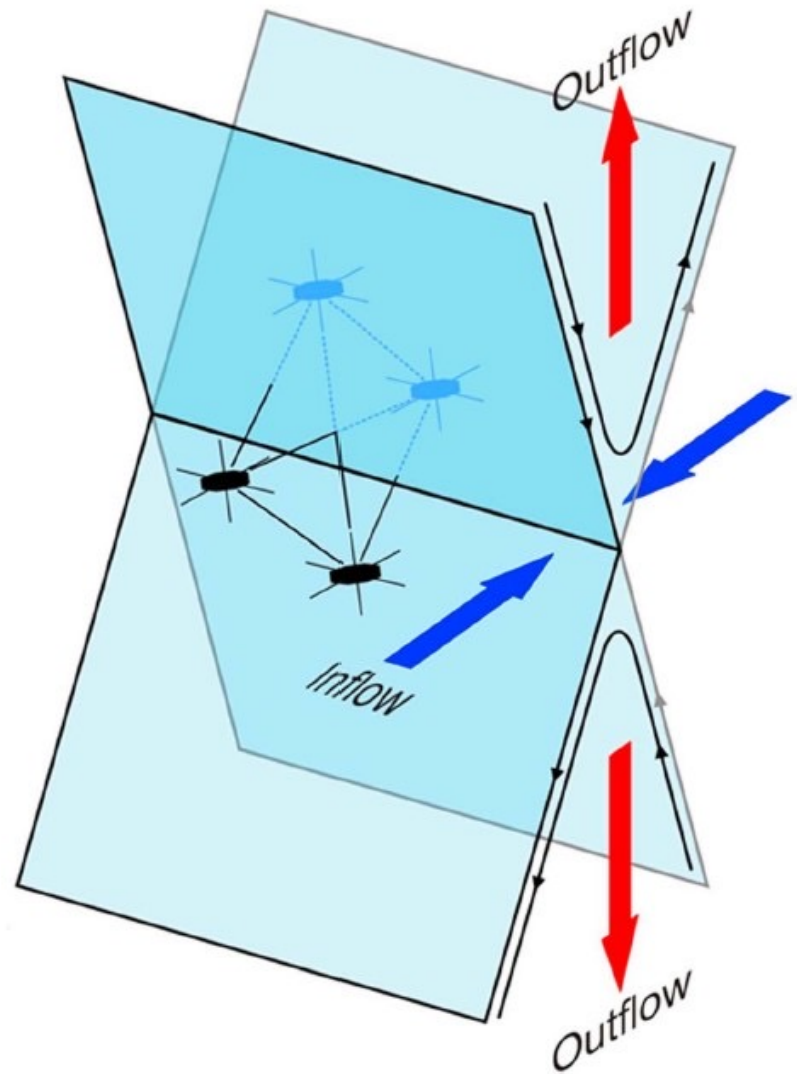
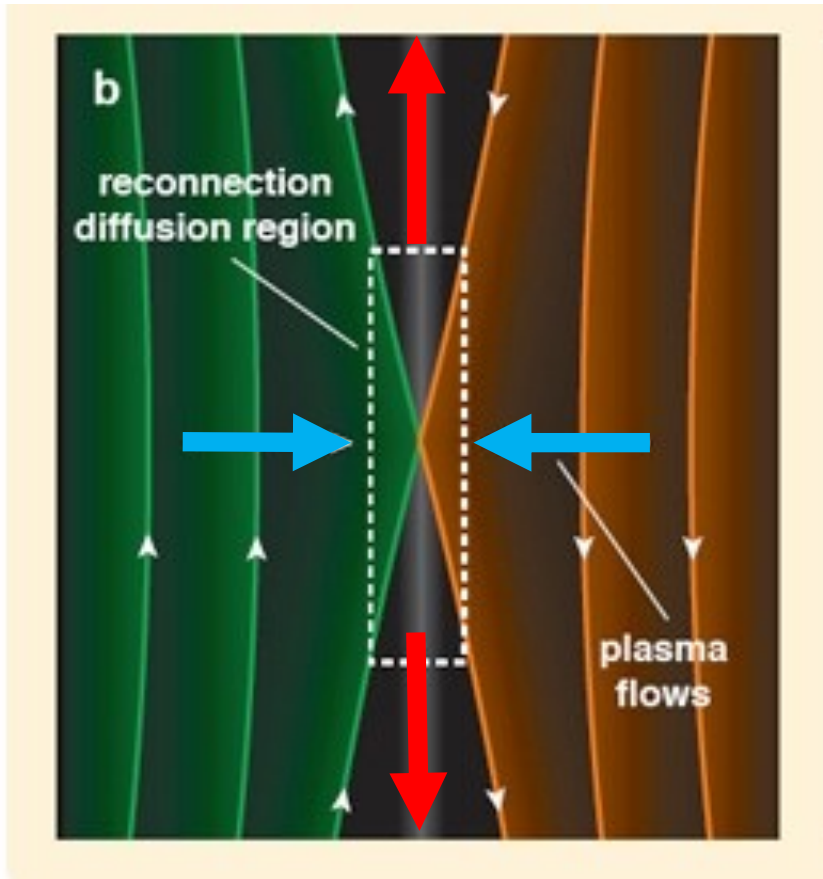
Particles “frozen-in” with a magnetic field (\mathbf{B}) gyrate about it. When \mathbf{B} moves, then particles move along with it at the $\mathbf{V} = (\mathbf{E} \times \mathbf{B})/B^2$ drift (yellow arrows).

In this case, there must be an electric field $\mathbf{E} = -\mathbf{V} \times \mathbf{B}$ pointing out of the plane.

“Failure of the “field-line” concept ... is captured by the term *reconnection* ... this term can be used to refer to the **changing connectivity** in a vacuum potential field ...or... the **decoupling of particle motions from the background magnetic field** ... we can say that **reconnection occurs whenever the approximation of frozen-in flux fails.**”

2-D versus

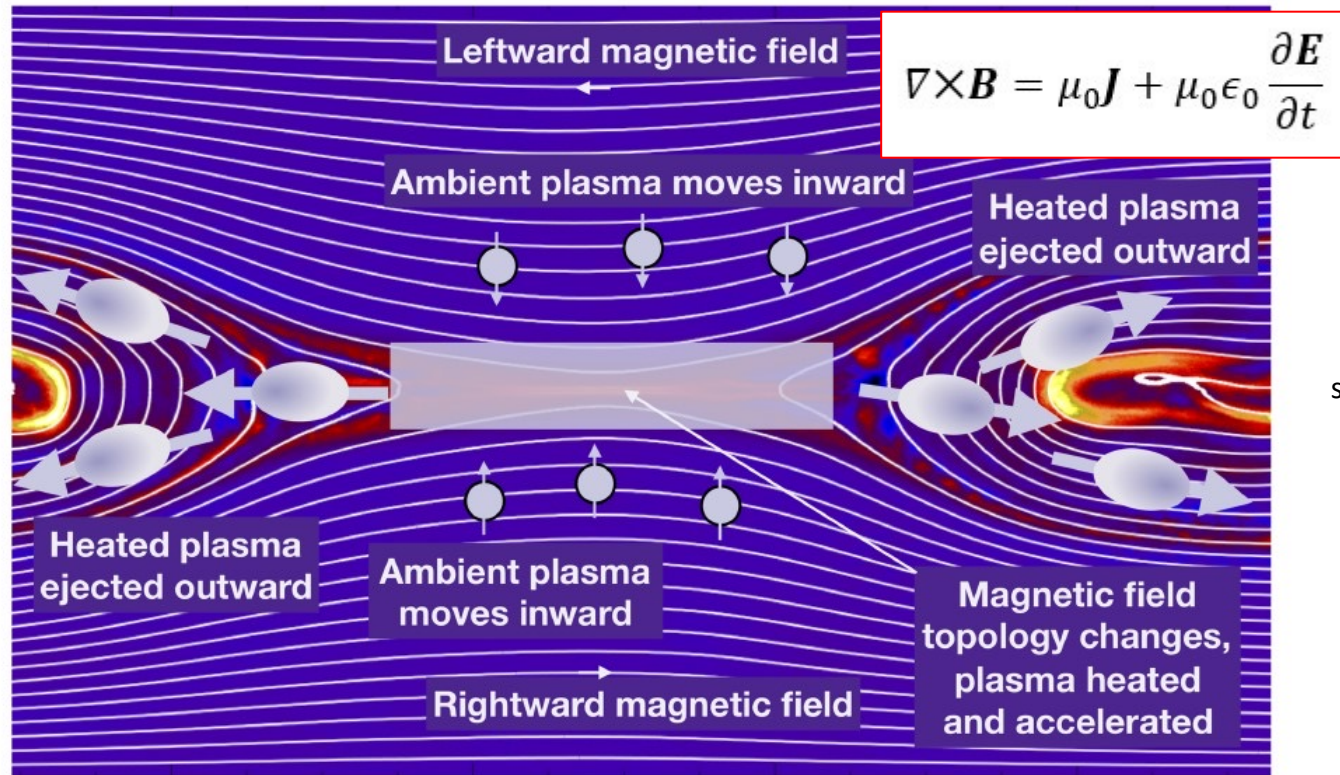
3-D



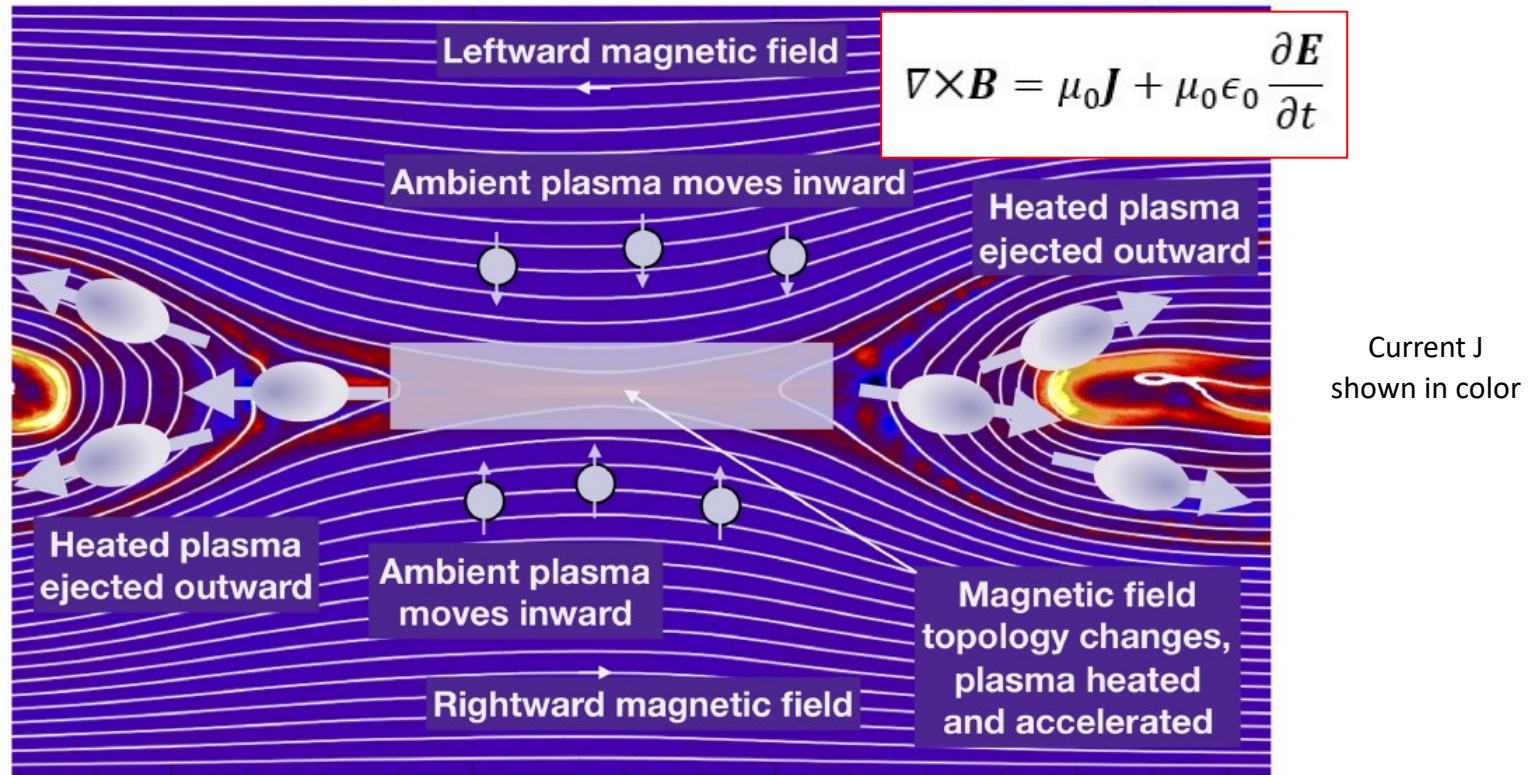
Burch, J.L., & J.F. Drake (2009). Reconnecting Magnetic Fields, American Scientist, Sept-Oct., vol. 97, number 5, doi:10.1511/2009.80.392

Gross, N. A., and W. J. Hughes (2015), A Decade of Questions About Magnetic Reconnection, Space Weather, 13, 606–610, doi:10.1002/2015SW001220

Magnetic Reconnection at Current Sheets



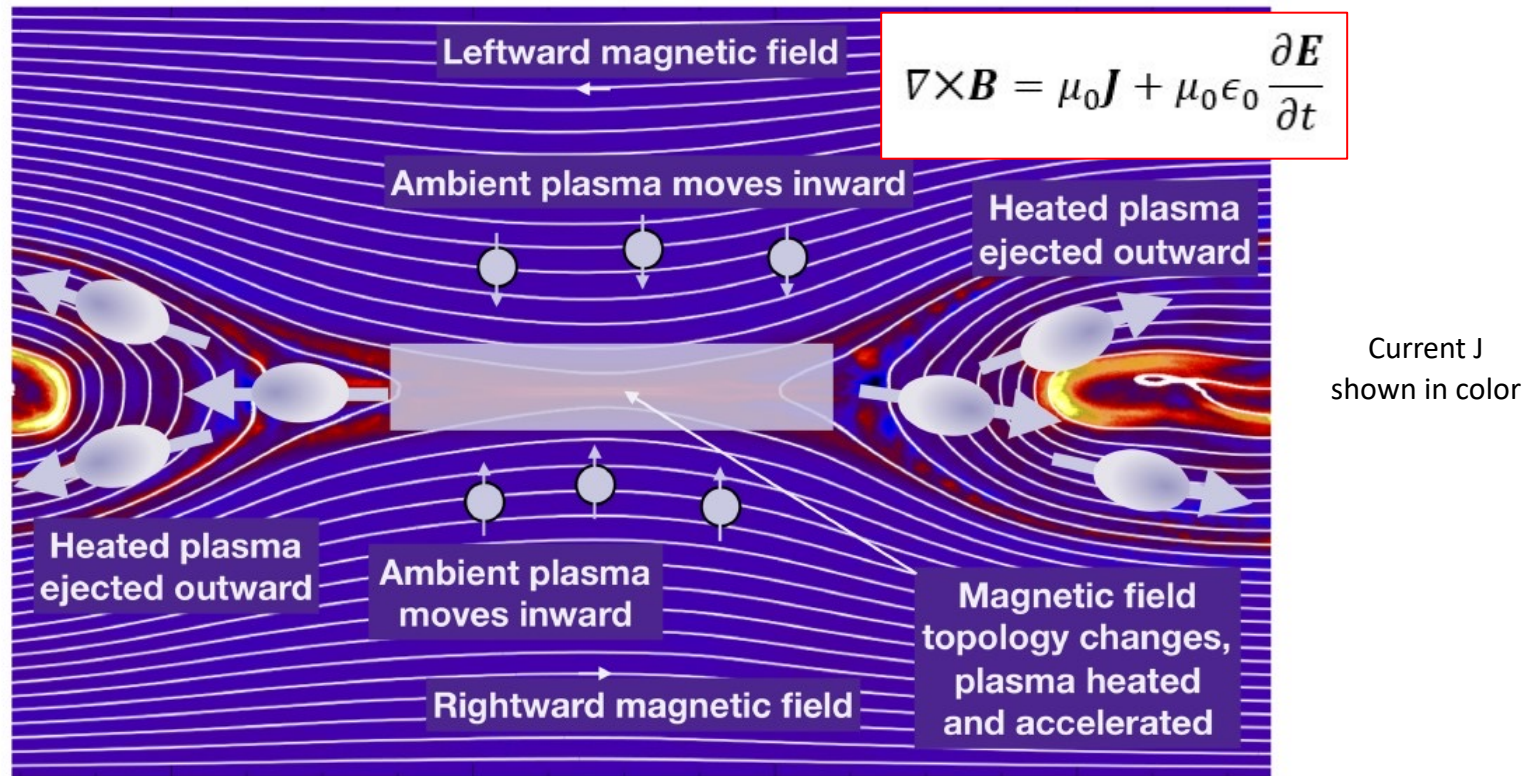
Magnetic Reconnection at Current Sheets



Reconnection diffusion region* is where the charged particles (i and e) are no longer “frozen-in” to \mathbf{B} , or $\mathbf{E} \neq -\mathbf{v} \times \mathbf{B}$ and the full particle motion is not a simple gyration about \mathbf{B}

* It is really a *finite volume of space* – not an “X-point” or “X-line” per se.

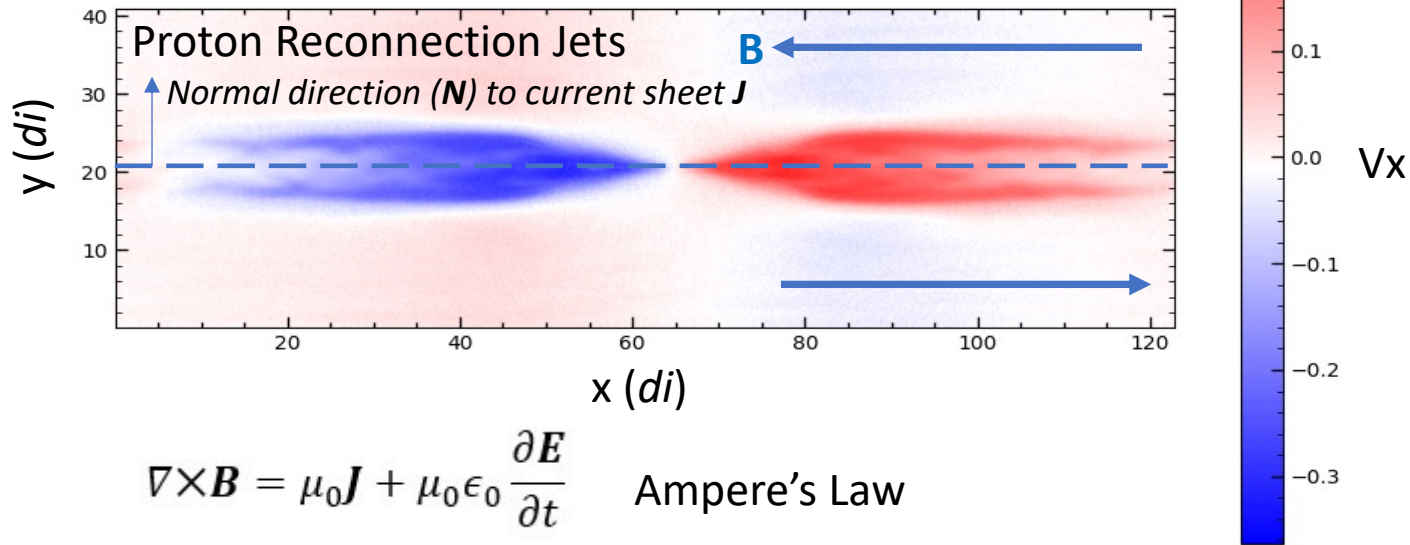
Magnetic Reconnection at Current Sheets



Reconnection jet regions: Newly reconnected fields are strongly bent. This magnetic tension force acts on the plasma (left & right) and results in two plasma jet regions.

Magnetic Reconnection

Particle-In-Cell (PIC) kinetic (ion and electron) simulations



Two main approaches exist to simulate the time-evolution of a plasma due to the presence of magnetic and electric fields.

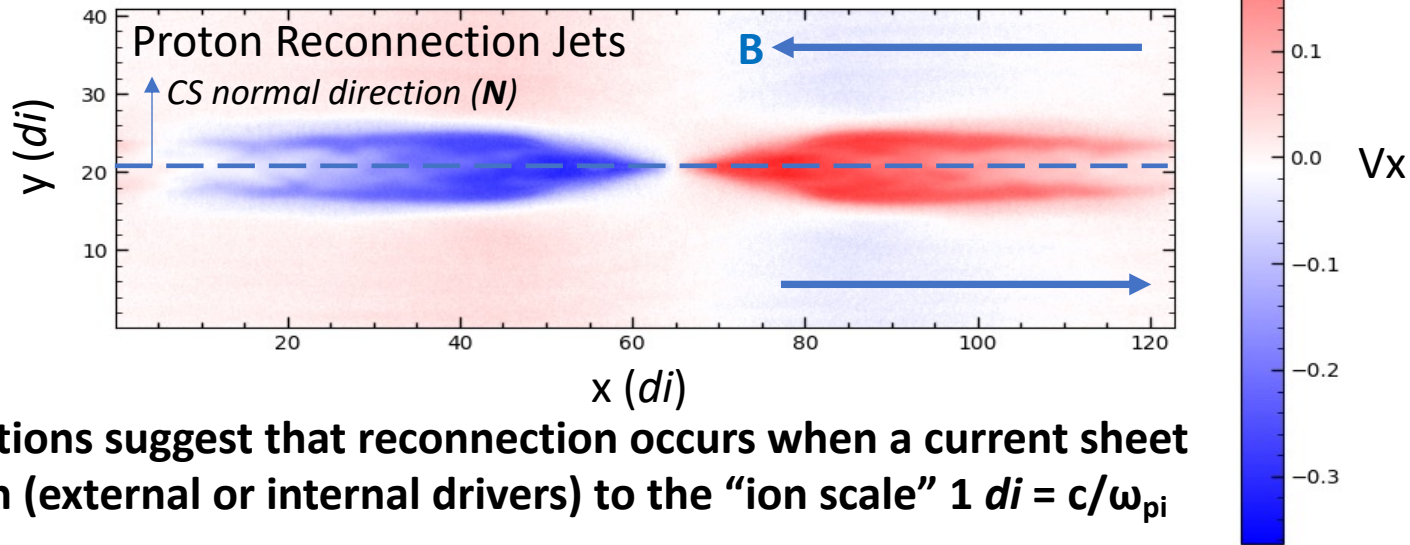
(1) Fluid methods (MHD) capture macroscopic system evolution.

Inaccuracies develop at small scales such as magnetic reconnection problem.

(2) Kinetic methods (PIC) aims to describe the full motion of ions and electrons from Maxwell's equations and the Vlasov transport equation. Often computationally expensive to use 3-D in a "big box" with full mass ratio of proton to electrons $m_p/m_e=1836$.

Magnetic Reconnection Ion Scale

PIC kinetic simulation



PIC simulations suggest that reconnection occurs when a current sheet thins down (external or internal drivers) to the “ion scale” $1 di = c/\omega_{pi}$

Here, c is speed of light and $\omega_{pi}^2 = N_p * e^2 / m_p * \epsilon_0$ is the proton plasma frequency.

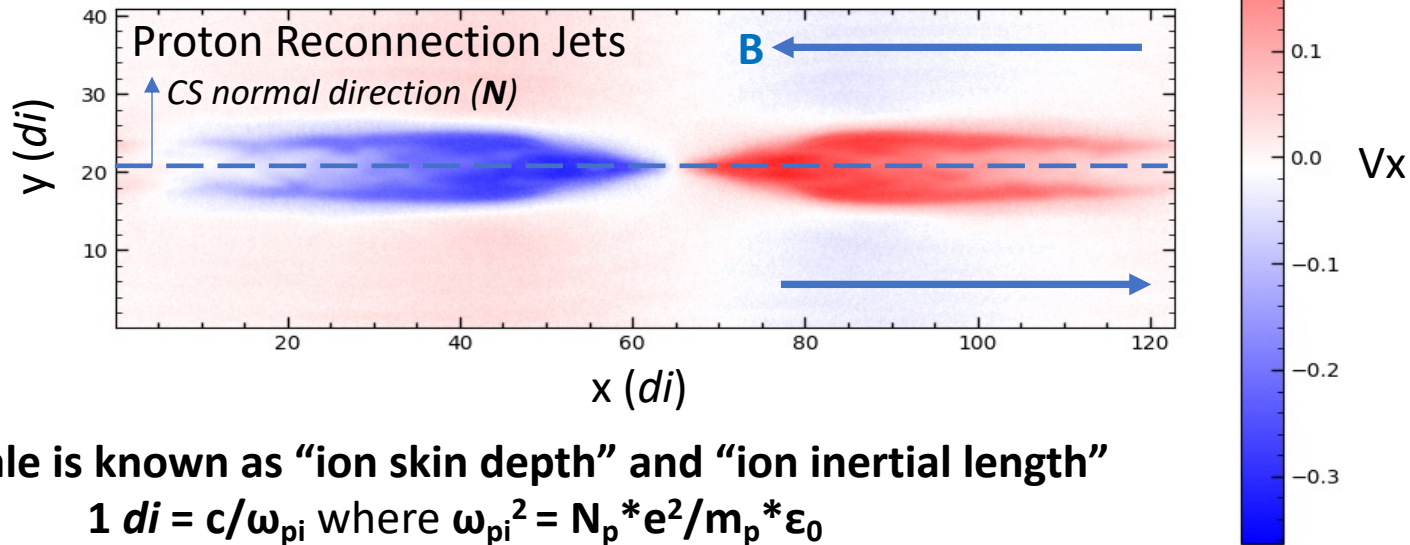
ω_{pi} is a fundamental time-scale in plasma physics. It represents a typical electrostatic oscillation frequency of a plasma in response to a local and small charge separation.

A plasma is ‘quasi-neutral’ ($N=N_i \sim N_e$) such that a given small **charge displacement \mathbf{x}** will generate an electric field $E_x = -\rho/\epsilon_0$ for a charge density $\rho = e * N * \mathbf{x}$ that will act on the charged particles to return them to their original position.

$$\text{From Newton's law: } m * d^2(\mathbf{x})/dt^2 = e * E_x = -e^2 * N * \mathbf{x} / \epsilon_0 = -m * \omega_{pi}^2 * \mathbf{x}$$

Magnetic Reconnection Ion Scale

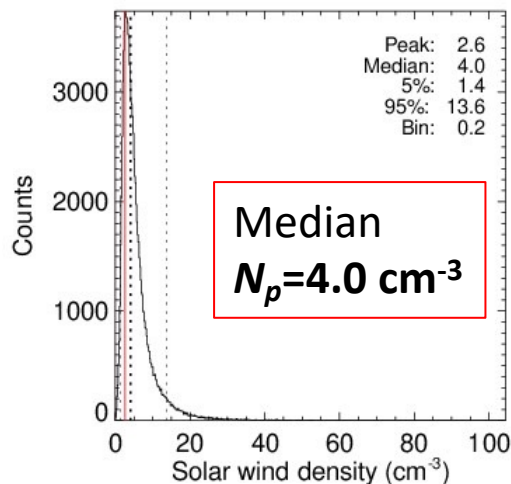
PIC kinetic simulation



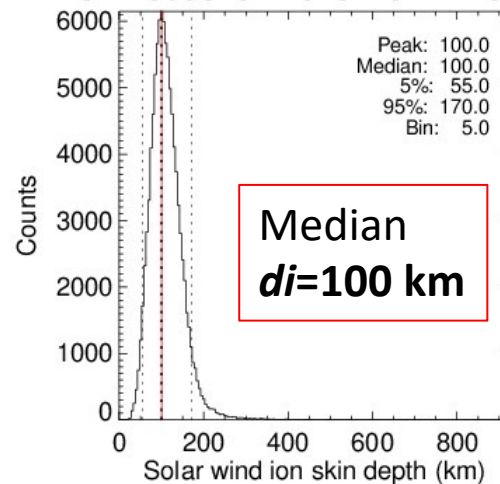
The di scale is known as “ion skin depth” and “ion inertial length”

$$1 di = c/\omega_{pi} \text{ where } \omega_{pi}^2 = N_p * e^2/m_p * \epsilon_0$$

ACE 19990101-20151231 1hr:99404



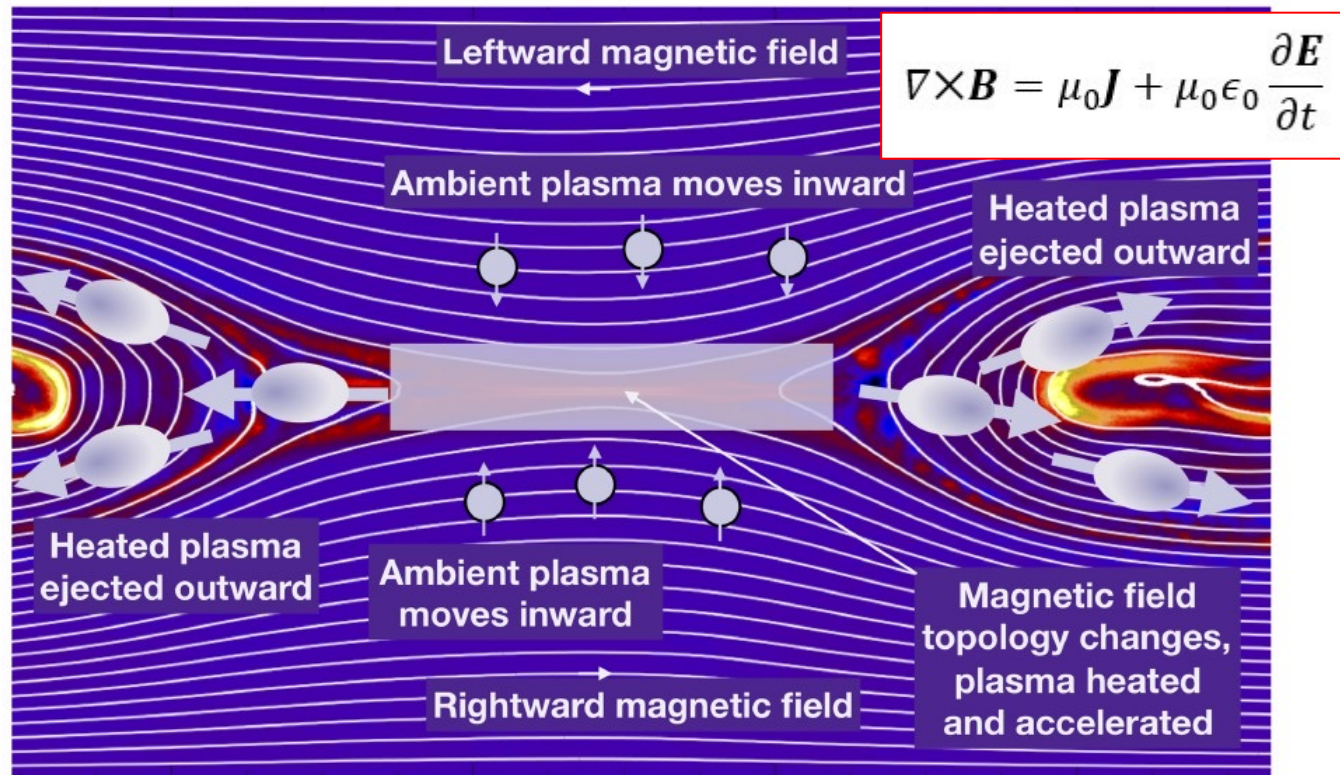
ACE 19990101-20151231 1hr:99404



Overview

- **Current sheets: Magnetic field rotations** [$J = \nabla \times B / \mu_0$] from the very wide Heliospheric Current Sheet to “narrow” M’pause
- **Multi-spacecraft missions: A brief introduction to tetrahedron formations and the Curlometer technique**
- **Near-Earth space regimes & boundaries**
- **The magnetic reconnection process at current sheets:**
 - (a) Schematic overviews, 2D vs 3D & ion (di) scale
 - (b) “To be or not to be” frozen-in? The G.O.L. vs Hall 😊
 - (c) Reconnection rate v_{in}/v_{out}
- **Observations of Reconnection Jets:**
 - (a) Cluster in the solar wind vs “timing normal” concept
 - (b) MMS at the magnetopause: J from “curlB” vs $J = Ne(V_i - V_e)$
- **Summary**

Magnetic Reconnection – G.O.L.



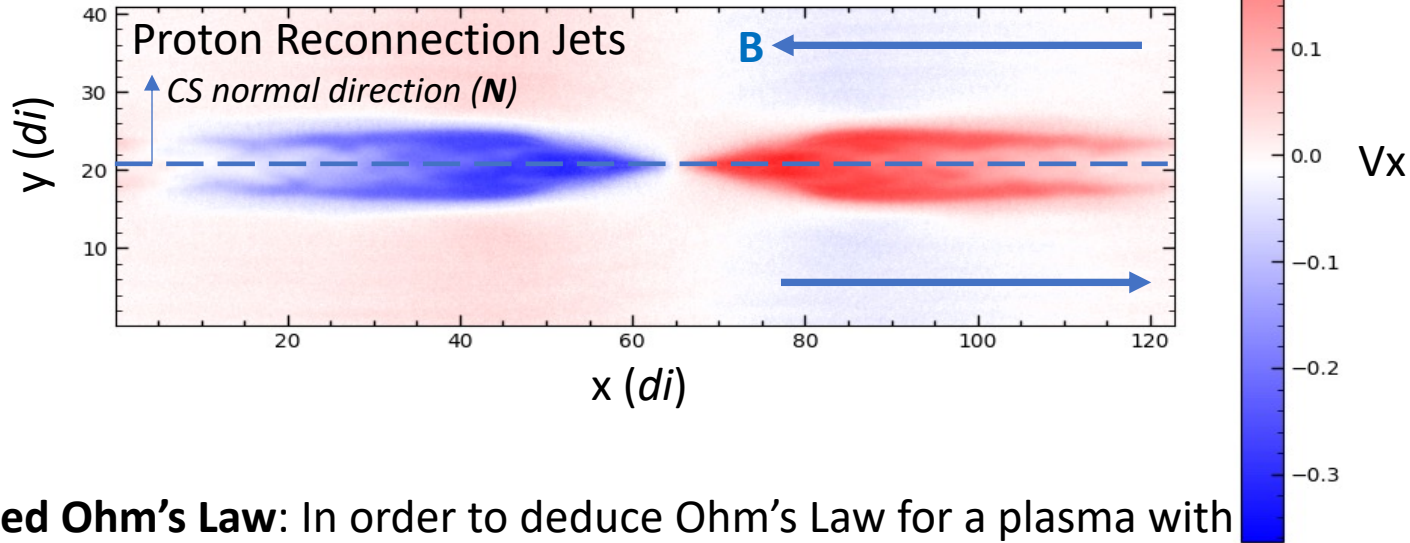
Since $\mathbf{E} = -\mathbf{v} \times \mathbf{B}$ (frozen-in condition) just outside the narrow current layer (both inflow regions), then there must be an electric field \mathbf{E} of that magnitude also inside the localized diffusion region where $\mathbf{E} \neq -\mathbf{v} \times \mathbf{B}$.

If \mathbf{E} is **not** equal to $-(\mathbf{v} \times \mathbf{B})$ there, then what supports this \mathbf{E} locally?

We must explore the *particle motions and the forces acting on them* in this small current layer region where the in-plane \mathbf{B} is weak (special case: $|\mathbf{B}| \ll 1$).

Magnetic Reconnection – G.O.L.

PIC kinetic simulation



Generalized Ohm's Law: In order to deduce Ohm's Law for a plasma with magnetic field \mathbf{B} , we consider at least *two equations of motion* – one each for electrons and ions - under the influence of the **forces** acting on the particles

Newton's 2nd Law of Motion for particles in collisionless plasma:

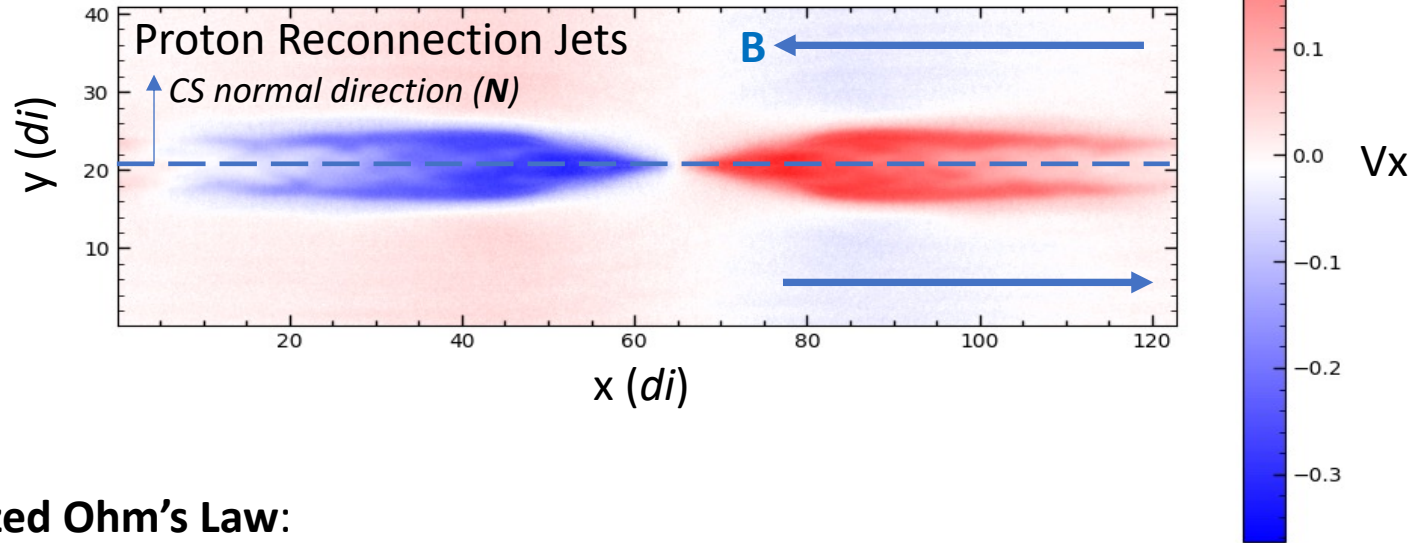
$$(1) m_e \mathbf{a}_e = \mathbf{F}_{Ee} + \mathbf{F}_{Be} - \nabla p_e / n_e + m_e \mathbf{g} \quad [\mathbf{F}_{Ee} = -e\mathbf{E} \text{ and } \mathbf{F}_{Be} = -e(\mathbf{v}_e \times \mathbf{B})]$$

$$(2) m_i \mathbf{a}_i = \mathbf{F}_{Ei} + \mathbf{F}_{Bi} - \nabla p_i / n_i + m_i \mathbf{g} \quad [\mathbf{F}_{Ei} = e\mathbf{E} \text{ and } \mathbf{F}_{Bi} = e(\mathbf{v}_i \times \mathbf{B})]$$

where $p_e = n_e k_B T_e$ and $p_i = n_i k_B T_i$ are electron and ion *scalar* pressures for an assumed isotropic plasma temperature. In anisotropic plasmas (e.g., $T_{e||} > T_{e\perp}$) $\nabla p \rightarrow \nabla \cdot \mathbf{P}$ where $\mathbf{P} = P_{ij}$ is a 3x3 pressure tensor.

Magnetic Reconnection – G.O.L.

PIC kinetic simulation



Generalized Ohm's Law:

Newton's 2nd law for a plasma with number density $n_i=n_e=n$ (quasi-neutral):

$$(1) \quad nm_e d\mathbf{v}_e/dt = -ne[\mathbf{E} + \mathbf{v}_e \times \mathbf{B}] - \nabla p_e + nm_e \mathbf{g}$$

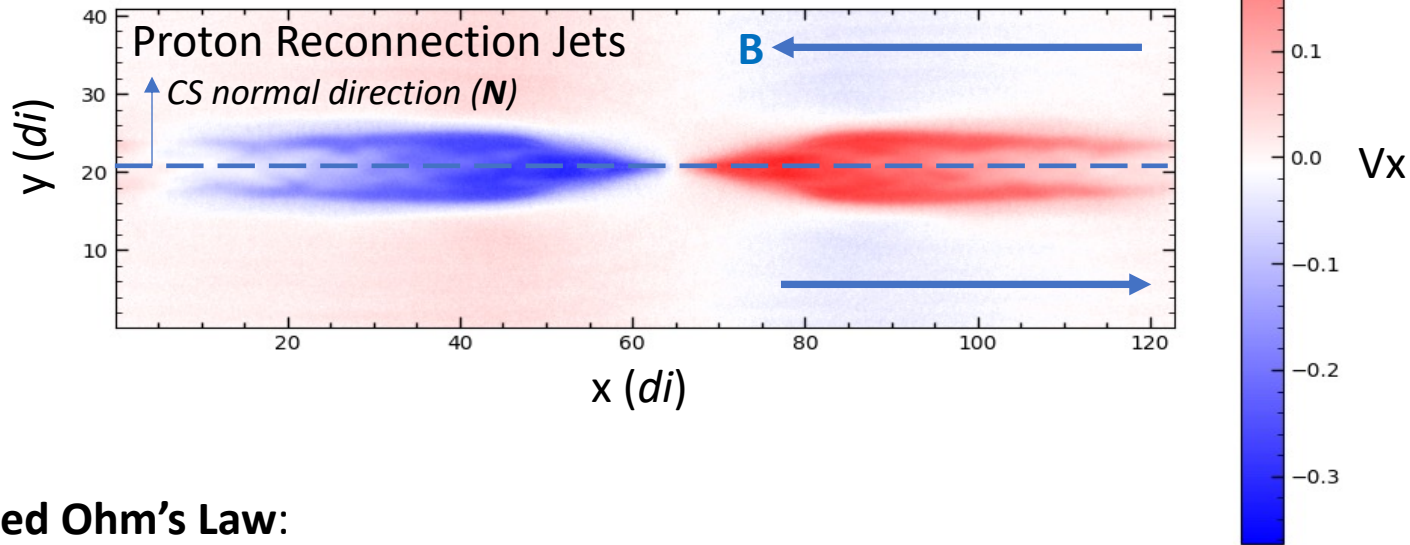
$$(2) \quad nm_i d\mathbf{v}_i/dt = ne[\mathbf{E} + \mathbf{v}_i \times \mathbf{B}] - \nabla p_i + nm_i \mathbf{g}$$

Adding (1) + (2) using mass density $\rho=n(m_i+m_e)$, momentum $\rho\mathbf{v}=n(m_i\mathbf{v}_i+m_e\mathbf{v}_e)$, and current density $\mathbf{J} = ne(\mathbf{v}_i-\mathbf{v}_e)$ results in:

$$\text{Plasma Equation of Motion: } \rho d\mathbf{v}/dt = \mathbf{J} \times \mathbf{B} - \nabla p + \rho \mathbf{g}$$

Magnetic Reconnection – G.O.L.

PIC kinetic simulation



Generalized Ohm's Law:

Newton's 2nd law for a plasma with number density $n_i=n_e=n$ (quasi-neutral):

$$(1) \quad nm_e d\mathbf{v}_e/dt = -ne[\mathbf{E} + \mathbf{v}_e \times \mathbf{B}] - \nabla p_e + nm_e \mathbf{g}$$

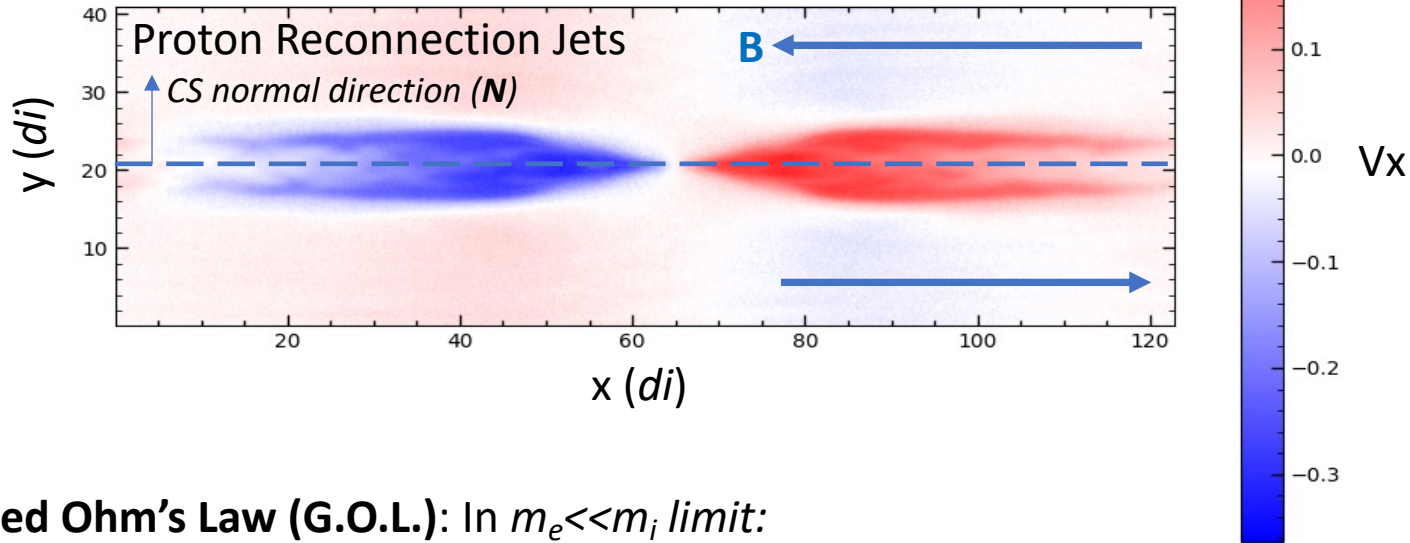
$$(2) \quad nm_i d\mathbf{v}_i/dt = ne[\mathbf{E} + \mathbf{v}_i \times \mathbf{B}] - \nabla p_i + nm_i \mathbf{g}$$

Taking (Eq2)* $m_e/(m_i n_e)$ **minus** (Eq1)* $1/ne$ **with** $\mathbf{v}_i \sim \mathbf{v}$ and $\mathbf{v}_e \sim (\mathbf{v} - \mathbf{J}/ne)$ from $\mathbf{J} = ne(\mathbf{v}_i - \mathbf{v}_e)$ [$m_e \ll m_i$ limit] results in:

$$\text{G.O.L.} \quad \mathbf{E} + \mathbf{v} \times \mathbf{B} = \mathbf{J} \times \mathbf{B}/ne - [\nabla p_e - m_e \nabla p_i/m_i]/ne + m_e/ne^2 d\mathbf{J}/dt$$

Magnetic Reconnection – G.O.L.

PIC kinetic simulation



Generalized Ohm's Law (G.O.L.): In $m_e \ll m_i$ limit:

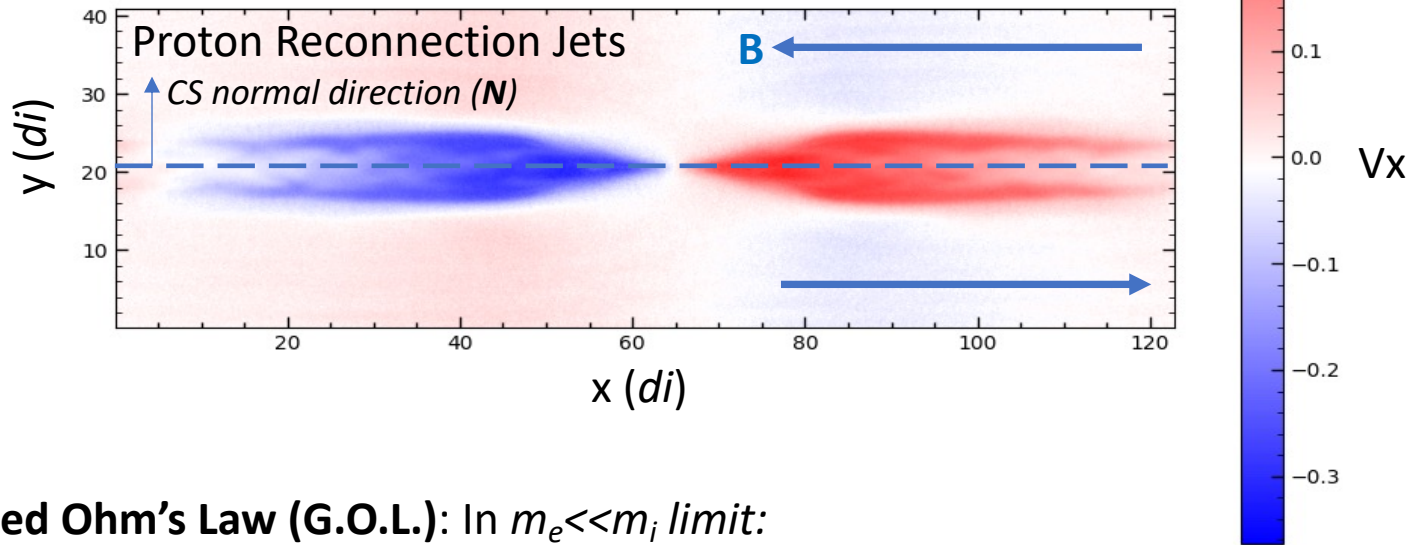
$$\text{G.O.L.} \quad \mathbf{E} + \mathbf{v} \times \mathbf{B} = \mathbf{J} \times \mathbf{B} / n_e - \nabla \cdot \mathbf{P}_e / n_e + m_e / n_e^2 d\mathbf{J} / dt \quad [\mathbf{P}_e : \text{electron pressure tensor}]$$

$$\mathbf{E}' = \text{“Hall”} - \text{“electron pressure divergence”} + \text{“electron inertia” terms}$$

In kinetic treatments of plasmas (non-MHD), the presence of a non-ideal electric field $\mathbf{E}' = \mathbf{E} + \mathbf{v} \times \mathbf{B} \neq 0$ in the frame of the moving particles ($\mathbf{v} = \mathbf{v}_i$ or $\mathbf{v} = \mathbf{v}_e$) will contribute to this violation of the “frozen-in” condition.

Magnetic Reconnection – G.O.L.

PIC kinetic simulation



Generalized Ohm's Law (G.O.L.): In $m_e \ll m_i$ limit:

$$\text{G.O.L.} \quad \mathbf{E} + \mathbf{v} \times \mathbf{B} = \mathbf{J} \times \mathbf{B} / n_e - \nabla \cdot \mathbf{P}_e / n_e + m_e / n_e^2 d\mathbf{J} / dt \quad [\mathbf{P}_e : \text{electron pressure tensor}]$$

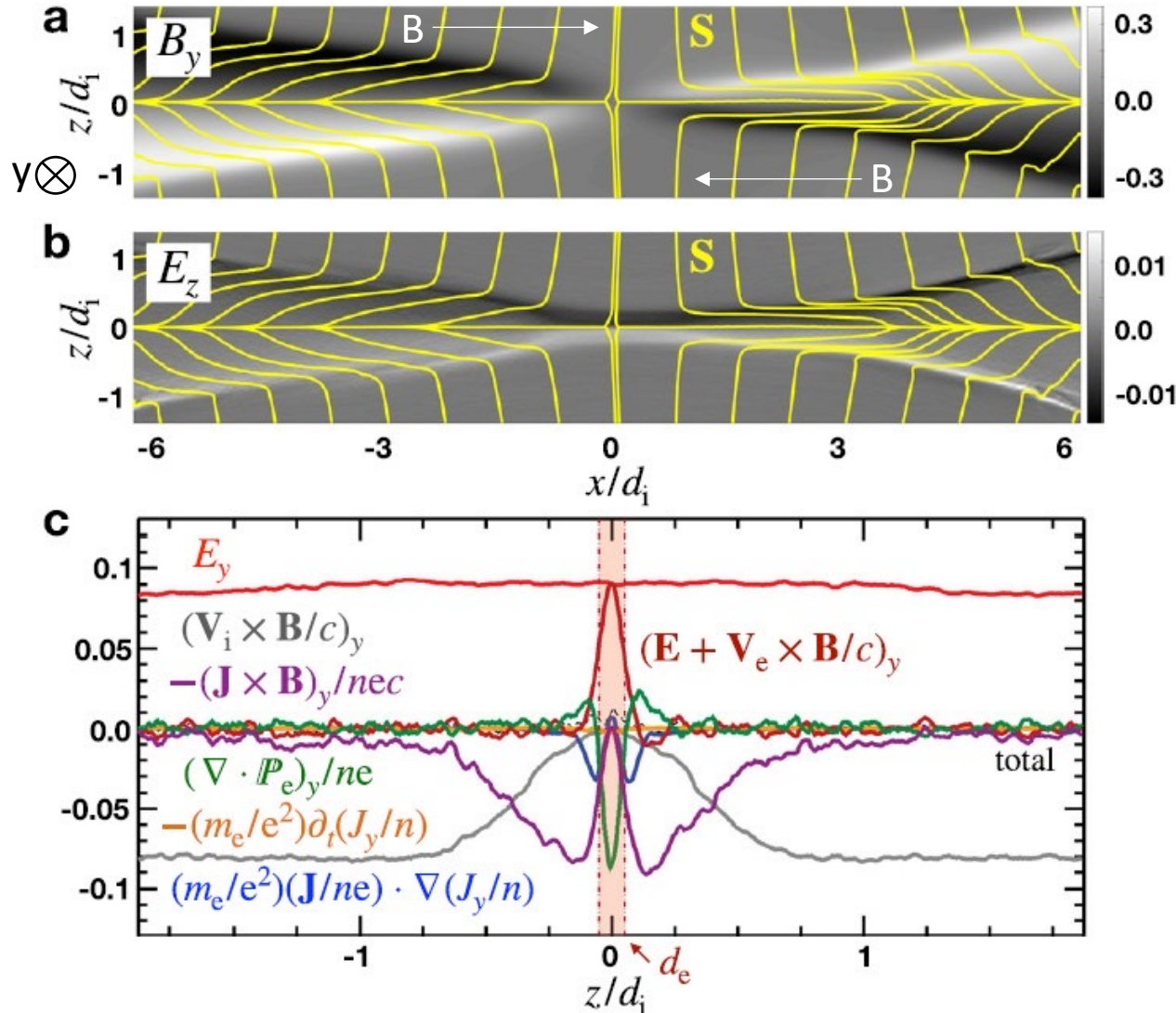
$$\mathbf{E}' = \text{“Hall”} - \text{“electron pressure divergence”} + \text{“electron inertia” terms}$$

The Objective of the MMS s/c constellation → Explore the RHS terms of G.O.L. where electron scales are crucial to measure. High measurement cadence a requirement.

Magnetic Reconnection – G.O.L. terms

Symmetric PIC simulation

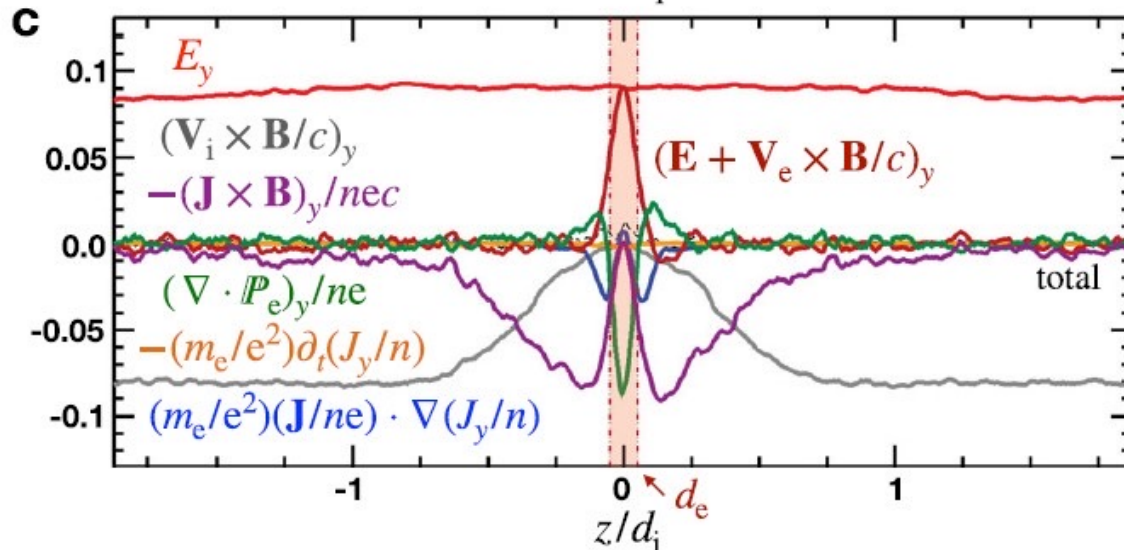
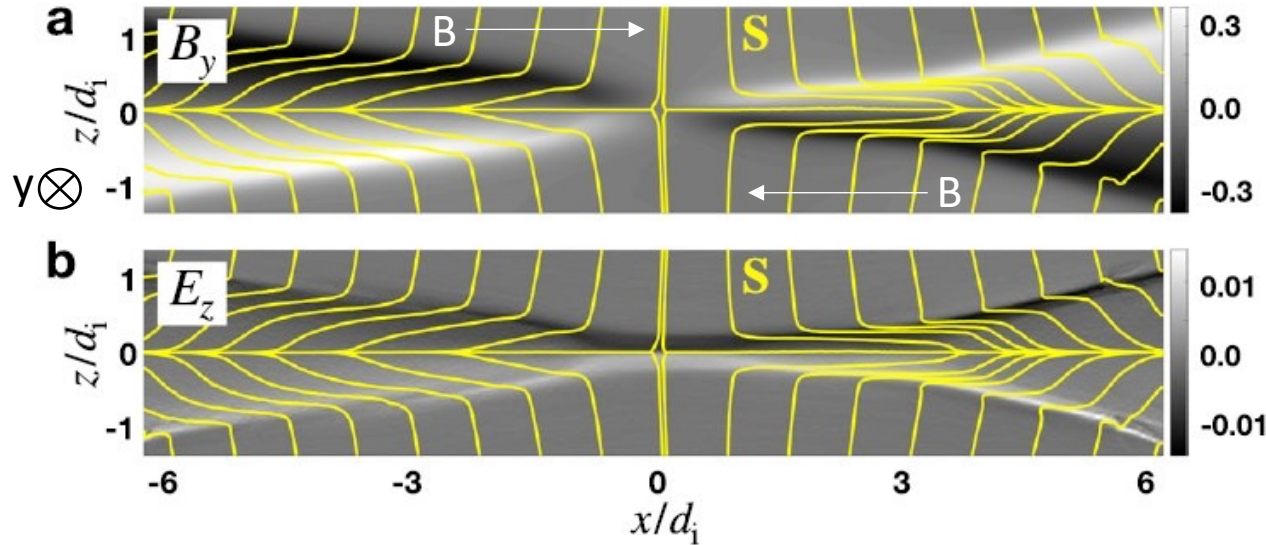
$$\mathbf{E} + \mathbf{v} \times \mathbf{B} = \mathbf{J} \times \mathbf{B} / ne - \nabla \cdot \mathbf{P}_e / ne + m_e / ne^2 d\mathbf{J} / dt$$



Magnetic Reconnection – G.O.L. terms

Symmetric PIC simulation

$$\mathbf{E} + \mathbf{v} \times \mathbf{B} = \mathbf{J} \times \mathbf{B} / ne - \nabla \cdot \mathbf{P}_e / ne + m_e / ne^2 d\mathbf{J} / dt$$



Note on scales:

$$m_p / m_e = 1836$$

$$d_e = c / \omega_{pe}$$

$$d_i = d_e * \text{SQRT}(m_p / m_e) \sim 43 * d_e$$

Example solar wind:

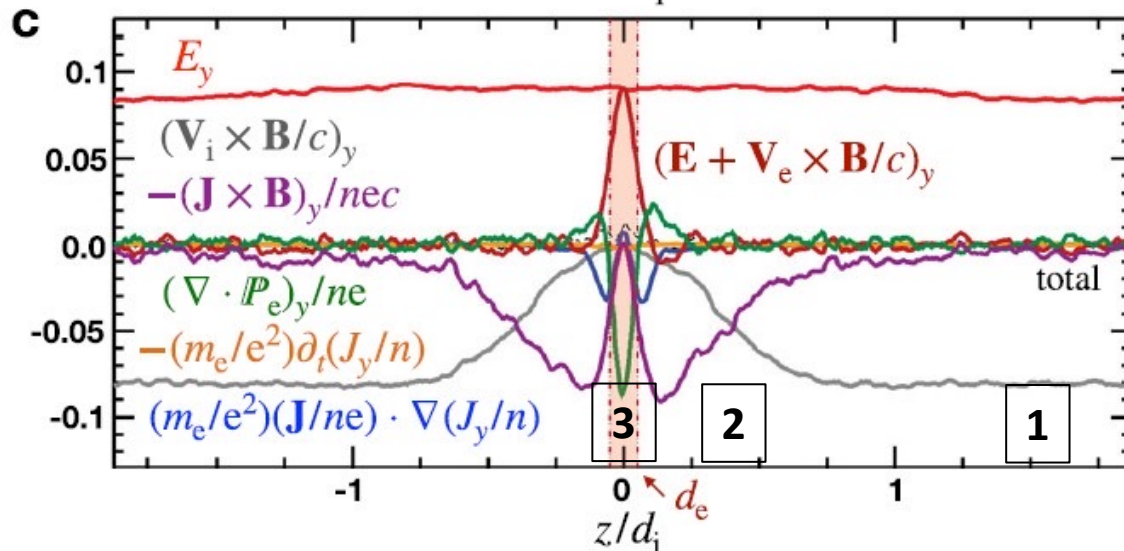
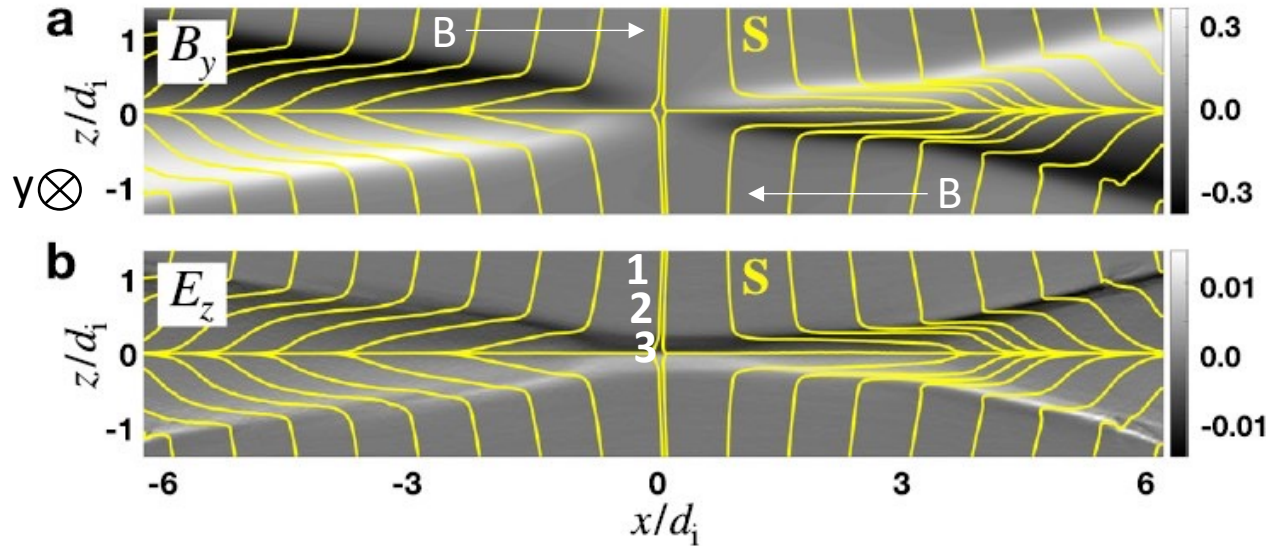
$$d_i = 100 \text{ km}$$

$$d_e = 2.3 \text{ km}$$

Magnetic Reconnection – 3 Regions

Symmetric PIC simulation

$$\mathbf{E} + \mathbf{v} \times \mathbf{B} = \mathbf{J} \times \mathbf{B} / ne - \nabla \cdot \mathbf{P}_e / ne + m_e / ne^2 d\mathbf{J} / dt$$



1. Upstream Inflow Region

$$\mathbf{E} = -\mathbf{V}_i \times \mathbf{B}$$

Plasma ExB inflow

i & e “frozen-in” to B

2. Ion Diffusion Region

$$\mathbf{E} + \mathbf{V}_i \times \mathbf{B} = \mathbf{J} \times \mathbf{B} / ne$$

i “de-coupled” & e “frozen-in”

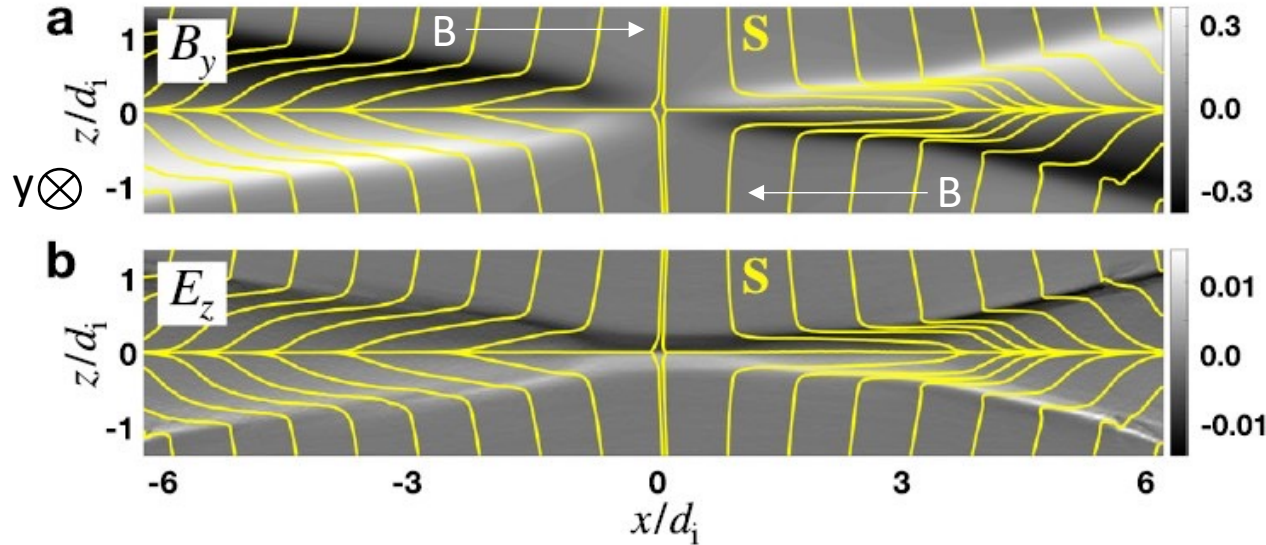
3. Electron Diffusion Region

$$\mathbf{E} + \mathbf{V}_e \times \mathbf{B} = -\nabla \cdot \mathbf{P}_e / ne$$

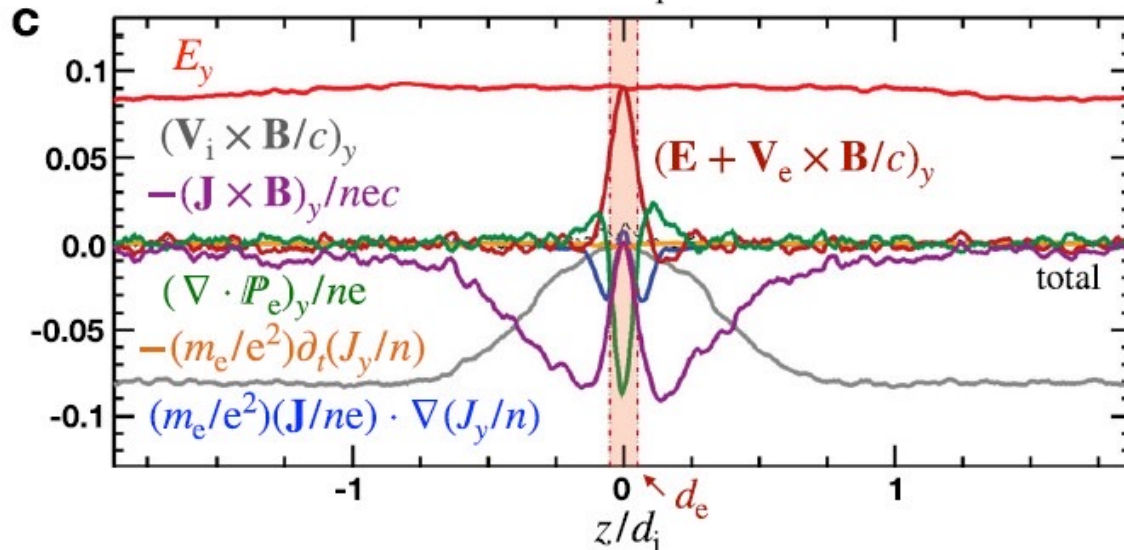
i & e “de-coupled”

Magnetic Reconnection – Hall E

Symmetric PIC simulation

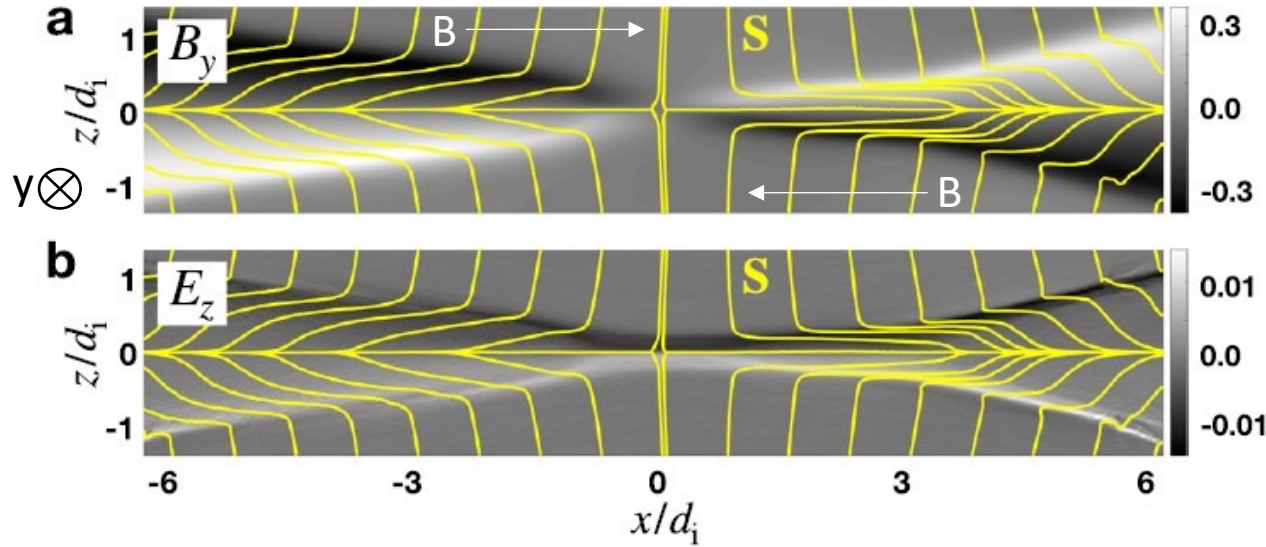


Since electrons decouple from \mathbf{B} closer to the current layer than ions, an inward (E_z) polarization electric field is generated that prevents a large charge separation.

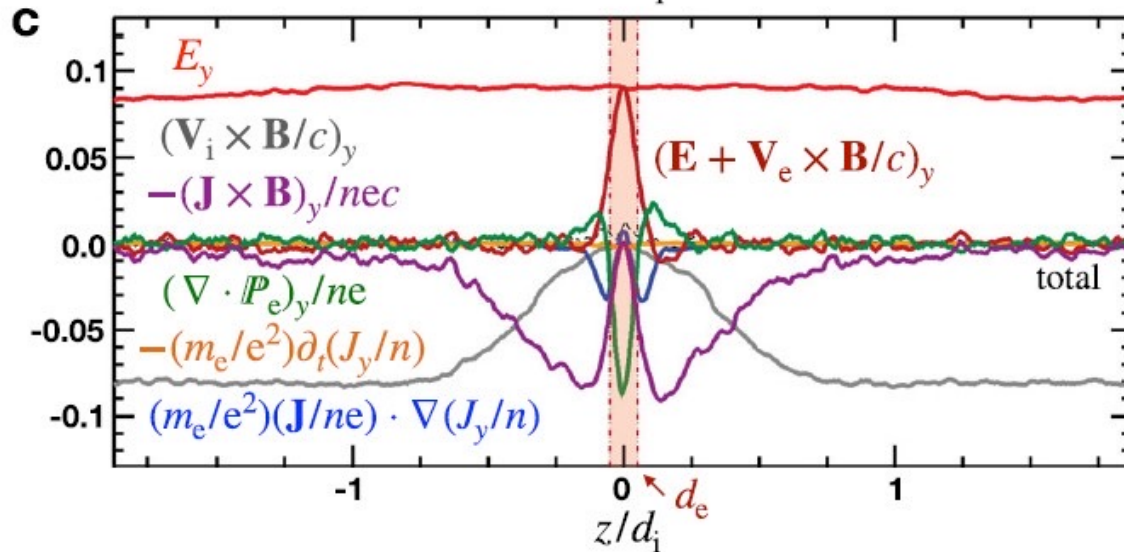


Magnetic Reconnection – Hall B

Symmetric PIC simulation

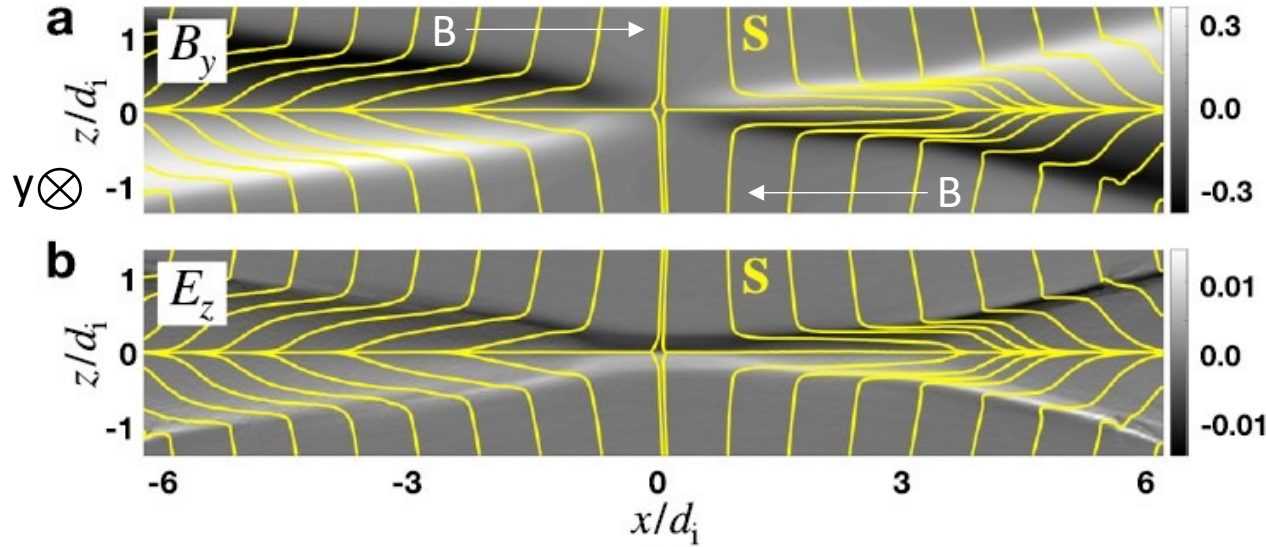


Likewise, a magnetic field (B_y) perturbation is generated from the inward and outward electron motions (current).

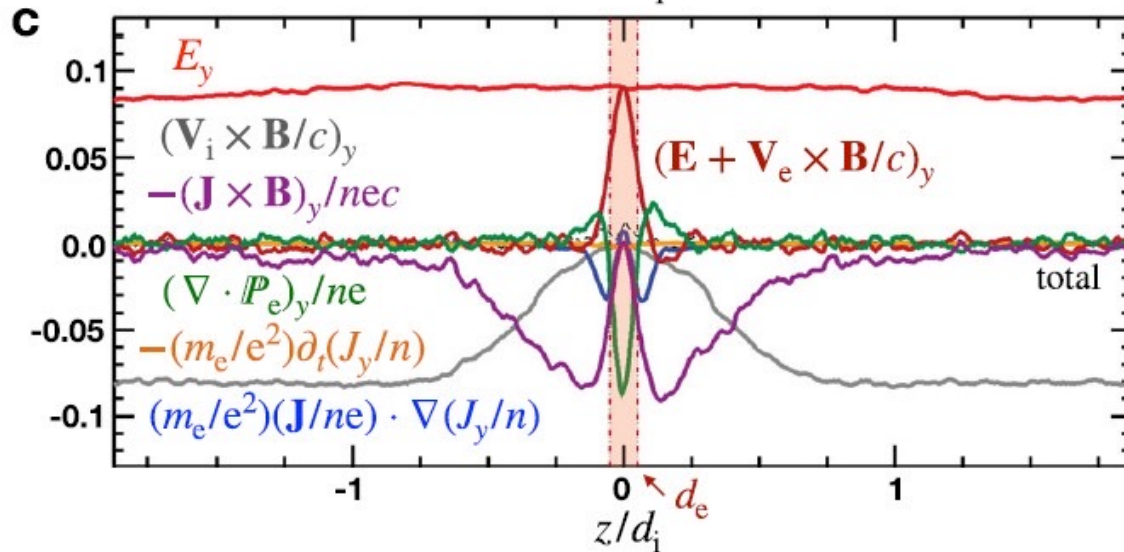


Magnetic Reconnection – Hall E & B

Symmetric PIC simulation

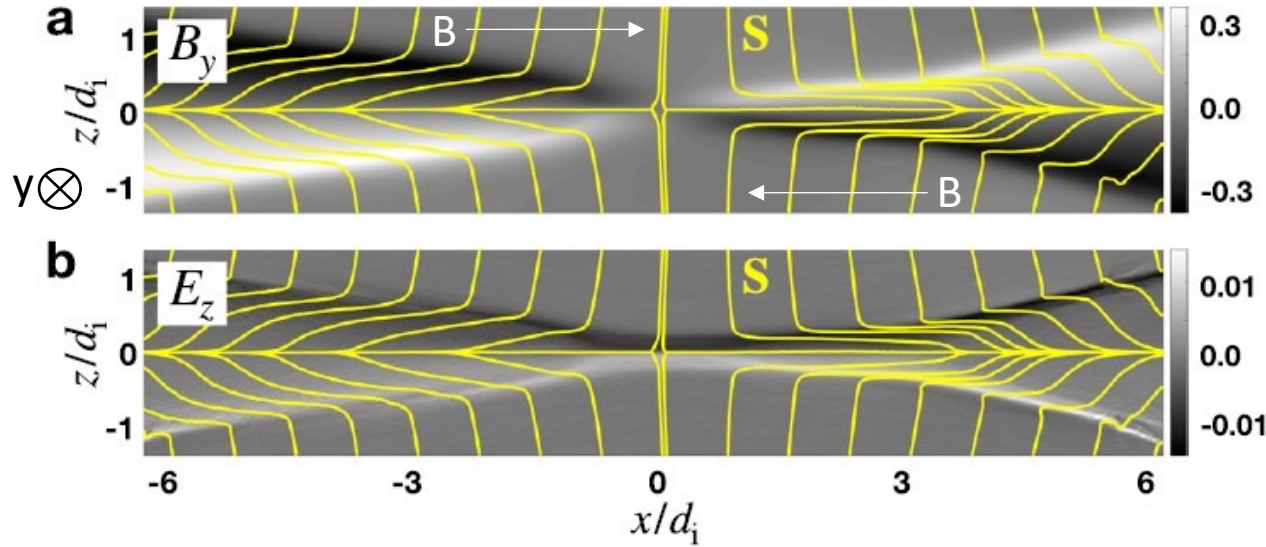


We refer to these effects of the Hall $\mathbf{J} \times \mathbf{B}$ term of the G.O.L. in the ion diffusion region as the **Hall magnetic field and Hall electric field.**

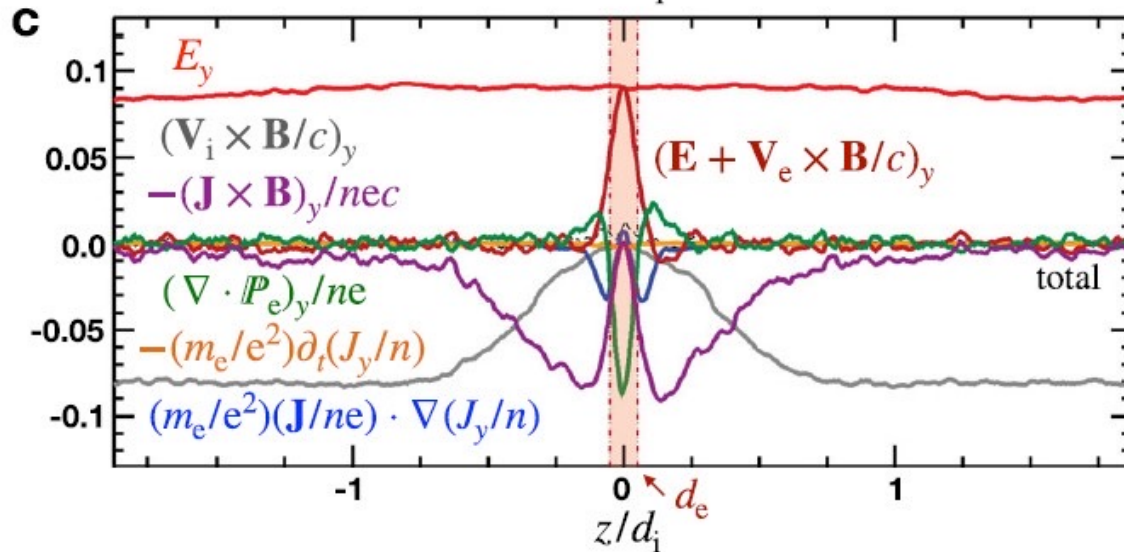


Magnetic Reconnection – Hall E & B

Symmetric PIC simulation

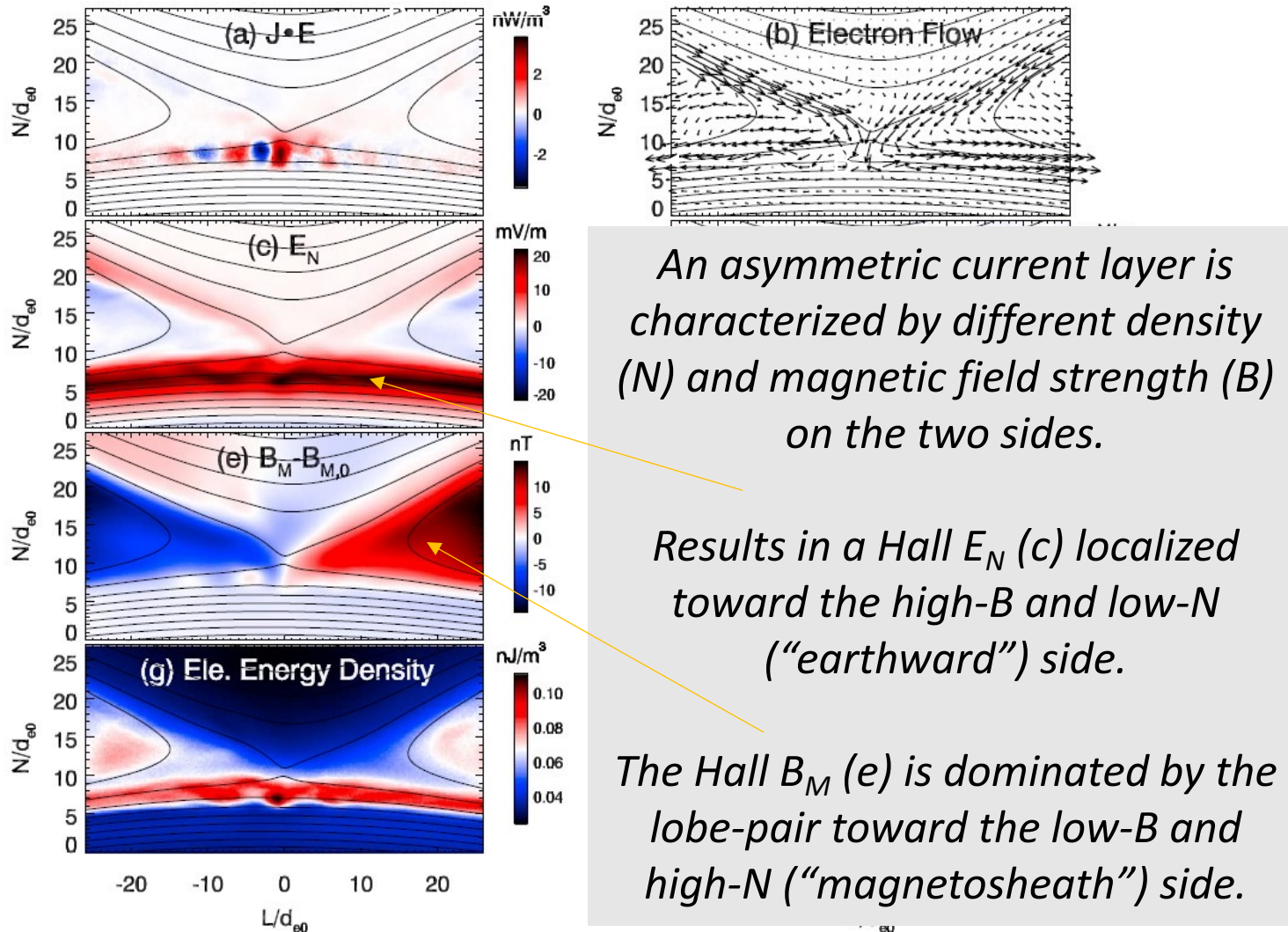


Streamlines $\mathbf{S} = \mathbf{E} \times \mathbf{B} / \mu_0$ is the Poynting flux (directional energy flux) due to Hall E_z and B_y terms.



Magnetic Reconnection – Hall E & B

Asymmetric PIC simulation (dayside magnetopause) & $[x, y, z] \leftrightarrow [L, M, N]$



Magnetic Reconnection – Hall B Summary

Symmetric two-fluid simulation

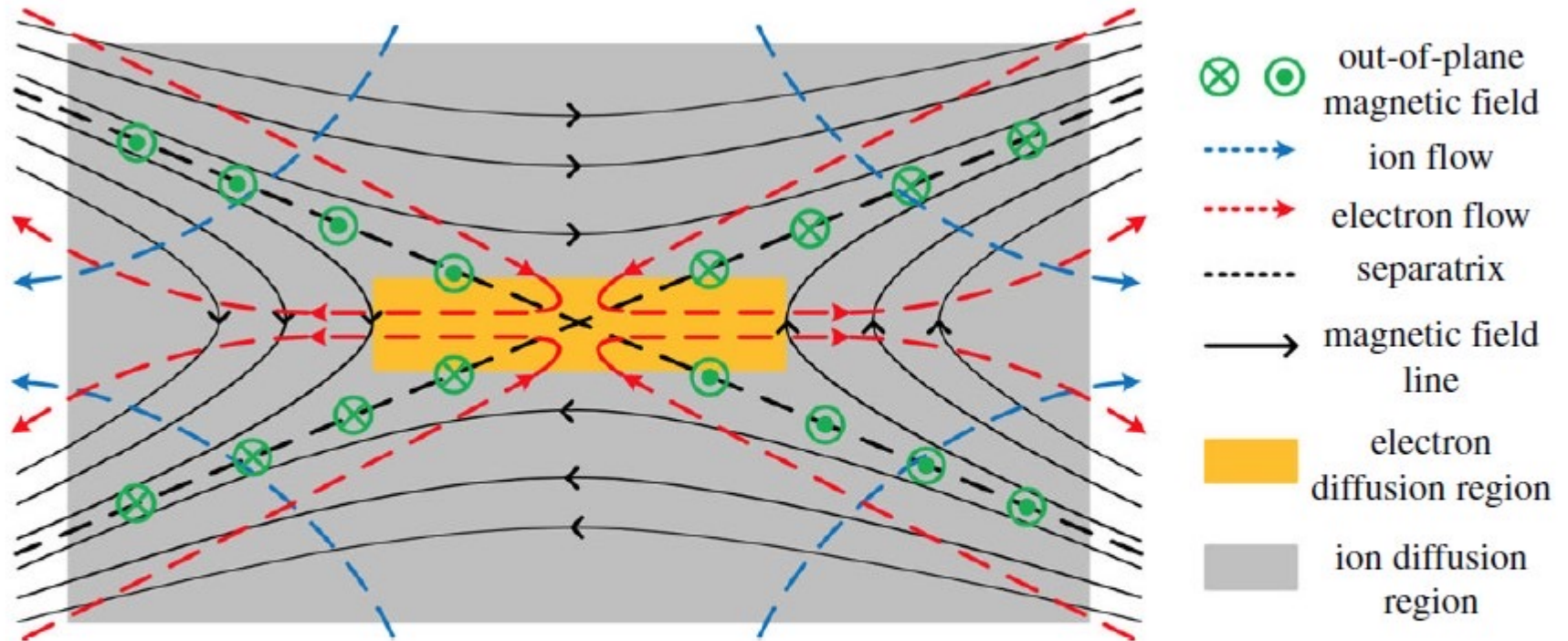


Figure 5. Schematic of two-fluid reconnection. Ions decouple from electrons in the ion diffusion region (grey colour). Electrons are frozen to the field lines until they reach the electron diffusion region (orange colour). The electron flow pattern creates a quadrupole out-of-plane magnetic field, a signature of the Hall effect.

Overview

- **Current sheets: Magnetic field rotations** [$J = \nabla \times B / \mu_0$] from the very wide Heliospheric Current Sheet to “narrow” M’pause
- **Multi-spacecraft missions: A brief introduction to tetrahedron formations and the Curlometer technique**
- **Near-Earth space regimes & boundaries**
- **The magnetic reconnection process at current sheets:**
 - (a) Schematic overviews, 2D vs 3D & ion (d_i) scale
 - (b) “To be or not to be” frozen-in? The G.O.L. vs Hall 😊
 - (c) **Reconnection rate v_{in}/v_{out}**
- **Observations of Reconnection Jets:**
 - (a) Cluster in the solar wind vs “timing normal” concept
 - (b) MMS at the magnetopause: J from “curlB” vs $J = Ne(V_i - V_e)$
- Summary

Magnetic Reconnection Rate

How fast can a magnetic field B_i enter a diffusion region (DR) at an external inflow speed v_i ?
In other words, what is the “reconnection rate” v_{in}/v_{out} ratio?

$E = v_i B_i$ (just outside DR) and $E = J / \sigma$ (Ohm's law inside DR) $\rightarrow v_i B_i = J / \sigma$

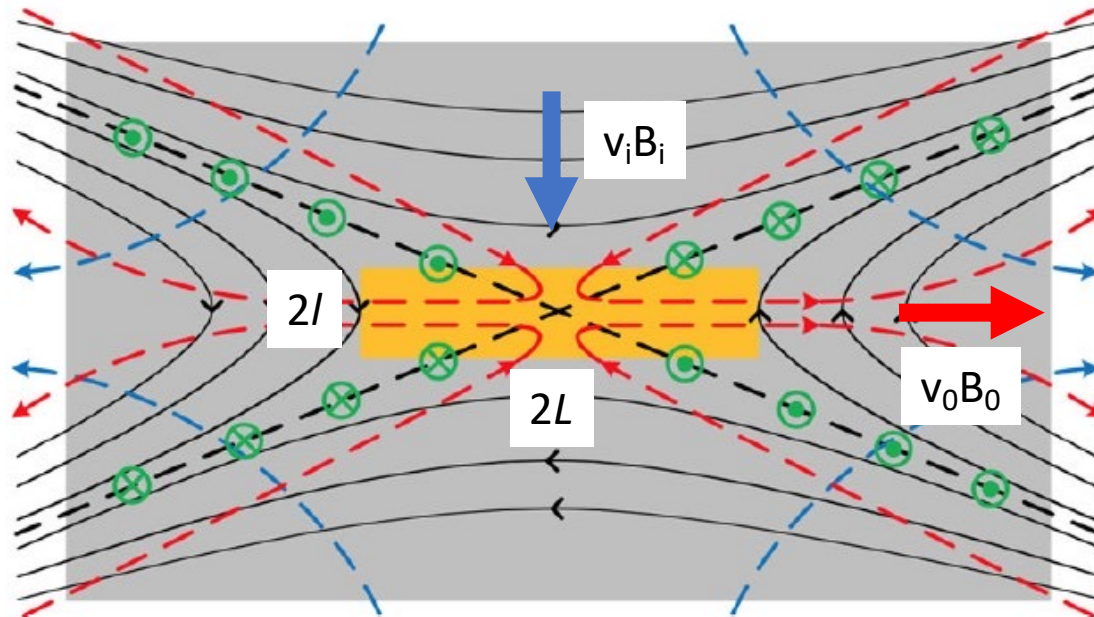
Using Ampere's Law (inside DR) $J = B_i / (\mu_0 l)$ $\rightarrow v_i l = 1 / (\sigma \mu_0)$ (1)

Mass conservation implies that inflow rate (up & down) equals outflow rate (left & right):

$\rho v_i * 2L * 2 = \rho v_o * 2l * 2$ or $v_o l = v_i L$ or $l = (v_i L) / v_o$ which combined with (1)

$\rightarrow v_i^2 = v_o / L (\sigma \mu_0)$ and using the Magnetic Reynolds number of the inflow plasma

$R_m \equiv v_{Ai} L (\sigma \mu_0)$ $\rightarrow v_i^2 = v_o v_{Ai} / R_m$ where v_{Ai} is the Alfvén speed of the inflow plasma.



Magnetic Reconnection Rate

How fast can a magnetic field B_i enter a diffusion region (DR) at an external inflow speed v_i ?
 In other words, what is the “reconnection rate” v_{in}/v_{out} ratio?

$$v_i^2 = v_0 v_{Ai} / R_m \quad (1) \quad \dots \quad \text{but what is the outflow speed } v_0?$$

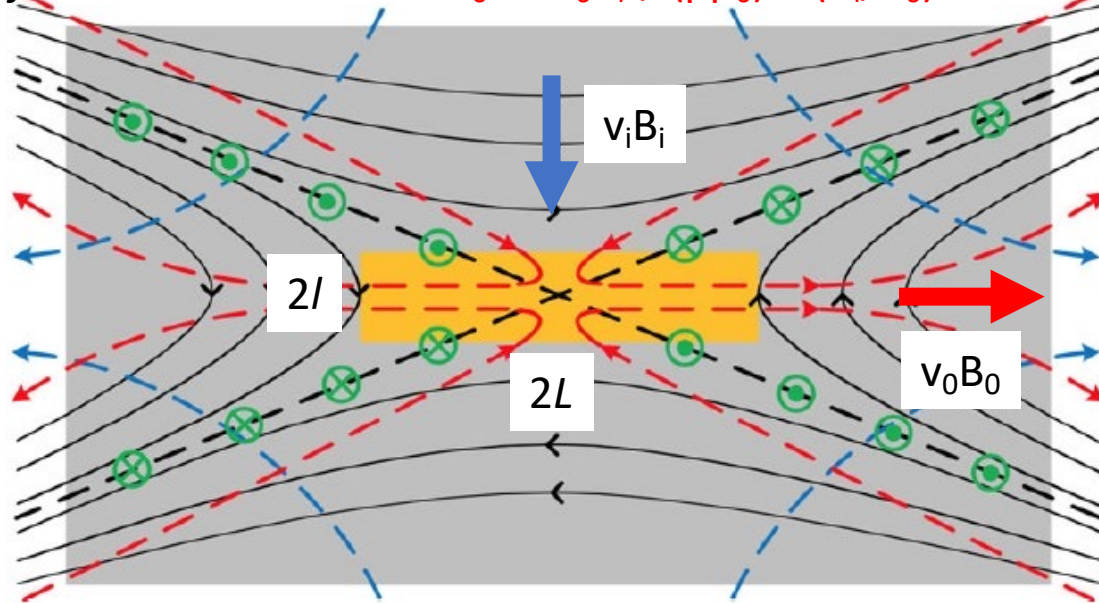
Plasma Equation of Outflow Motion: $\rho \, d\mathbf{v}/dt = \mathbf{J} \times \mathbf{B}$ where $d\mathbf{v}/dt = \partial\mathbf{v}/\partial t + (\mathbf{v} \cdot \nabla)\mathbf{v}$

$$\rightarrow \rho v_0^2 / L = J B_0 \quad (\text{steady state}) \quad \text{and using Ampere's law } J = B_i / (\mu_0 l)$$

$$\rightarrow \rho v_0^2 / L = B_0 B_i / (\mu_0 l)$$

$$\rightarrow v_0^2 = (L/\rho) * B_0 B_i / (\mu_0 l) = (L/l) * B_0 B_i / (\rho \mu_0)$$

Now $(L/l) = (v_0/v_i)$ from mass conservation and $(v_0/v_i) = (B_i/B_0)$ from magnetic flux conservation and $v_0^2 = B_0 B_i / (\rho \mu_0) * (B_i/B_0) \rightarrow v_0 = B_i / \text{SQRT}(\mu_0 \rho) = v_{Ai} \quad (2)$



The original Sweet-Parker reconnection rate from (1) and (2):

$$v_i = v_{Ai} / \text{SQRT}(R_m)$$

or

$$v_i/v_{Ai} \sim 1/\text{SQRT}(R_m)$$

Magnetic Reconnection Rate

The original Sweet-Parker reconnection rate $v_{in}/v_{out} = v_i/v_{Ai} \sim 1/\text{SQRT}(R_m)$ is **too slow** if the *dimension L along the current sheet* is **long compared with thickness δ** and this theory alone failed to explain reconnection associated with solar flares.

The famous “GEM reconnection challenge” set of papers in 2001, with an introduction by *Birn, J. et al.*, Geospace Environmental Modeling (GEM) Magnetic Reconnection Challenge (2001), <https://doi.org/10.1029/1999JA900449>, were instrumental in validating the importance of the **$\mathbf{J} \times \mathbf{B}$ Hall term** of the G.O.L. to obtain fast $v_i/v_A \sim 0.1$ rates.

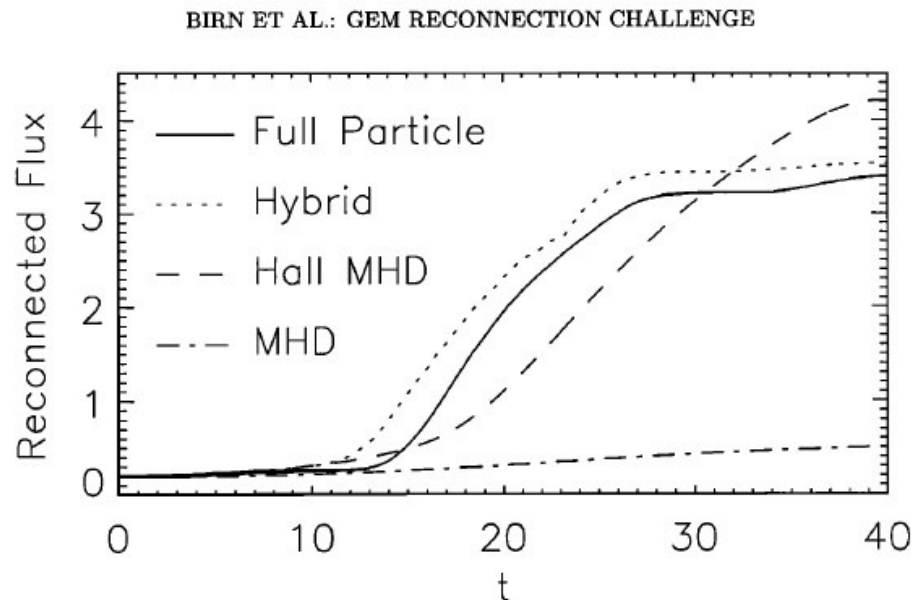


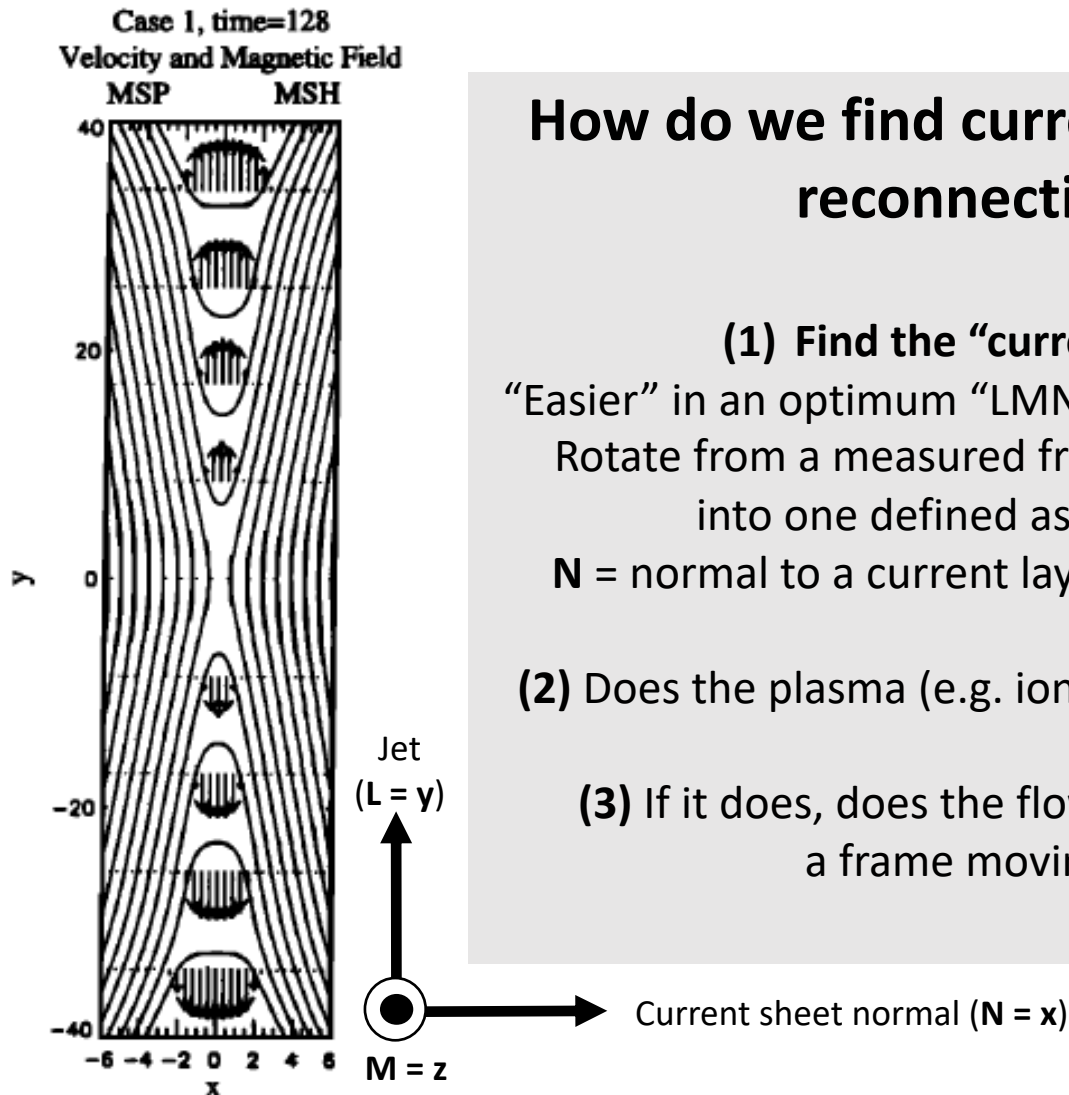
Figure 1. The reconnected magnetic flux versus time from a variety of simulation models: full particle, hybrid, Hall MHD, and MHD (for resistivity $\eta = 0.005$).

Overview

- Current sheets: *Magnetic field rotations [$J = \nabla \times B / \mu_0$] from the very wide Heliospheric Current Sheet to “narrow” M’pause*
- Multi-spacecraft missions: *A brief introduction to tetrahedron formations and the Curlometer technique*
- Near-Earth space regimes & boundaries
- The magnetic reconnection process at current sheets:
 - (a) *Schematic overviews, 2D vs 3D & ion (di) scale*
 - (b) *“To be or not to be” frozen-in? The G.O.L. vs Hall ☺*
 - (c) *Reconnection rate v_{in}/v_{out}*
- **Observations of Reconnection Jets:**
 - (a) ***Cluster in the solar wind vs “timing normal” concept***
 - (b) *MMS at the magnetopause: J from “curlB” vs $J = Ne(V_i - V_e)$*
- Summary

Magnetic Reconnection - Observations

Magnetohydrodynamic (MHD) simulations



How do we find current sheets associated with reconnection jets in space?

(1) Find the “current sheet” – rotation of \mathbf{B} .

“Easier” in an optimum “LMN” system (c.f. *simulation coordinates*).

Rotate from a measured frame (e.g. GSE, GSM, s/c frame etc)

into one defined as: \mathbf{L} = maximum change in \mathbf{B} ,

\mathbf{N} = normal to a current layer (various methods) and $\mathbf{M} = \mathbf{N} \times \mathbf{L}$

(2) Does the plasma (e.g. ion) velocity peak (+/-) across the layer?

(3) If it does, does the flow change satisfy \sim Alfvén speed in a frame moving with the boundary?

The four-spacecraft Cluster mission: Spacecraft separations

Year	Minimum (km)	Maximum (km)
2005	600	1700
2006	6000	12300
2007	400	12400
2008	40	10400
2009	3300	8500

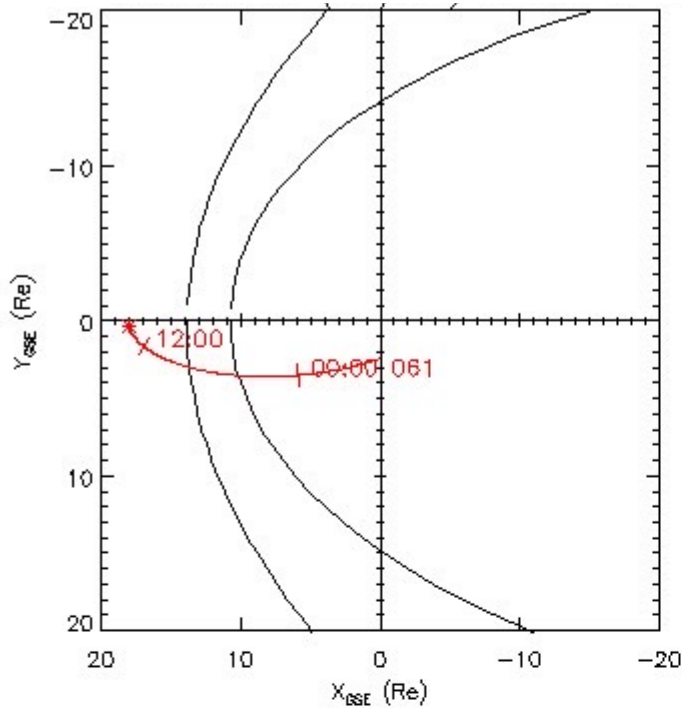
Note: Solar wind density results in a most common $d_i \sim 100$ km

The four-spacecraft Cluster mission: Spacecraft separations

Year	Minimum (di)	Maximum (di)
2005	6	17
2006	60	123
2007	4	124
2008	0.4	104
2009	33	85

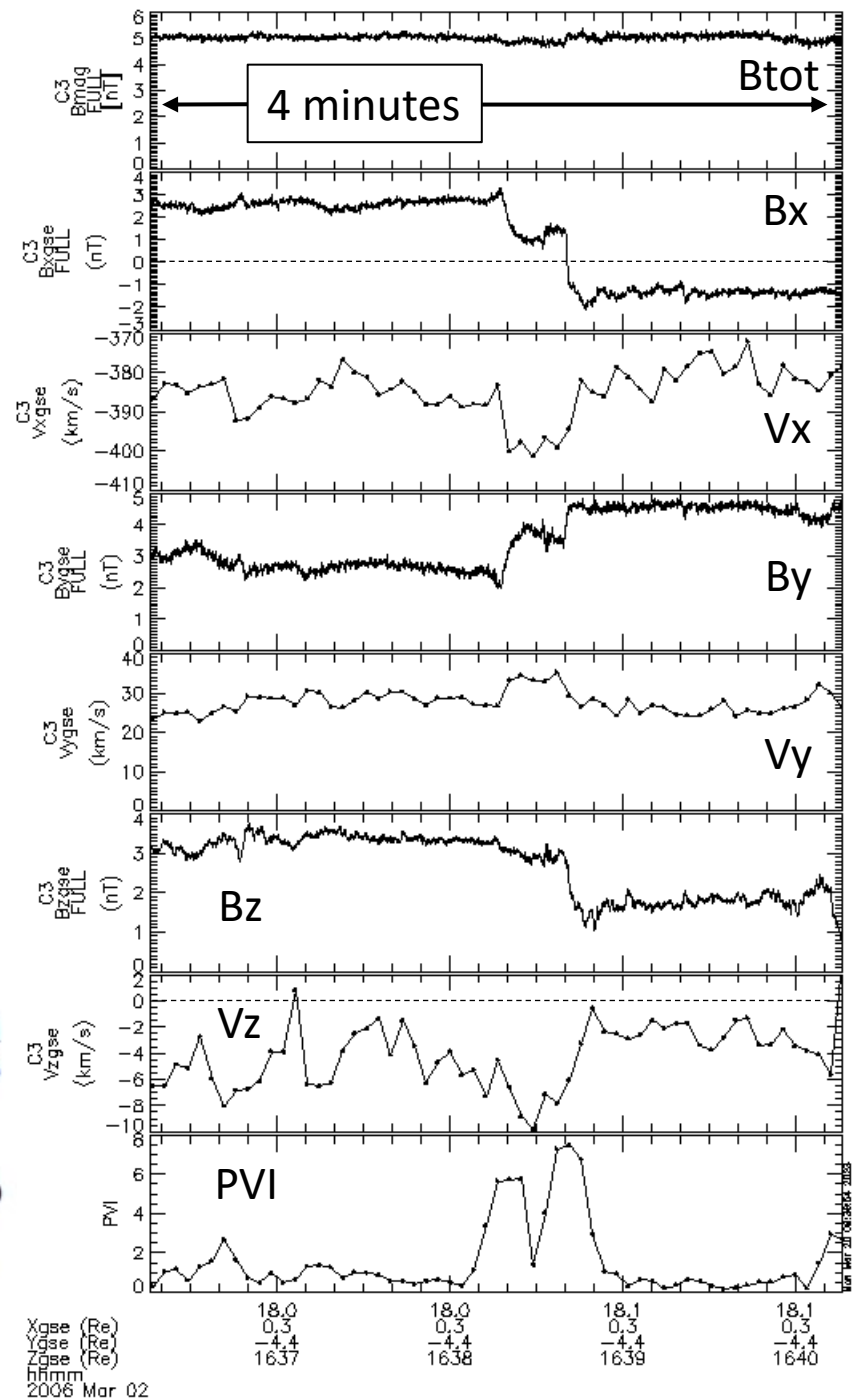
Note: Solar wind density results in a most common $di \sim 100$ km

Exploring Cluster in the solar wind



The PVI time series is defined in terms of the magnetic field increment vector $\Delta B(t, \tau) = B(t + \tau) - B(t)$ (Greco et al. 2008):

$$PVI(t, \tau) = \frac{|\Delta B(t, \tau)|}{\sqrt{(|\Delta B(t, \tau)|)^2}} \quad (1)$$



Exploring Cluster in the solar wind

We confirm a presence of an Alfvénic reconnection exhaust across a current sheet by using the so-called “Walén” relation (*Paschmann et al., 1986*):

whether it may also satisfy the Walén relation $V_{\text{WL}} = V_{\text{L0}} \pm \Delta V_{\text{AL}}$ as expected for a magnetic reconnection exhaust (*Paschmann et al. 1986*), where ΔV_{AL} is given as

$$\Delta V_{\text{AL}} = \sqrt{\rho_0 / \mu_0} (B_L / \rho - B_{\text{L0}} / \rho_0).$$

Here, $\mu_0 = 4\pi \times 10^{-7}$ Vs/Am is the permeability of free space and the other parameters indicated with a subscript “0” (V_{L0} , B_{L0} , ρ_0) correspond to the given external parameter at the start time of the Walén prediction, whether that is before the CS (leading side) or after the CS (trailing side). The positive and negative signs of ΔV_{AL} are chosen automatically according to the direction of the potential jet ($\Delta V_{\text{L}} > 0$ or $\Delta V_{\text{L}} < 0$).

Paschmann G., Papamastorakis I., Baumjohann W. et al., The magnetopause for large magnetic shear: AMPTE/IRM observations, JGR 91 11099, 1986

Eriksson et al., The Astrophysical Journal, 933:181 (21pp), 2022 July 10, <https://doi.org/10.3847/1538-4357/ac73f6>

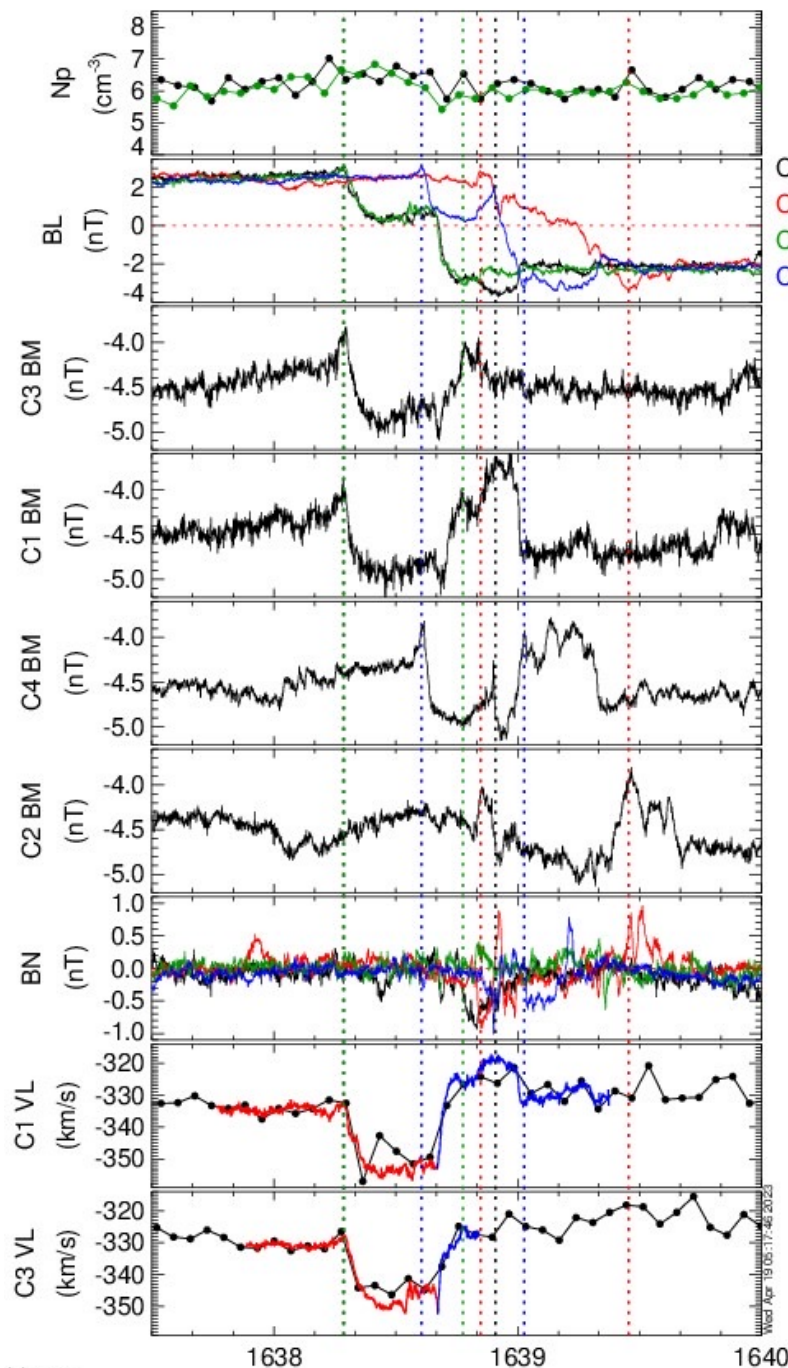
Exploring Cluster in the solar wind

Event duration: 70.1 s (1.2 min)

Solar wind external flow:

$$\langle V_L, V_M, V_N \rangle = [-329.8, 59.5, -194.8] \text{ km/s}$$

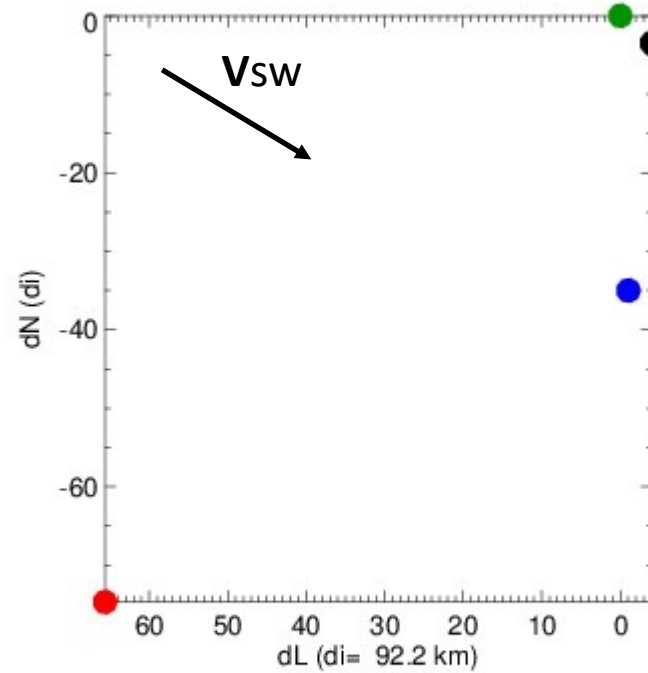
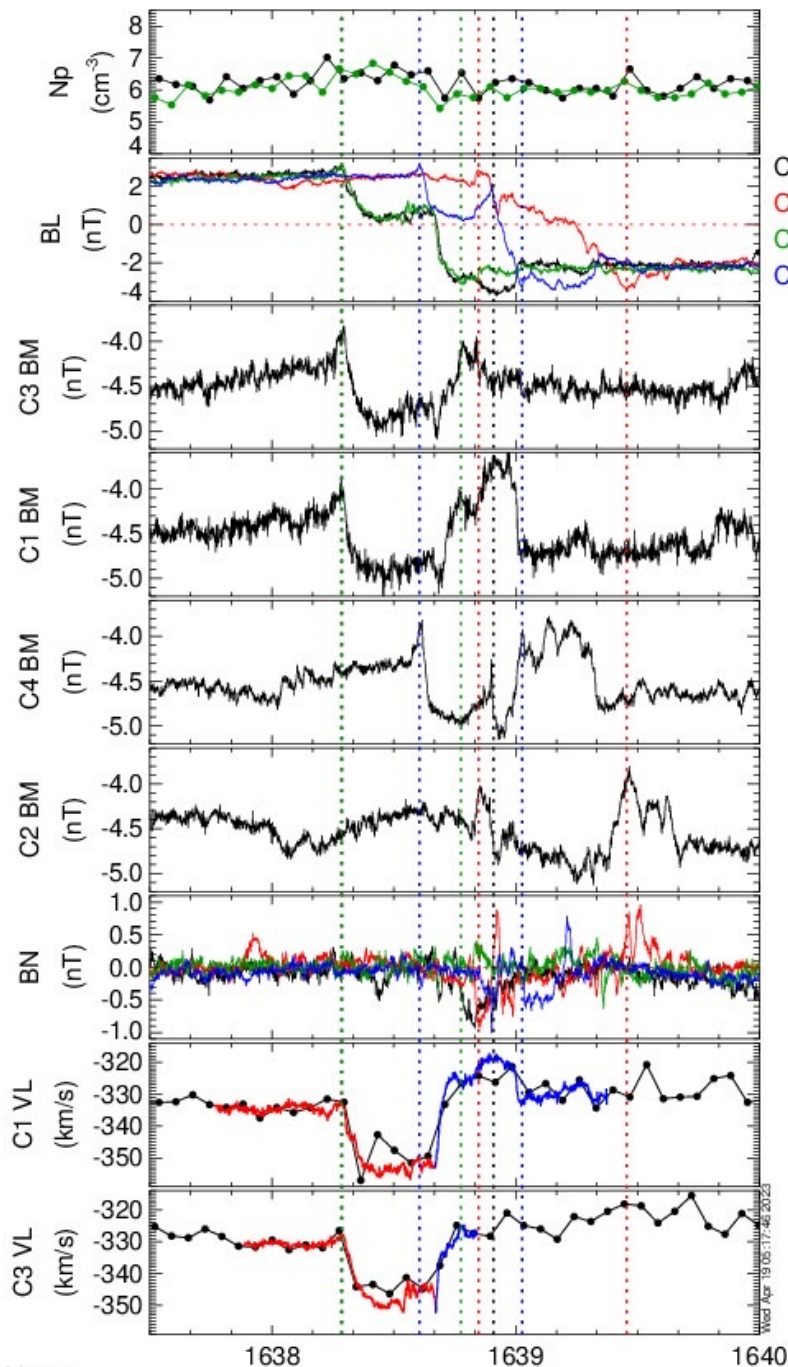
$$\langle di \rangle = 92.2 \text{ km}$$



	C1	C2	C3	C4
Δt_{cs} (s)	37.3	36.4	29.3	25.3
ΔN (di)	79	77	62	53
ΔL (di)	133	130	105	90
ΔM (di)	24	24	19	16
B_{rot} ($^\circ$)	79	75	74	78
B_{M1}/B_{L1}	1.6	1.7	1.7	1.9
B_{M2}/B_{L2}	2.2	2.3	1.9	2.1

Exploring Cluster in the solar wind

C3 C1 C4 C2 at T=2006-03-02/16:38:17.2 UT

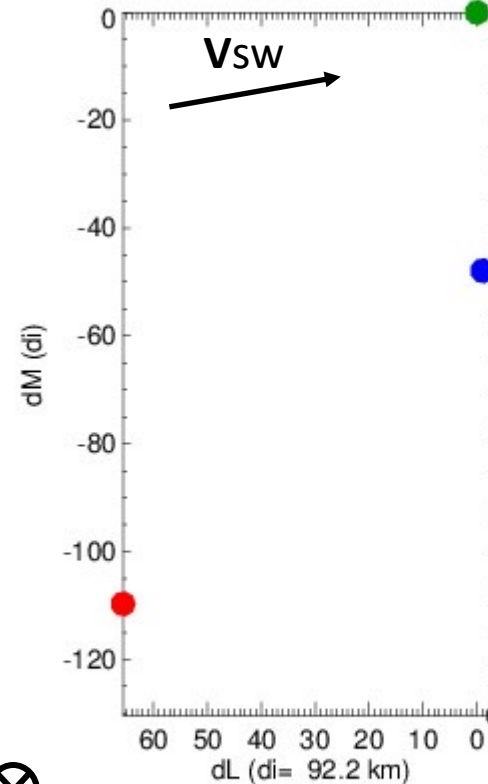
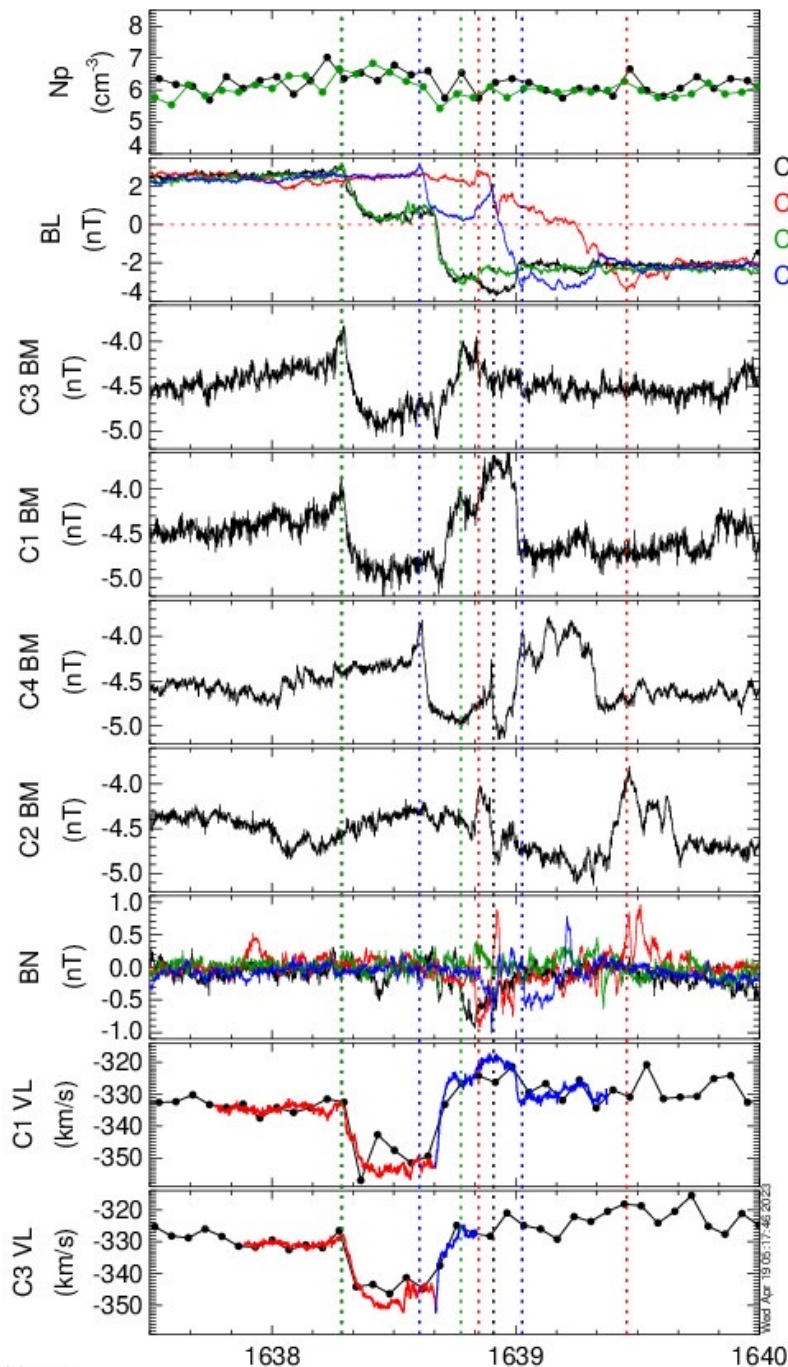


C3 $R_{GSE} = (18.05 \ 0.32 \ -4.37) R_E$
 $N_{GSE} = (0.505808 \ 0.434122 \ -0.745451)$
 $L_{GSE} = (0.850924 \ -0.393063 \ 0.348469)$
 $M_{GSE} = (-0.141731 \ -0.810580 \ -0.568219)$



Exploring Cluster in the solar wind

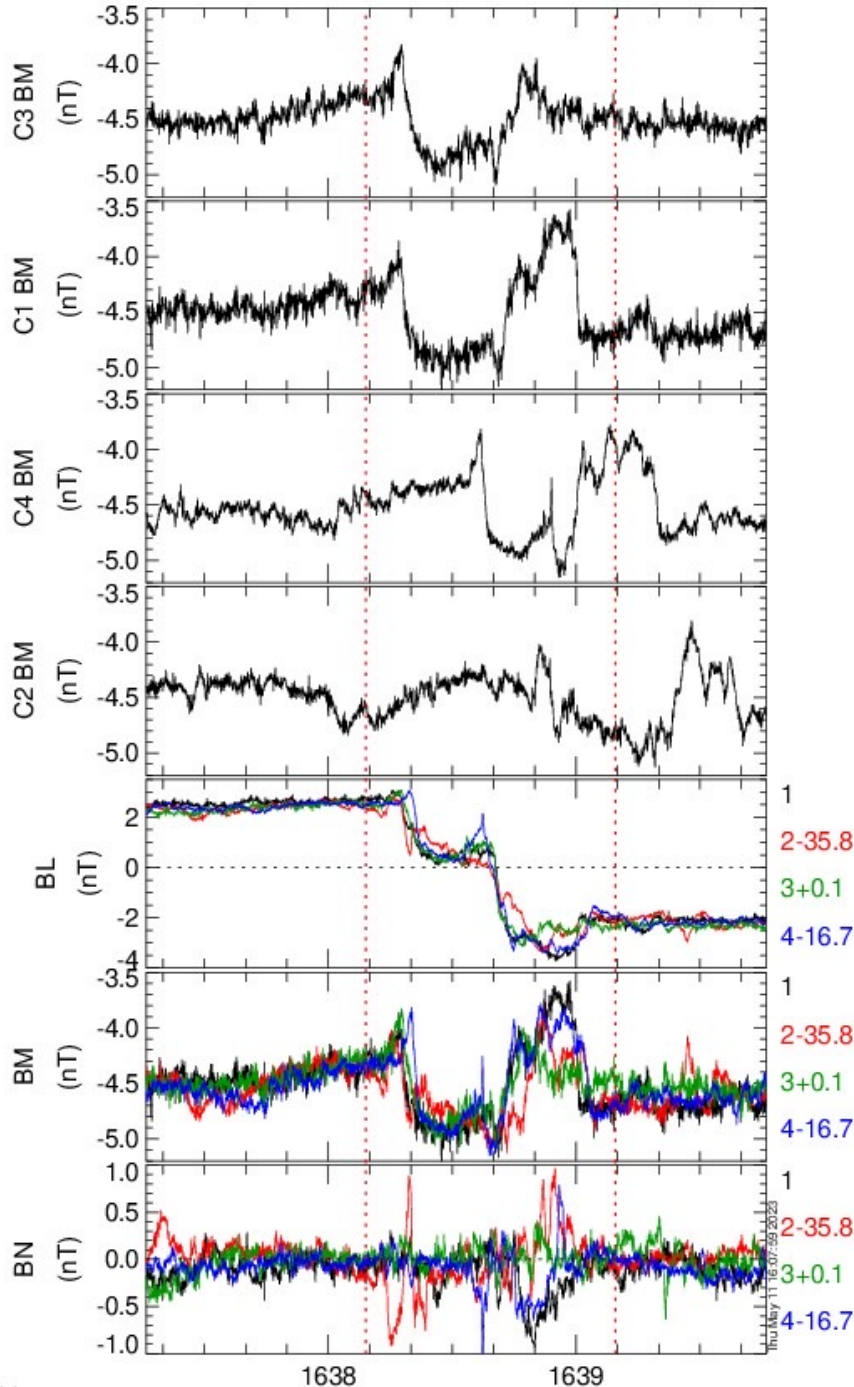
C3 C1 C4 C2 at T=2006-03-02/16:38:17.2 UT



N

C3 $R_{GSE} = (18.05 \ 0.32 \ -4.37) R_E$
 $N_{GSE} = (0.505808 \ 0.434122 \ -0.745451)$
 $L_{GSE} = (0.850924 \ -0.393063 \ 0.348469)$
 $M_{GSE} = (-0.141731 \ -0.810580 \ -0.568219)$

Timing Analysis

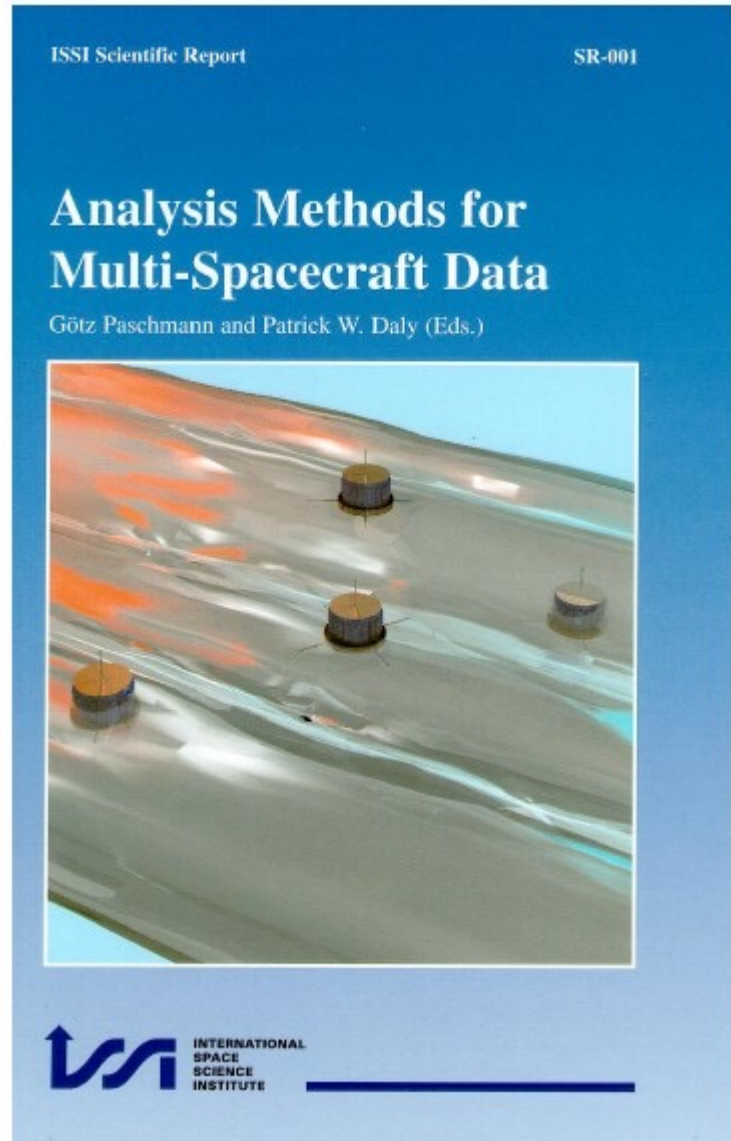
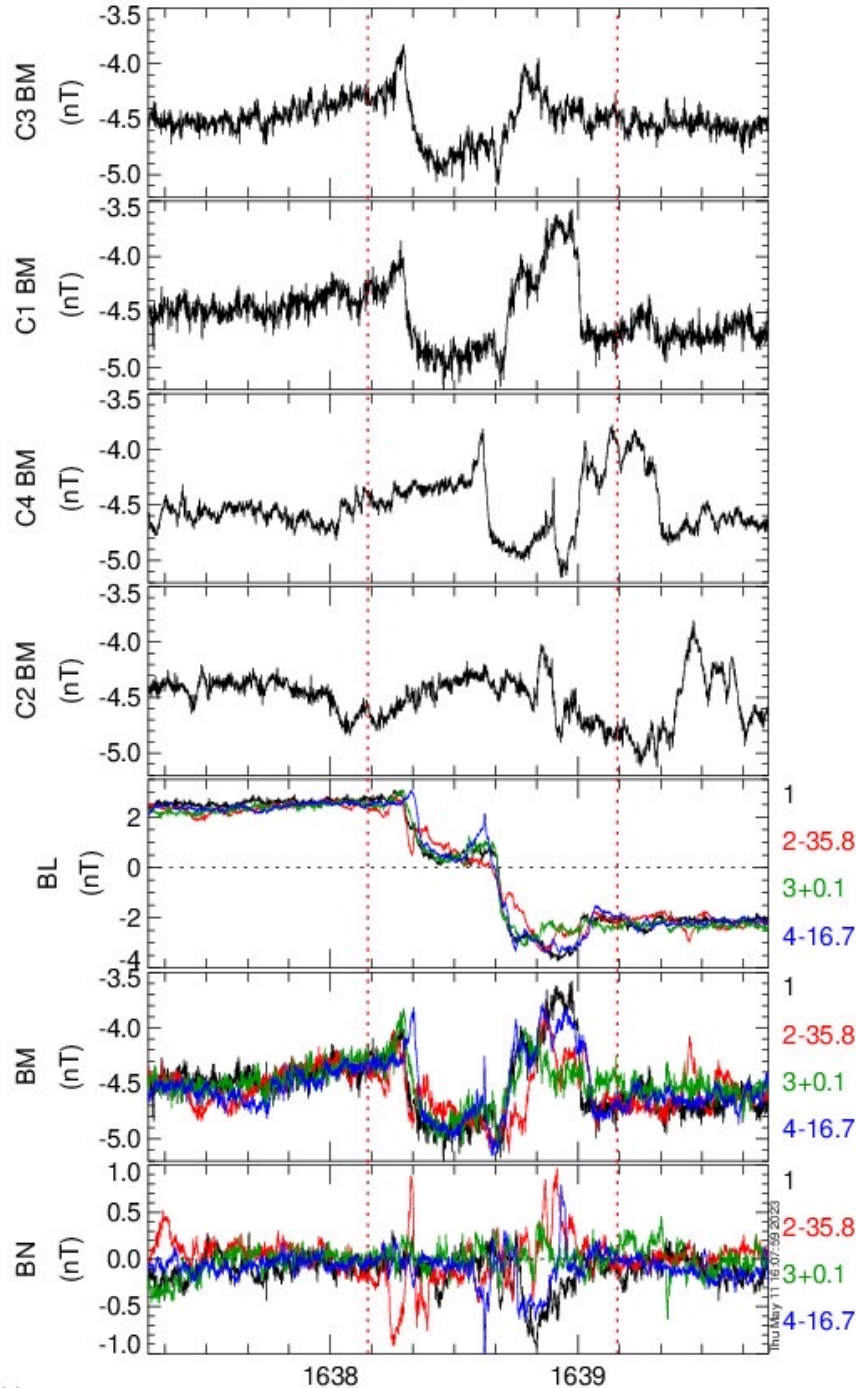


If you “only” had one s/c to go by ...
you would not know what the **actual structure** of the current layer looks like.

A multi-formation mission demonstrates
how the *same* current sheet has
important structure in, e.g., BM and BN.

In this case, structure exists over
the ~100 di separation.

Timing Analysis



Ch.10 Shock & Discontinuity Normals... by Steven J. Schwartz

10.4.3 Multi-Spacecraft Timings

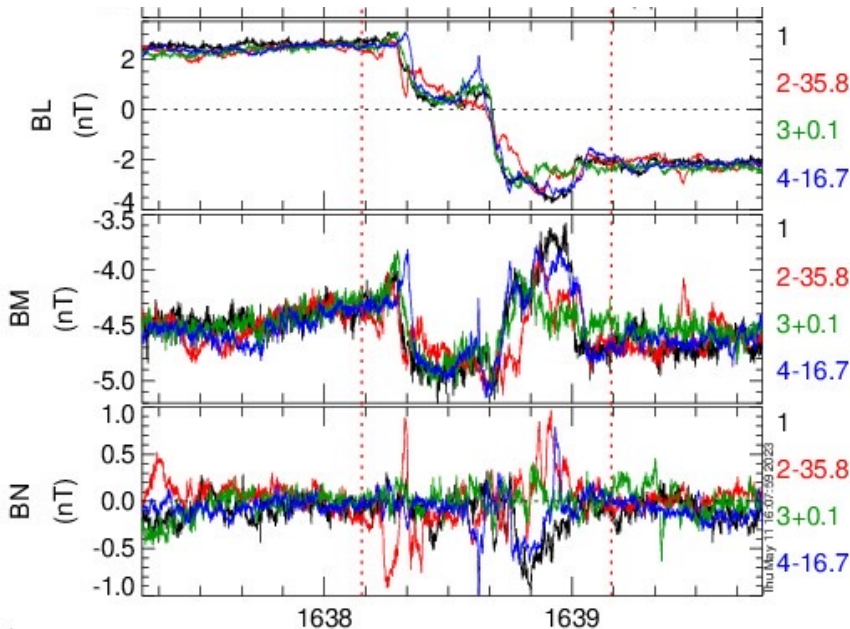
Timing Analysis

If the same boundary passes several spacecraft, the relative positions and timings can be used to construct the boundary normal and speed, since

$$(V_{sh}^{arb} t_{\alpha\beta}) \cdot \hat{n} = r_{\alpha\beta} \cdot \hat{n} \quad (10.19)$$

where $r_{\alpha\beta}$ is the separation vector between any spacecraft pair and $t_{\alpha\beta}$ the time difference between this pair for a particular boundary. Thus given 4 spacecraft, the normal vector and normal propagation velocity $V_{sh}^{arb} \equiv V_{sh}^{arb} \cdot \hat{n}$ are found from the solution of the following system:

$$\begin{pmatrix} r_{12} \\ r_{13} \\ r_{14} \end{pmatrix} \cdot \frac{1}{V_{sh}^{arb}} \begin{pmatrix} n_x \\ n_y \\ n_z \end{pmatrix} = \begin{pmatrix} t_{12} \\ t_{13} \\ t_{14} \end{pmatrix} \quad (10.20)$$



At 2006-03-02/16:38:41 UT :

$$r_{12} = [1873, -6929, 6043] \text{ km}$$

$$r_{13} = [-1229, -9761, -6947] \text{ km}$$

$$r_{14} = [-2313, -7544, -2066] \text{ km}$$

Relative C1 = [18.2, 1.8, -3.3] Re (GSE)

$$t_{12} = -35.8 \text{ s}$$

$$t_{13} = +0.1 \text{ s}$$

$$t_{14} = -16.7 \text{ s}$$

Solving (e.g. inverting separation matrix):

$$Nt = \pm[0.343745, 0.409645, -0.845003]$$

$$|Vt| = 58.5 \text{ km/s}$$

10.4.3 Multi-Spacecraft Timings

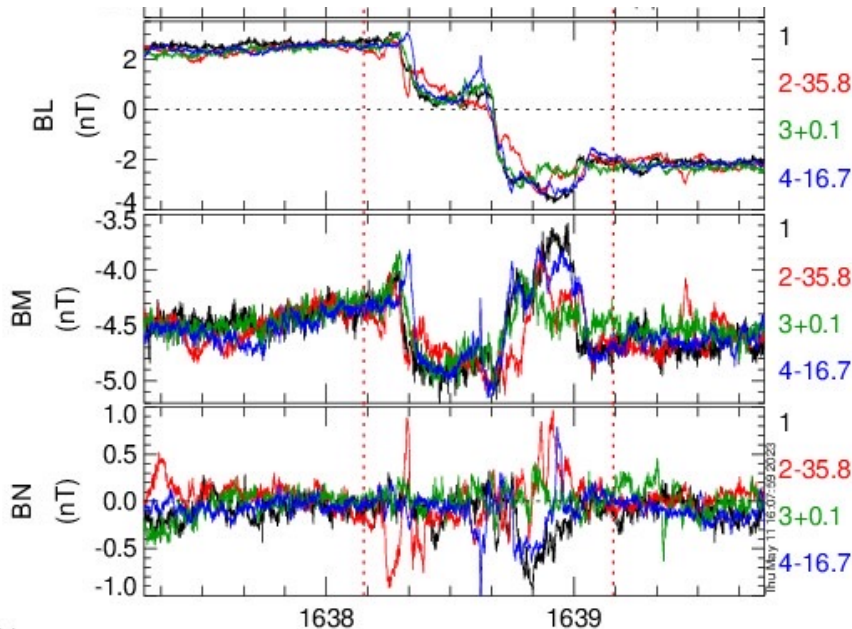
Timing Analysis

If the same boundary passes several spacecraft, the relative positions and timings can be used to construct the boundary normal and speed, since

$$(V_{sh}^{arb} t_{\alpha\beta}) \cdot \hat{n} = r_{\alpha\beta} \cdot \hat{n} \quad (10.19)$$

where $r_{\alpha\beta}$ is the separation vector between any spacecraft pair and $t_{\alpha\beta}$ the time difference between this pair for a particular boundary. Thus given 4 spacecraft, the normal vector and normal propagation velocity $V_{sh}^{arb} \equiv V_{sh}^{arb} \cdot \hat{n}$ are found from the solution of the following system:

$$\begin{pmatrix} r_{12} \\ r_{13} \\ r_{14} \end{pmatrix} \cdot \frac{1}{V_{sh}^{arb}} \begin{pmatrix} n_x \\ n_y \\ n_z \end{pmatrix} = \begin{pmatrix} t_{12} \\ t_{13} \\ t_{14} \end{pmatrix} \quad (10.20)$$



$$\mathbf{Nt} = \pm[0.343745, 0.409645, -0.845003]$$

$$|\mathbf{Vt}| = 58.5 \text{ km/s}$$

$$\mathbf{Nc} = \mathbf{B}_1 \times \mathbf{B}_2 / |\mathbf{B}_1 \times \mathbf{B}_2| =$$

$$= [0.505808, 0.434122, -0.745451]$$

$$\text{Angle difference: } \mathbf{Nt} \cdot \mathbf{Nc} = 11^\circ$$

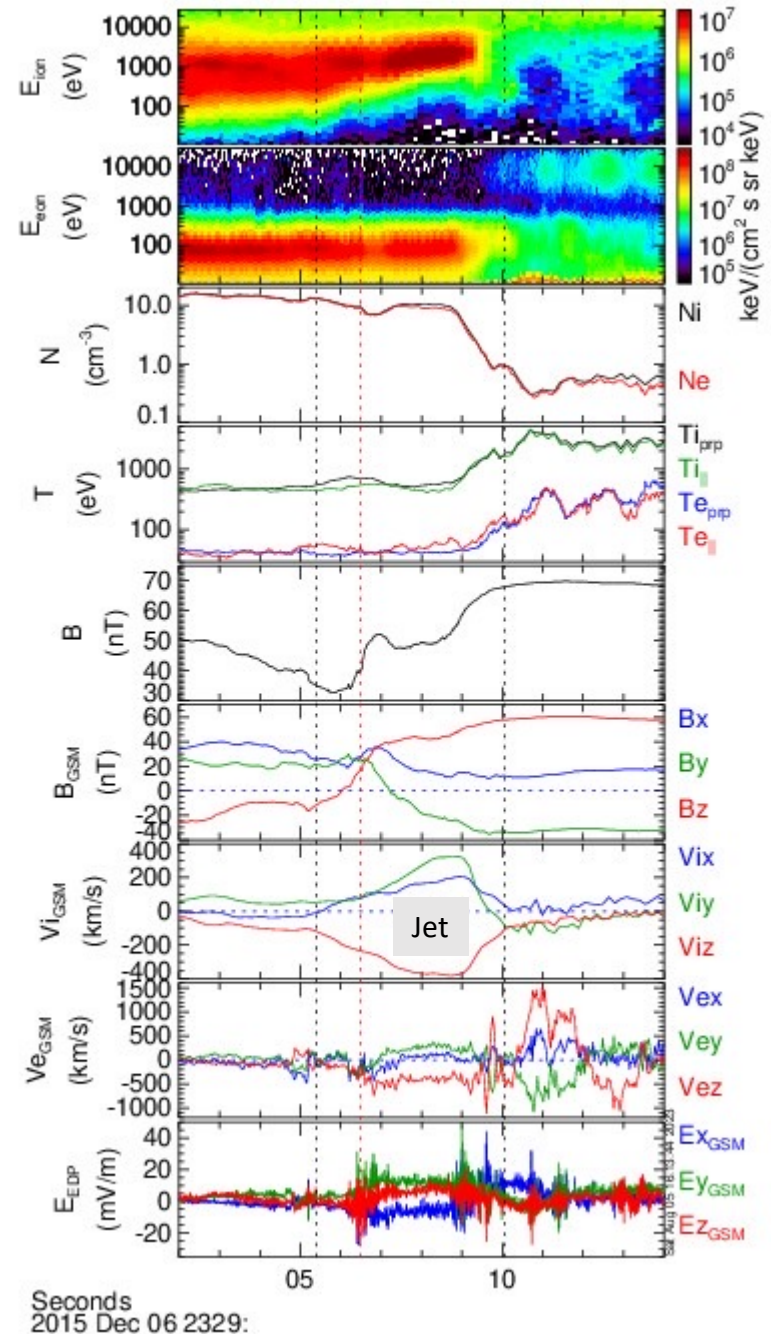
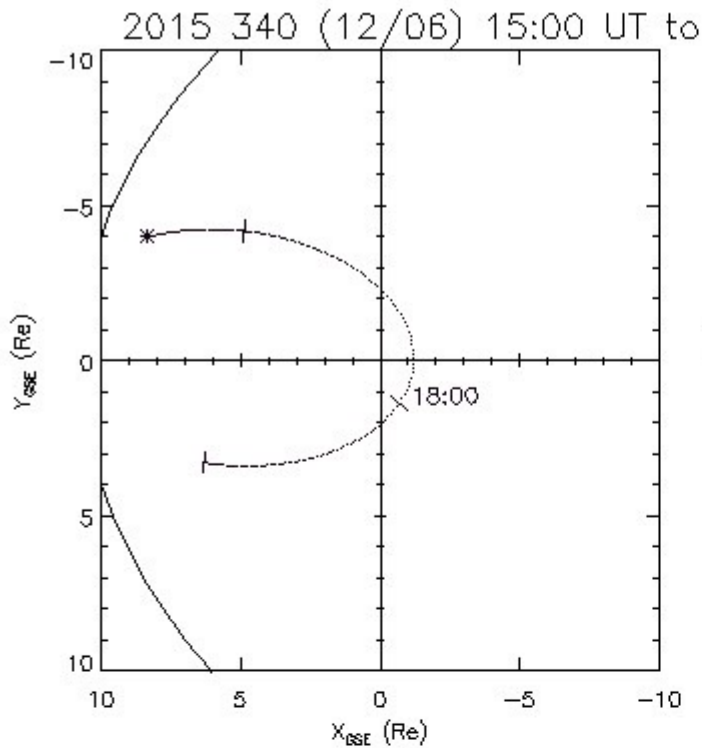
Caveats:

- (1) Sharp signal gradient observed at all s/c
- (2) Tetrahedron *formation* v.s. *s/c alignment* relative the (assumed) planar boundary

Overview

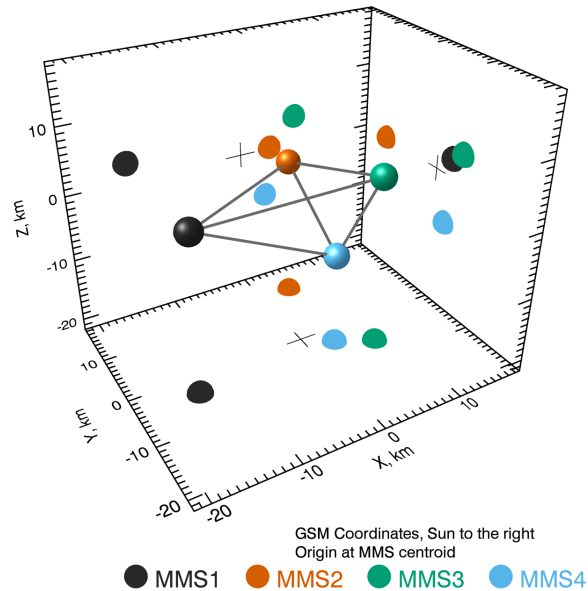
- Current sheets: *Magnetic field rotations [$J = \nabla \times B / \mu_0$] from the very wide Heliospheric Current Sheet to “narrow” M’pause*
- Multi-spacecraft missions: *A brief introduction to tetrahedron formations and the Curlometer technique*
- Near-Earth space regimes & boundaries
- The magnetic reconnection process at current sheets:
 - (a) *Schematic overviews, 2D vs 3D & ion (di) scale*
 - (b) *“To be or not to be” frozen-in? The G.O.L. vs Hall ☺*
 - (c) *Reconnection rate v_{in}/v_{out}*
- **Observations of Reconnection Jets:**
 - (a) *Cluster in the solar wind vs “timing normal” concept*
 - (b) *MMS at the magnetopause: J from “curlB” vs $J = Ne(V_i - V_e)$*
- Summary

Exploring MMS at the Dayside Magnetopause: GSM



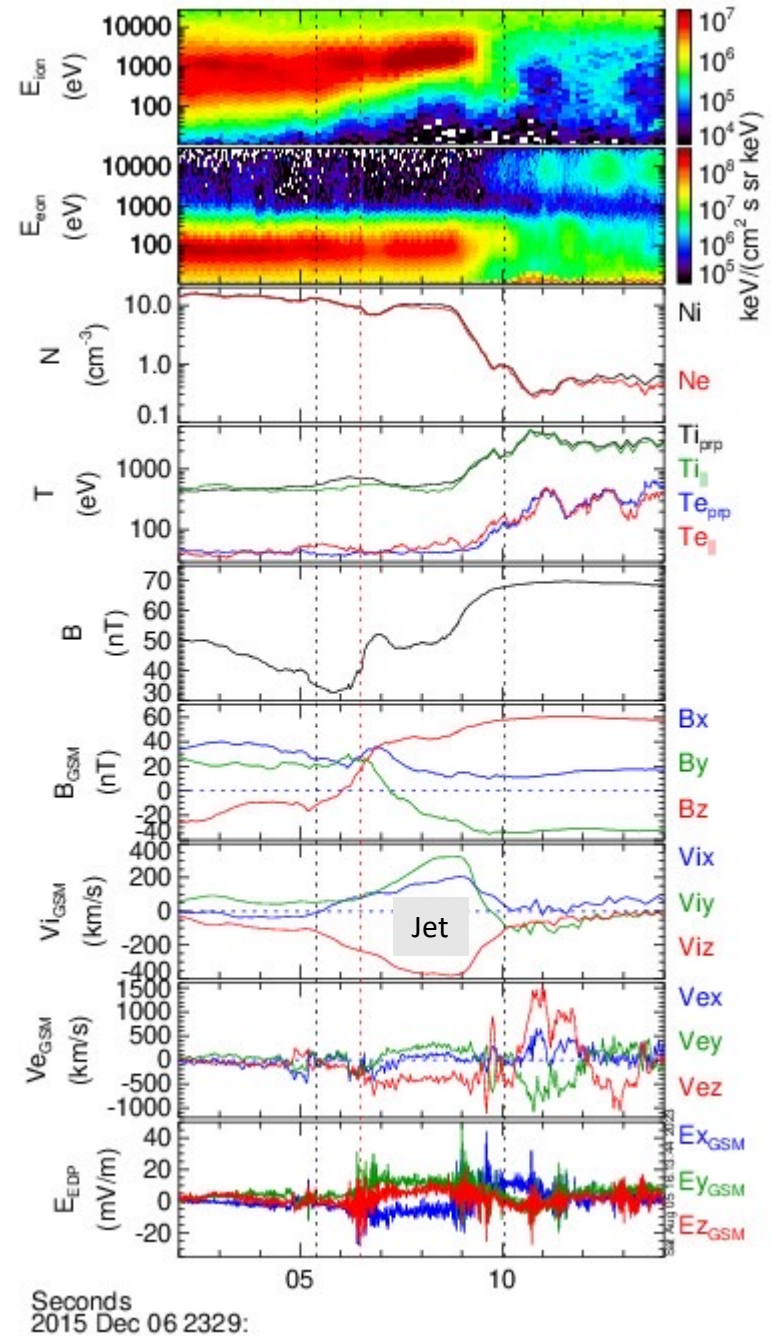
Exploring MMS at the Dayside Magnetopause: GSM

MMS Formation
 2015-12-06/23:29:06 UTC
 TQF=0.763



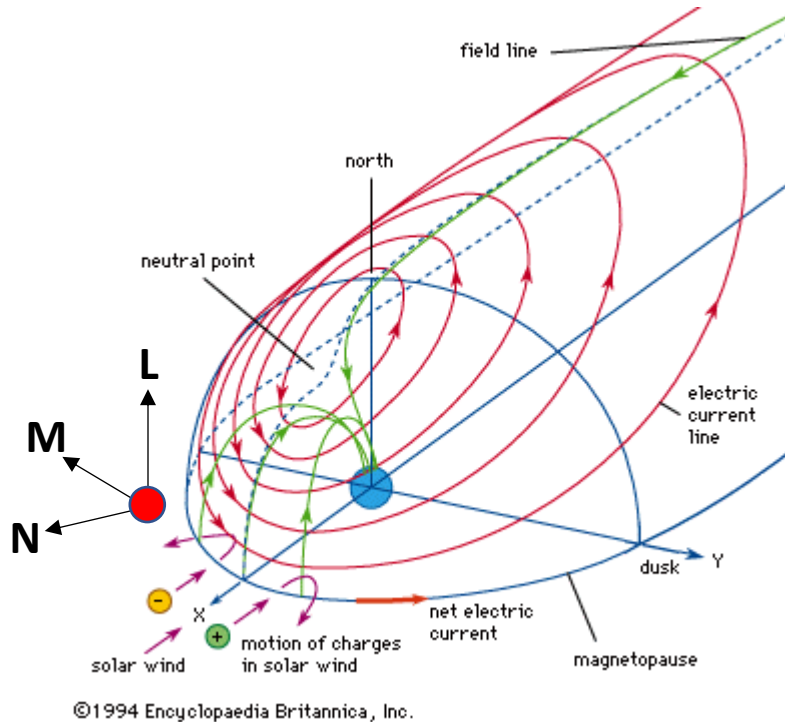
TQF = Tetrahedron Quality Factor

TQF = 1 <-> "regular" tetrahedron



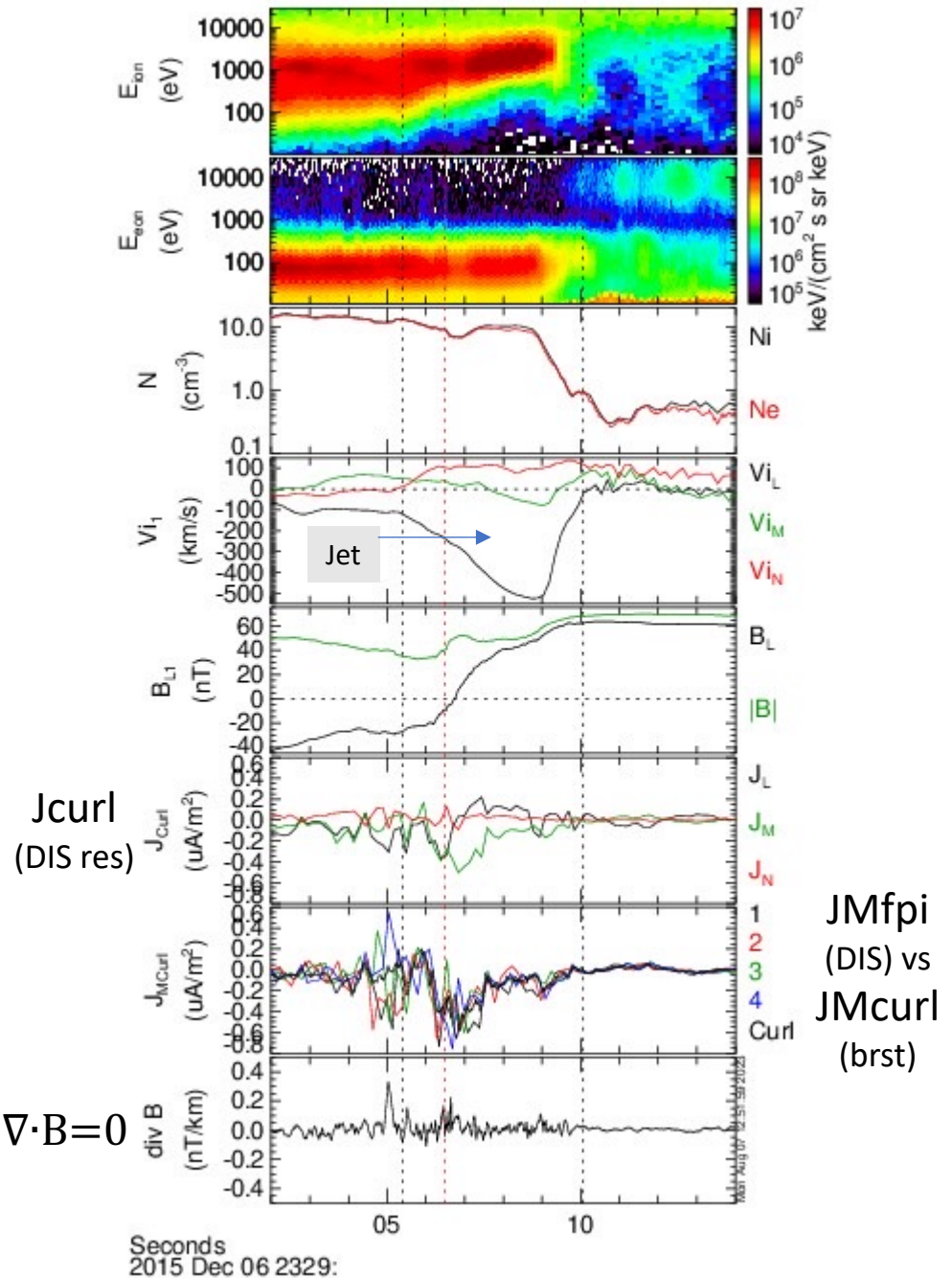
Seconds
 2015 Dec 06 2329:

Exploring MMS at the Dayside Magnetopause: LMN & $J = \text{Curl} B / \mu_0$ vs $J = Ne(V_i - V_e) = J_{fpi}$



$L_{gsm} = [-0.1598, -0.6770, 0.7185]$
 $M_{gsm} = [-0.7211, -0.4170, -0.5533]$
 $N_{gsm} = [0.6742, -0.6065, -0.4215]$

$$\nabla \cdot B = 0$$



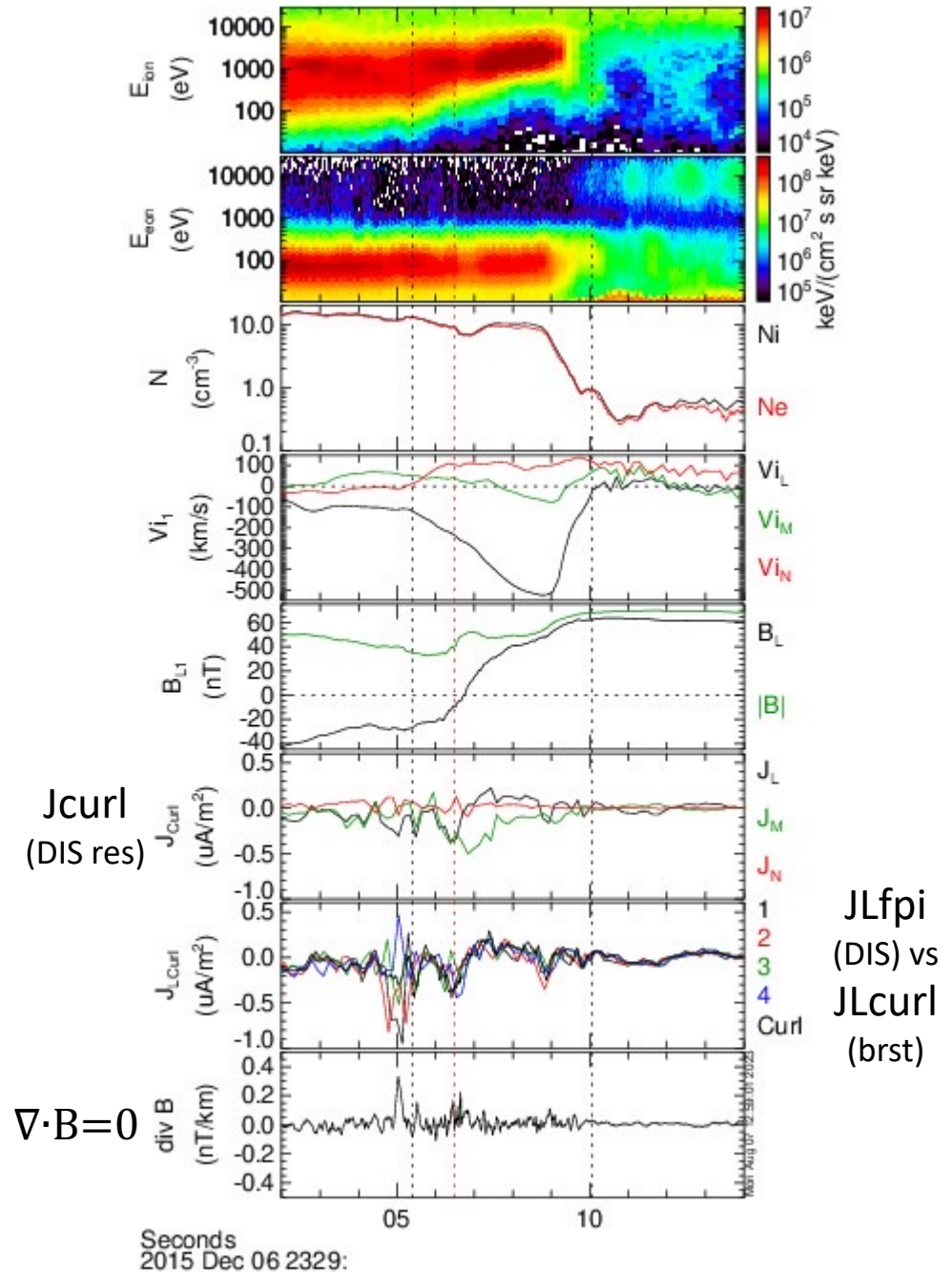
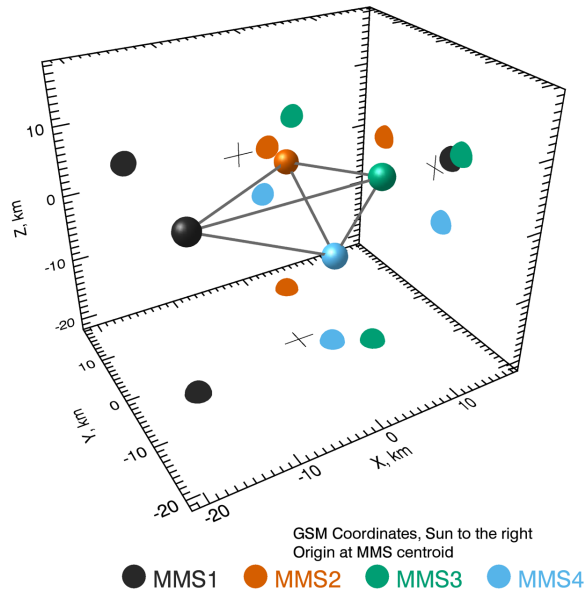
Exploring MMS at the Dayside Magnetopause: LMN & $J = \text{Curl} B / \mu_0$

vs $J = Ne(V_i - V_e) = J_{fpi}$

MMS Formation

2015-12-06/23:29:06 UTC

TQF=0.763



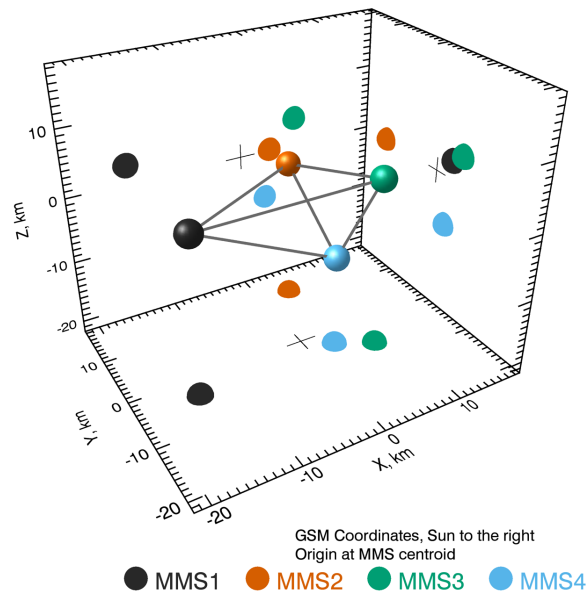
Exploring MMS at the Dayside Magnetopause: LMN & $J = \text{Curl} B / \mu_0$

vs $J = Ne(V_i - V_e) = J_{fpi}$

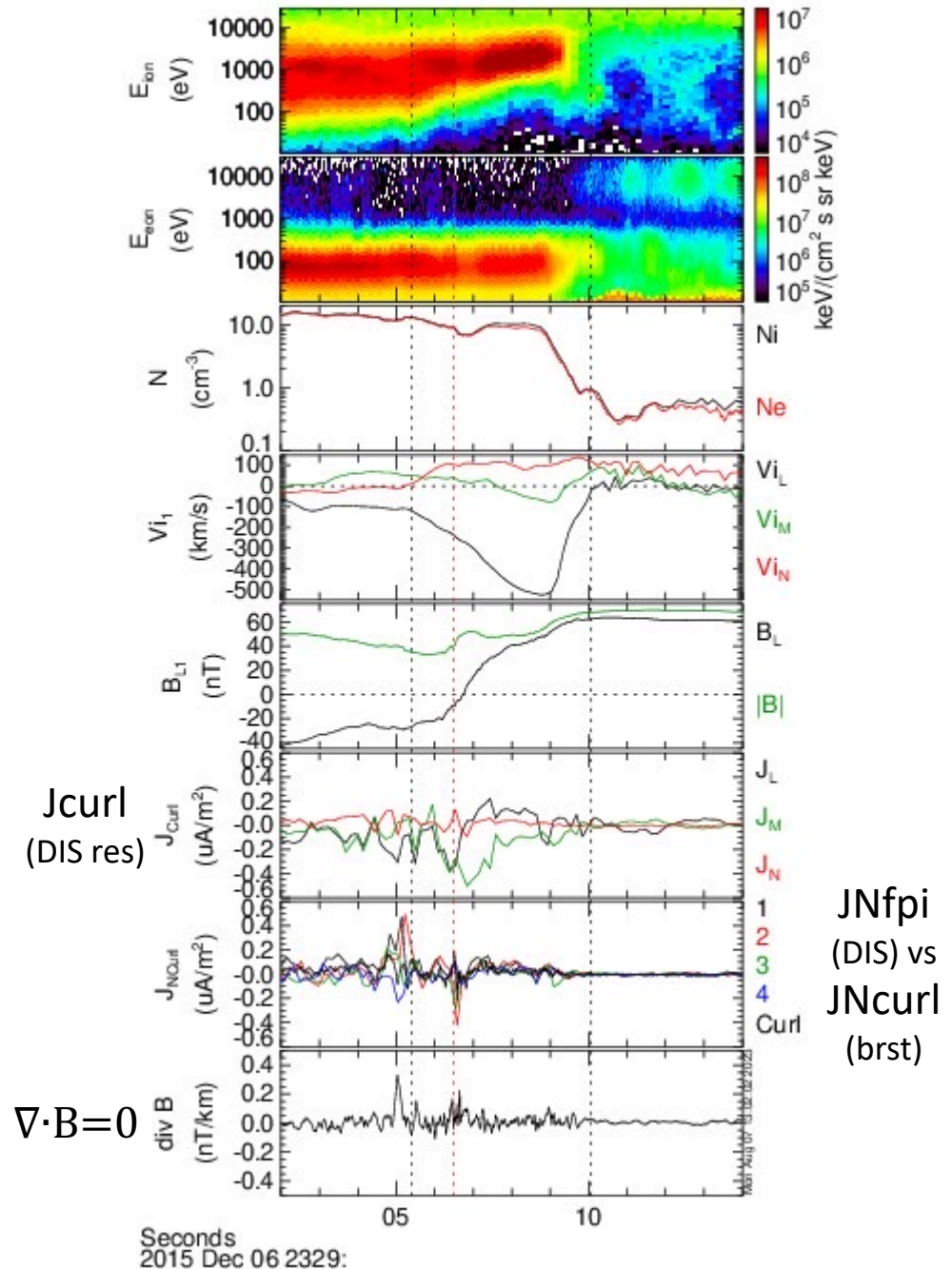
MMS Formation

2015-12-06/23:29:06 UTC

TQF=0.763

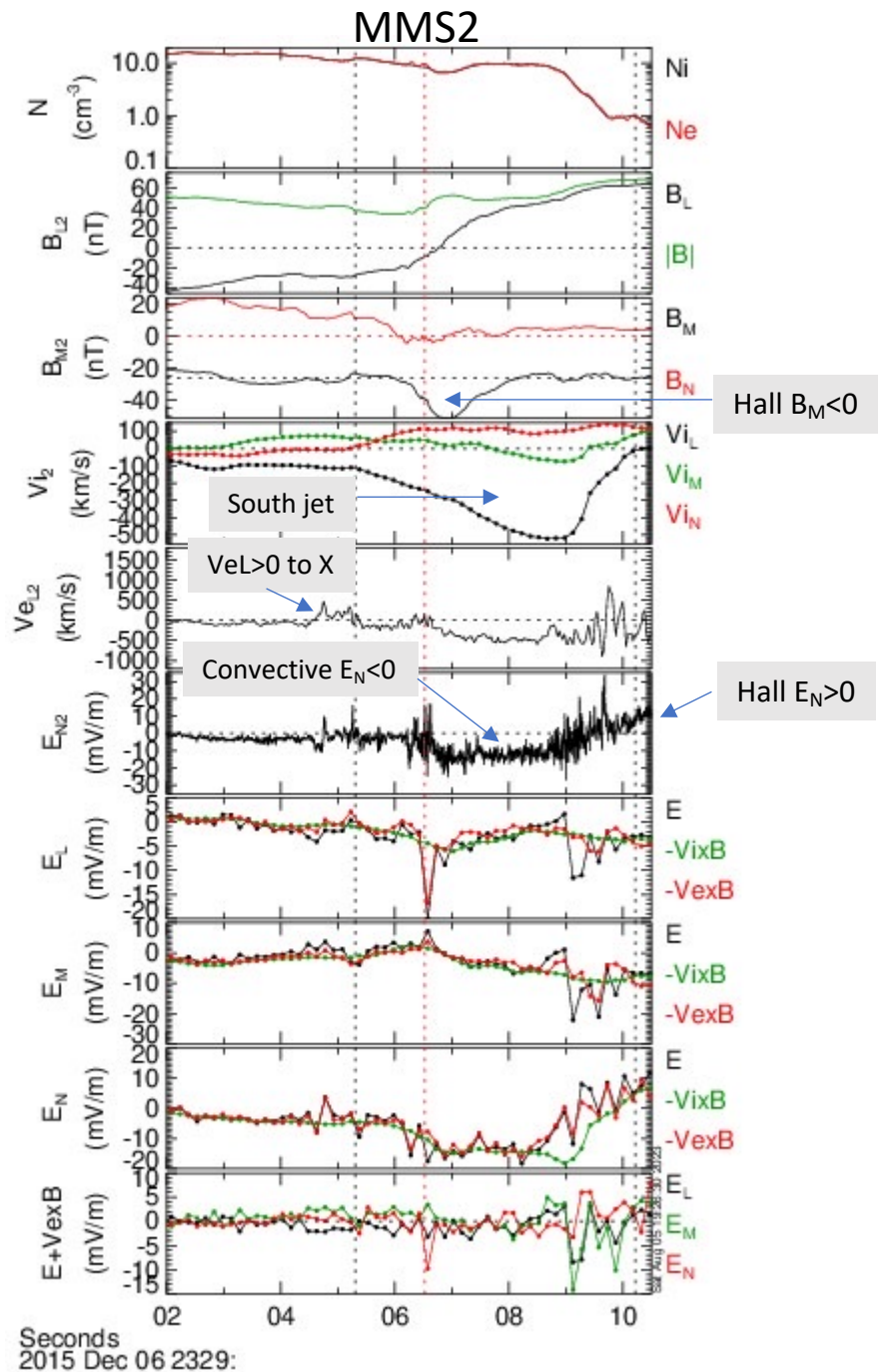
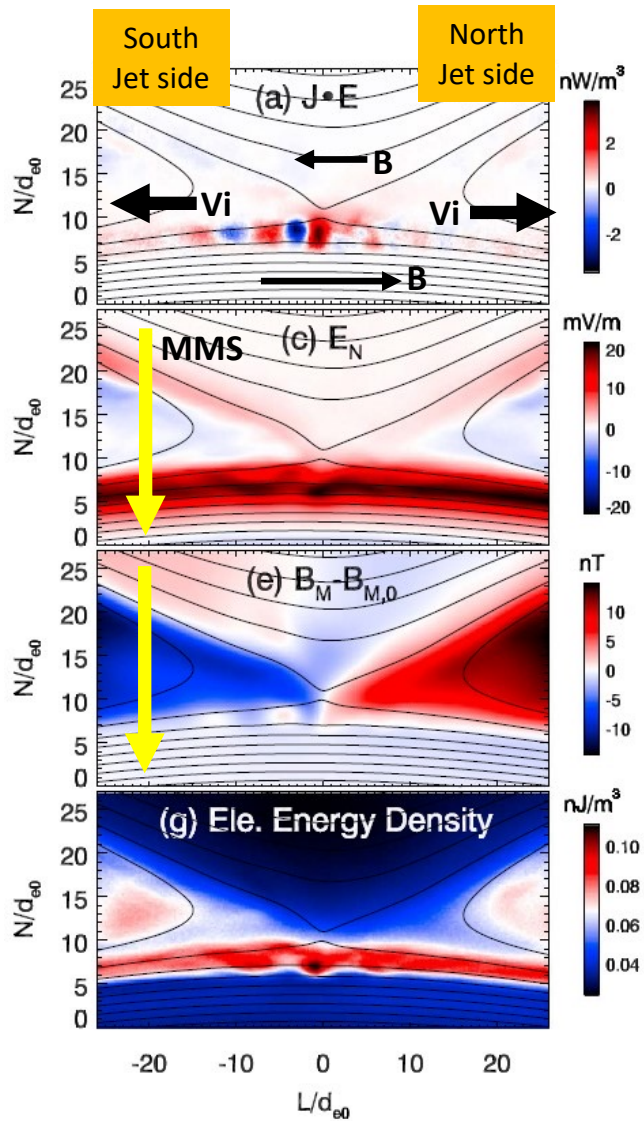


Tetrahedron conclusion:
 J_{curl} gives an average J .
 $J_{fpi} = Ne(V_i - V_e)$ is really good.
 One may confirm if $\text{div}(B) = 0$...



$\nabla \cdot B = 0$

Exploring MMS at the Dayside Magnetopause: Reconnection $E' = E + V_e \times B$

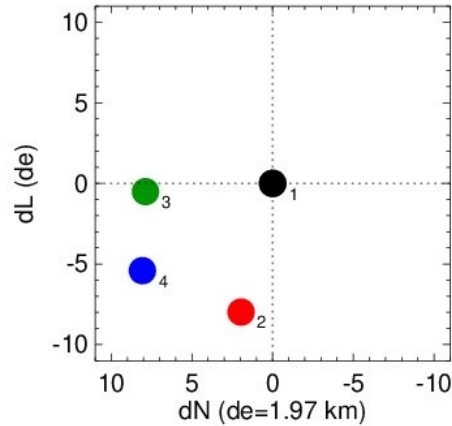


Exploring MMS at the Dayside Magnetopause: Reconnection

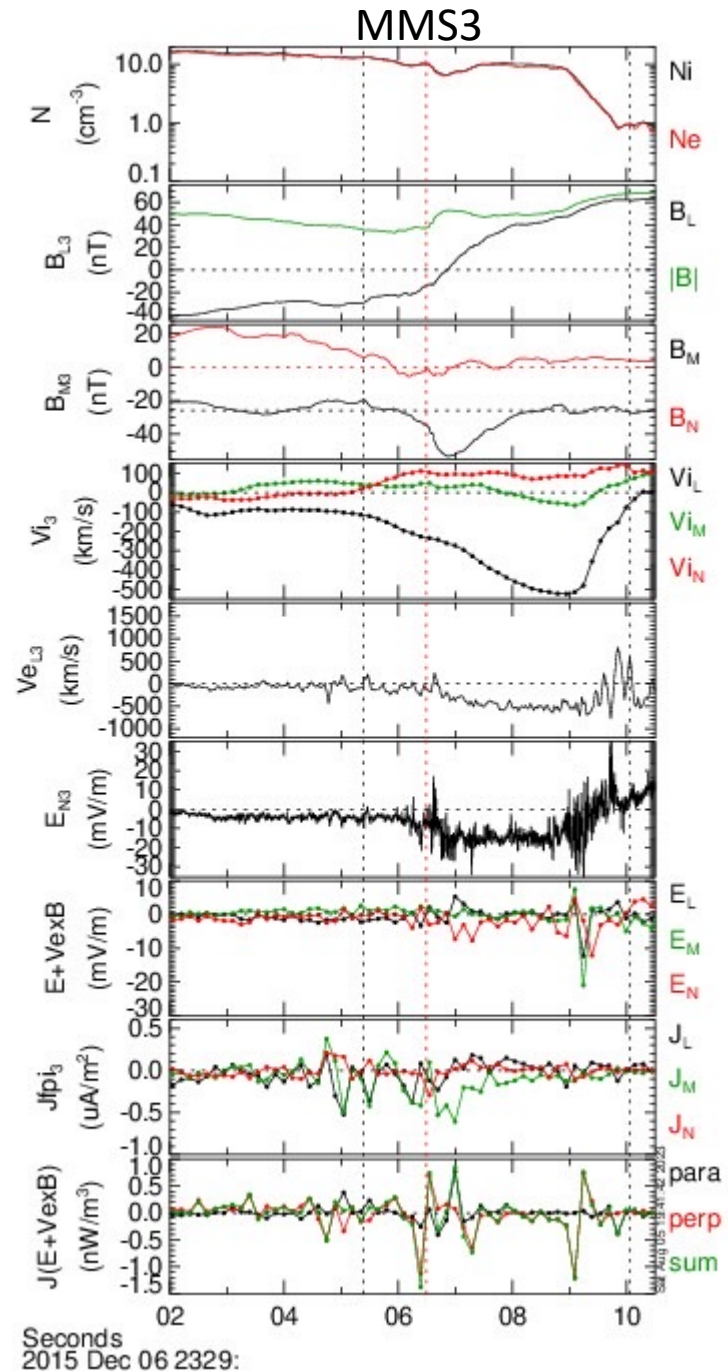
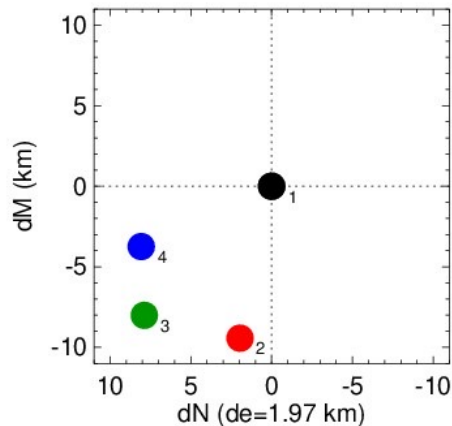
J · E'

$J \cdot E' > 0$ particles gain energy from EM
 $J \cdot E' < 0$ particles lose energy to EM

MMS at 2015-12-06/23:29:06.509



MMS1_{GSM}=[8.32 -3.96 -0.80] R_E
 N_{GSM}=[0.674 -0.607 -0.421]
 L_{GSM}=[-0.160 -0.677 0.718]
 M_{GSM}=[-0.721 -0.417 -0.553]



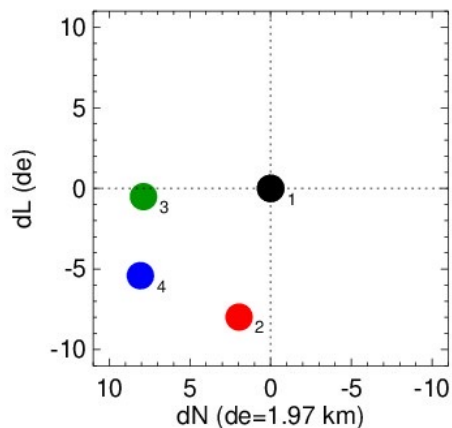
Seconds
 2015 Dec 06 2329:

Exploring MMS at the Dayside Magnetopause: Reconnection

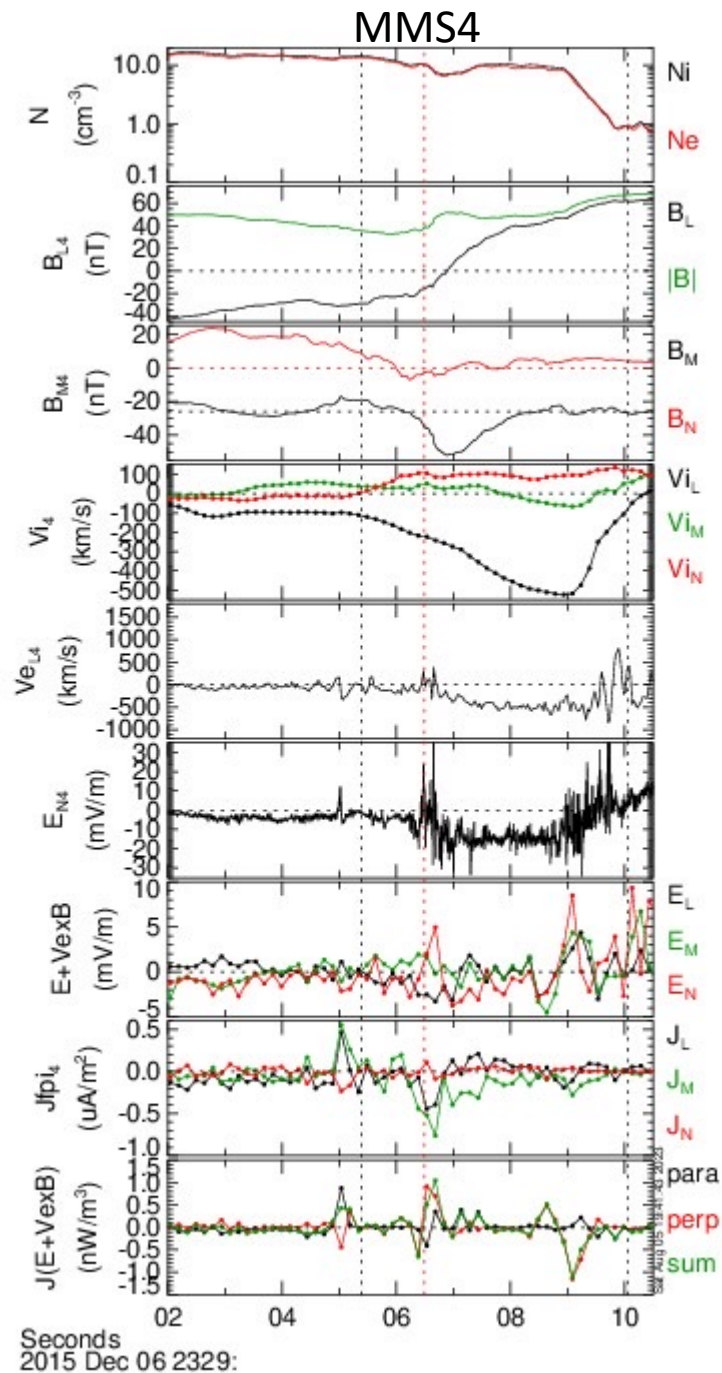
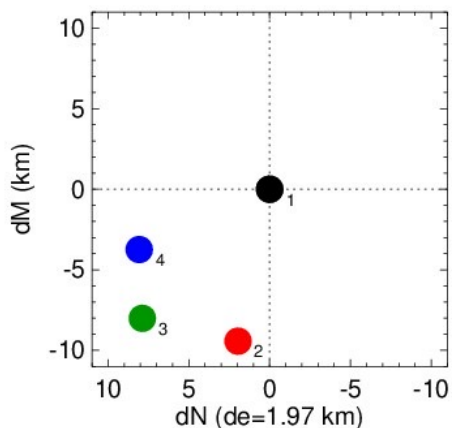
J · E'

$J \cdot E' > 0$ particles gain energy from EM
 $J \cdot E' < 0$ particles lose energy to EM

MMS at 2015-12-06/23:29:06.509



MMS1_{GSM}=[8.32 -3.96 -0.80] R_E
 N_{GSM}=[0.674 -0.607 -0.421]
 L_{GSM}=[-0.160 -0.677 0.718]
 M_{GSM}=[-0.721 -0.417 -0.553]



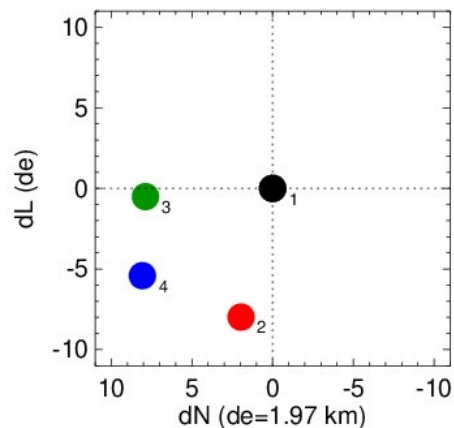
Seconds
 2015 Dec 06 2329:

Exploring MMS at the Dayside Magnetopause: Reconnection

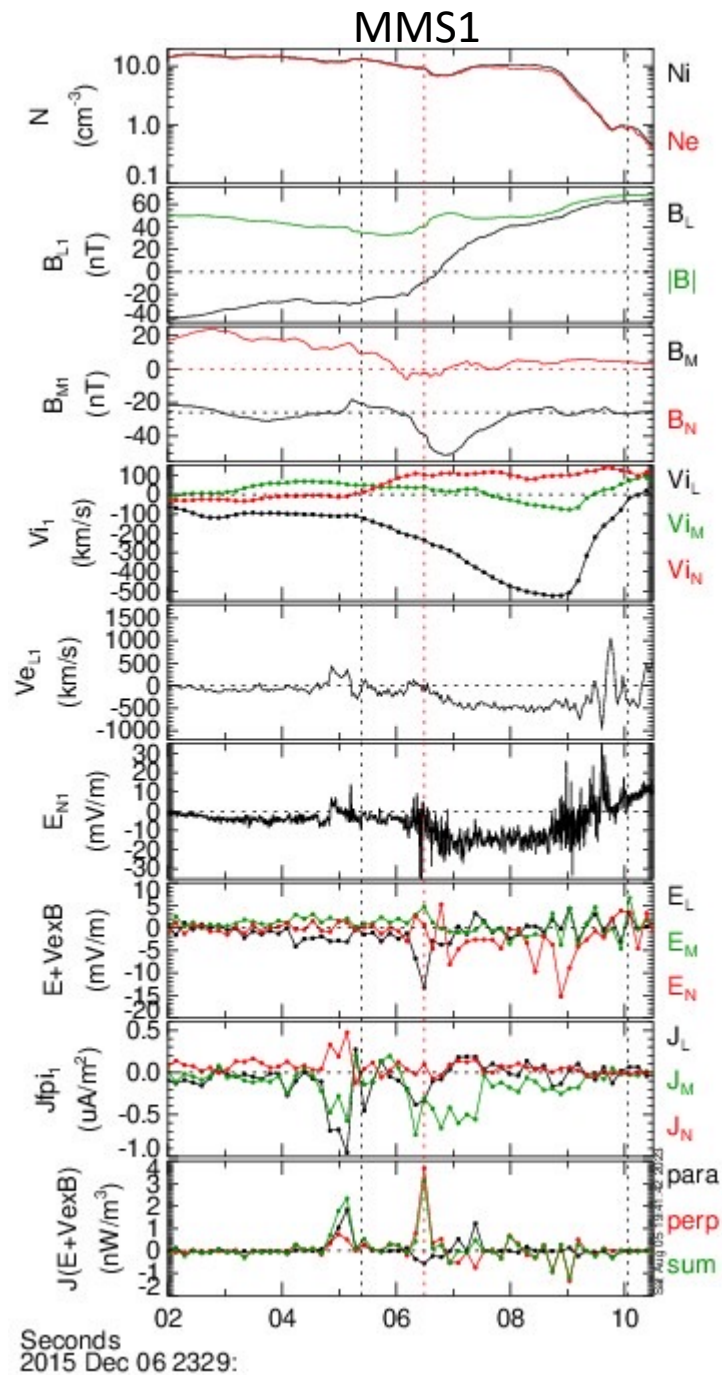
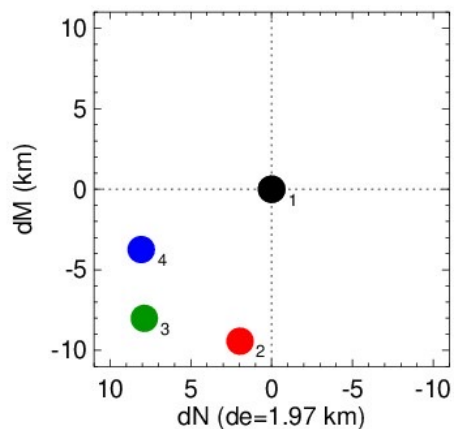
J · E'

$J \cdot E' > 0$ particles gain energy from EM
 $J \cdot E' < 0$ particles lose energy to EM

MMS at 2015-12-06/23:29:06.509



MMS1_{GSM}=[8.32 -3.96 -0.80] R_E
 N_{GSM}=[0.674 -0.607 -0.421]
 L_{GSM}=[-0.160 -0.677 0.718]
 M_{GSM}=[-0.721 -0.417 -0.553]



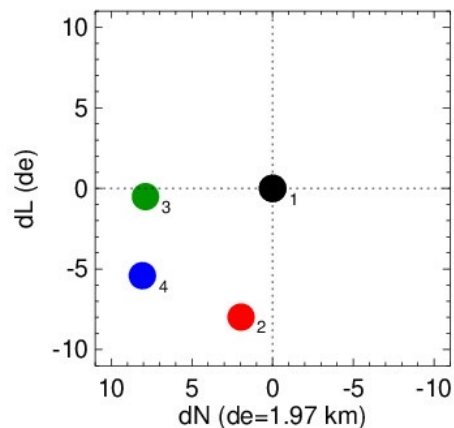
Seconds
 2015 Dec 06 2329:

Exploring MMS at the Dayside Magnetopause: Reconnection

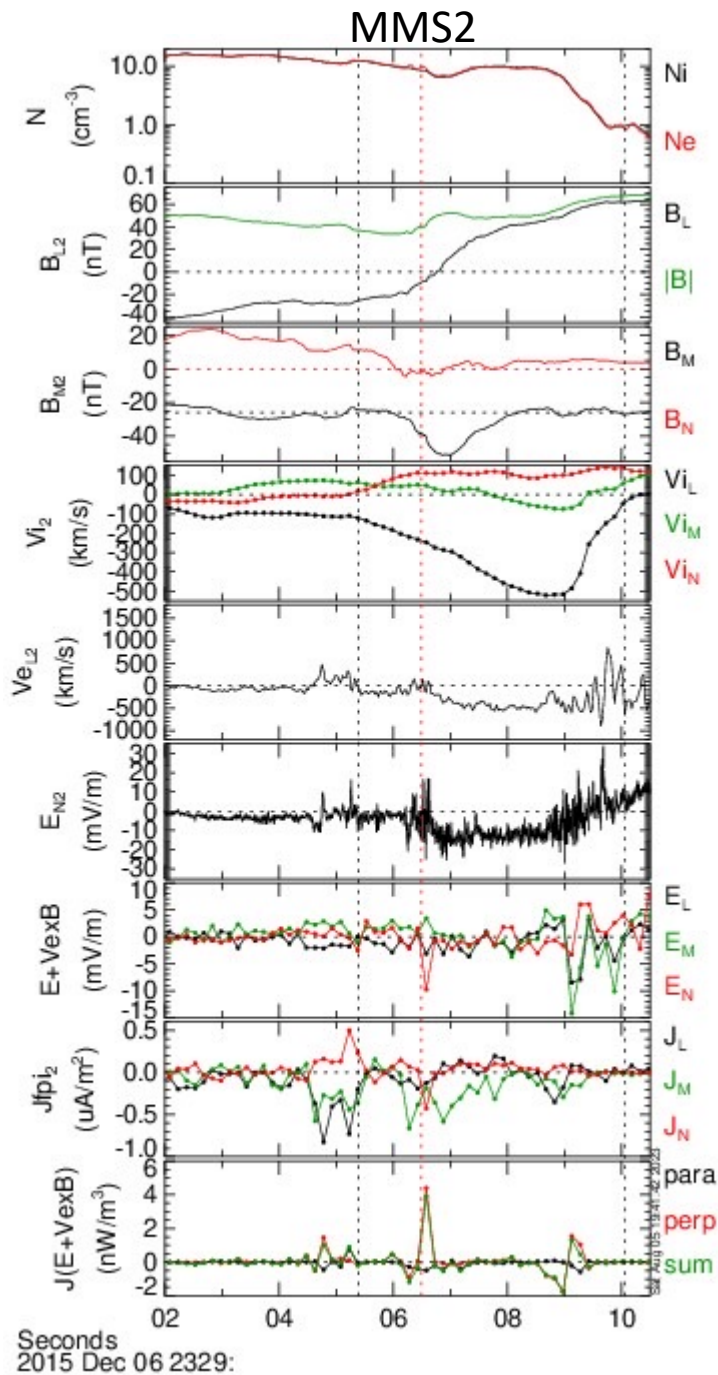
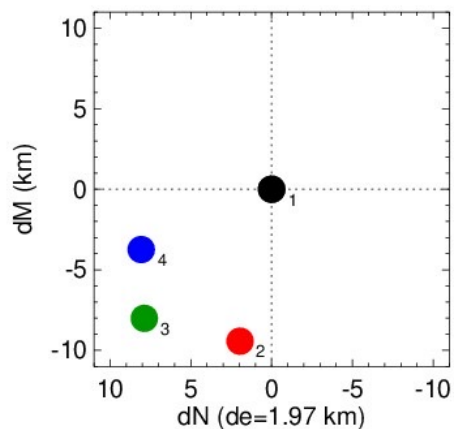
J · E'

$J \cdot E' > 0$ particles gain energy from EM
 $J \cdot E' < 0$ particles lose energy to EM

MMS at 2015-12-06/23:29:06.509

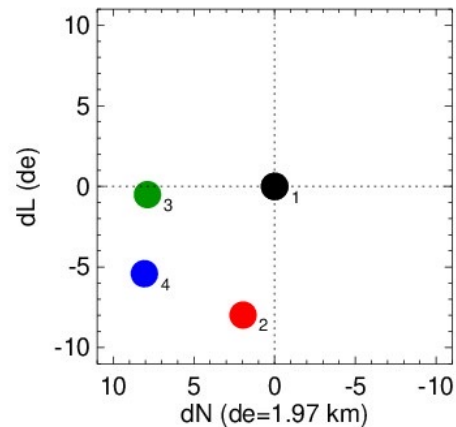


MMS1_{GSM}=[8.32 -3.96 -0.80] R_E
 N_{GSM}=[0.674 -0.607 -0.421]
 L_{GSM}=[-0.160 -0.677 0.718]
 M_{GSM}=[-0.721 -0.417 -0.553]

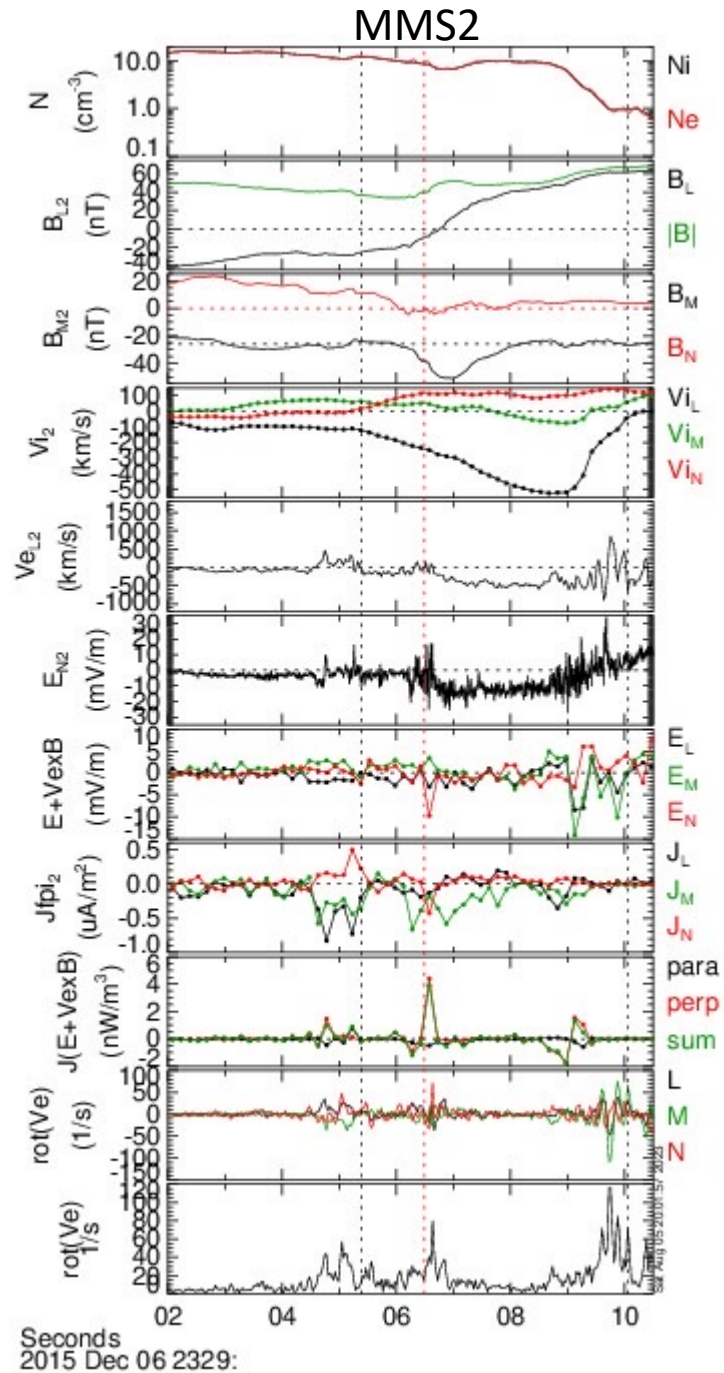
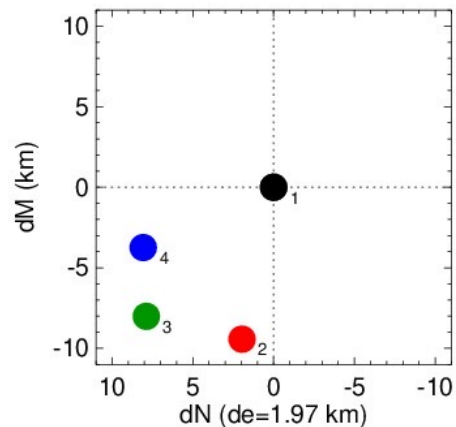


Exploring MMS at the Dayside Magnetopause: $\mathbf{J} \cdot \mathbf{E}'$ & $\nabla \times (\mathbf{V}_e)$

MMS at 2015-12-06/23:29:06.509



$MMS1_{GSM} = [8.32 \ -3.96 \ -0.80] R_E$
 $N_{GSM} = [0.674 \ -0.607 \ -0.421]$
 $L_{GSM} = [-0.160 \ -0.677 \ 0.718]$
 $M_{GSM} = [-0.721 \ -0.417 \ -0.553]$



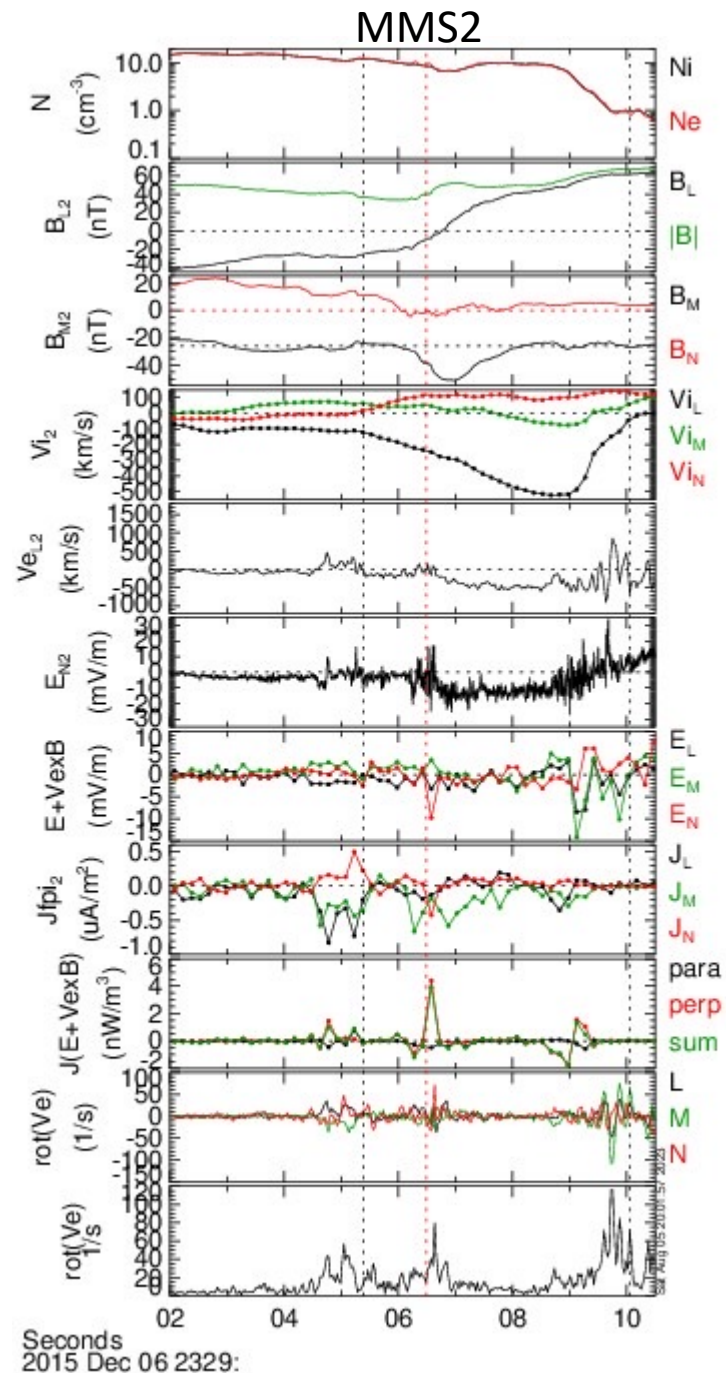
Exploring MMS at the Dayside Magnetopause: $\mathbf{J} \cdot \mathbf{E}'$ & $\nabla \times (\mathbf{V}_e)$

MMS allows unprecedented examinations of kinetic (ions & electrons) physics associated with reconnection & space physics in general.

This example has demonstrated many predicted (PIC) signatures of reconnection at the asymmetric magnetopause.

It also demonstrated a case of electron flow vorticity at both separatrices & inside exhaust.

An extended $\sim 8-10 d_e$ layer (L+M) exists inside the exhaust ($\Delta N \sim 2d_e$) with $J_{\text{perp}} \cdot \mathbf{E}' > 0$ (mms2+mms1)



Summary

- Current sheets can become unstable and reconnect. Whether big or small... [Yes, many HCSs near the Sun support exhausts!]
- The Alfvénic jets along the CS are a major characteristic.
- Other Rx parameters include Hall B and if (!) there are good 3D electric field measurements, you should see the Hall E.
- Multi-spacecraft tetrahedron formations allow us to obtain spatial gradients. Beware of “Tetrahedron Quality Factor” ... *not all formations are “regular” (TQF=1) and $\text{div}(\mathbf{B}) \neq 0$!*
- The Generalized Ohm’s Law helps us understand the plasma physics (particle motions) when $\mathbf{E} \neq -\mathbf{v} \times \mathbf{B}$... e.g. Rx
- Showed observations of Alfvénic reconnection jets across two current sheets – one in the solar wind and one at the m’pause.

Summary

- *I did NOT cover how you find the crucial **L,M,N** orientation of current sheets in space.*

*Many methods exist. Often one truly only knows the direction of maximum variance (**L**)... ☹*

*Normals (**N**) found using...to name a few.*

*(1) minimum variance of **B** (ISSI Chapter 8, Sonnerup & Scheible, 1998)*

*(2) cross-product of **B** on either side (Knetter et al 2004, J. Geophys. Res., 109, A06102, doi:10.1029/2003JA010099)*

(3) timing (if good s/c distribution – beware of poor alignments relative CS) (ISSI Chapter 10, Schwartz, 1998)